UNIVERSITÀ DEGLI STUDI DI PADOVA

UNIVERSITÀ DEGLI STUDI DI PADOVA

DIPARTIMENTO DI INGEGNERIA DELL'INFORMAZIONE

LAUREA MAGISTRALE IN
INGEGNERIA DELL'AUTOMAZIONE

Modeling and analysis of open-channel networks

Laureando:
Michele Frigo

Relatore:
Prof. Angelo Cenedese

Correlatore:
Dr. Marco Fabris

28 Febbraio, 2022
Anno Accademico 2021-2022

Contents

List of Figures

List of Tables

Abstract

Over the last decades, global warming has increased the frequency and intensity of storm water events by stressing the drainage system of urban areas that are not designed to manage these strong phenomena. This thesis deals with the analysis of the overflow risk in the network of open-channels focusing on the *Cavallino di Venezia* drainage network. For this purpose, it is presented a model that describes the dynamics of water flow in open-channel networks with a particular regard on the propagation of the *backwater effect* through channels and junctions. Such a model is used to analyse the functionality of the network when there is a large amount of rainwater be drained and to understand which places are at risk of overflow. To describe the fluid dynamics and build the network model, Saint-Venant equations are taken into account. In particular, the thesis focuses on the *Integrator Delay Zero model* that describes the main physical behaviour of the open-channel dynamics. This model is crucial in this thesis as it represents the core of the network model. Furthermore, different models are analysed and compared to characterize the behaviour of water in a junction. In particular, the the well-known *Equality model* is tested in order to find the conditions under which it operates properly. In conclusion, the *Integrator Delay Zero model* model and the *Equality model* are combined together with the support of graph theory to obtain the open-channel networks. In addition, this thesis deals with the problem of sensors placement. The aim of the latter investigation is to find the optimal sensor placement in order to estimate the flow in open-channel networks by minimising the estimation error. Finally, each topic presented in this thesis is supported by numerical simulations executed in MATLAB in order to to validate the theoretical results, by also resorting to using measurements of real drainage systems.

Abstract

Negli ultimi decenni, il riscaldamento globale ha aumentato la frequenza e l'intensità delle precipitazioni, sottoponendo a una forte sollecitazione i sistemi di drenaggio delle aree urbane che non sono progettati per gestire questi fenomeni violenti. Questa tesi si occupa dell'analisi del rischio di straripamento delle rete di canali concentrandosi sulla rete di drenaggio del *Cavallino di Venezia*. A questo scopo, viene proposto un modello che descrive la dinamica del flusso dell'acqua nelle reti di canali con un particolare riguardo alla propagazione dell'effetto *backwater*. Tale modello viene utilizzato per analizzare la funzionalità della rete e per capire quali luoghi sono a rischio di straripamento quando c'è un notevole quantitativo di acqua piovana da drenare. Per descrivere la dinamica dei fluidi e costruire il modello di rete, vengono prese in considerazione le equazioni di Saint-Venant (SVEs). In particolare, la tesi si concentra sul modello *Integrator Delay Zero* che fornisce una descrizione della dinamica dell'acqua nei canali semplificata rispetto le SVEs. Inoltre, si confrontano diversi modelli per descrivere il comportamento dell'acqua nella giunzioni tra canali. In particolare, il modello *Equality* è testato per trovare le condizioni in cui approssima adeguatamente la realtà. In conclusione, il modello *Integrator Delay Zero* e il modello *Equality* sono abbinati insieme con il supporto della teoria dei grafi per ottenere il modello per le reti di canali. Inoltre, questa tesi affronta il problema del posizionamento di sensori. Il suo scopo è quello di trovare il posizionamento ottimale di sensori al fine di stimare il flusso nelle reti di canali idrici minimizzando l'errore di stima. Infine, ogni tematica presentata in questa tesi è supportata da simulazioni numeriche eseguite in MATLAB al fine di convalidare i risultati teorici ricorrendo anche a misure del flusso di sistemi reali.

CHAPTER 1

Introduction

Drainage networks are complex large-scale systems composed by several components including transports structures as open-channel and pipelines, storage system and control structure. These networks have several purposes: the main one is to drain rainwater outside the urban areas in order to avoid flooding. At the same time, they have the aim of ensuring an appropriate water supply for the irrigation of the agricultural land around the cities. Over the last decades, global warming has increased the frequency, intensity and duration of storm water events in many areas causing flooding due to the inability of the drainage system to manage these strong phenomena. Flooding can cause major disruptions in cities, and lead to significant impacts on people, the economy and on the environment. For this reason the impact of flooding in cities is dealt with in several studies, such as in [1] which presents the state of the art of the literature on flood impact assessment in urban areas. On the other hand, climate change generates dry seasons that lead to water shortages causing droughts in crops. Therefore, the design of an advance control strategy to improve water management efficiency has become an objective of great importance in the last years. In particular, it is necessary to develop a strategy to minimise the flooding events during the rainy seasons and minimise water wastage in the distribution system in order to reduce the impact of droughts in the agriculture areas. This thesis focuses on the *Cavallino di Venezia* drainage network. This territory is a coastal peninsula that separates the northern Venetian Lagoon from the Adriatic Sea. The peninsula is separated from the mainland by the river Sile to the north and it extends toward south to the lagoon inlet *Lido*.

Figure 1.1 shows the peninsula highlighting the network under analyses. Note that the network is composed of open-channel and pipelines. Also, it is crossed by

Figure 1.1: Satellite view of the *Cavallino* peninsula.

the *Saccagnana* canal which divides the network into two parts: the main subnetwork is the one of the peninsula facing onto the Adriatic Sea, while the second subnetwork is in an urbanized area located further inland in the lagoon. The two networks are connected through two underground pipelines that lies on the *Saccagnana* canal bed. In addition, both the subnetworks communicate through hydraulic structures as gate with the lagoon, the rivers and the sea surrounding the peninsula. The peculiarity of this territory is that it is located under the sea level and it is protected from the sea by the elevated coastline and by the gate that can isolate the network of the peninsula from the external environment. Moreover, thanks to the proximity of the sea, the lagoon surrounding the *Cavallino* peninsula is affected by the tide. In addition to the normal fluctuation of the water level generated by the tide, the entire lagoon area is subject to a more extreme phenomenon called *Acqua alta* [2]. This phenomenon is caused by a combination of astronomical (tide), meteorological and geological events. This problem often occurs during rainy periods and forced the technicians to isolate the *Cavallino* network from the outside environment to prevent flooding in the Urban area of the *Cavallino* territory. However, this strategy removes the possibility of the network to drain rainwater outside. Also, due to climate change, the rainfalls have become increasingly violent and they are capable of releasing large amounts of water in a short time. The *Cavallino* network had the

problem that it is not design to withstand such extreme phenomena; indeed, *Acqua alta* events in combination with violent rainfalls cause flooding on the Urban area of the *Cavallino* territory. The main objective sought in this thesis is to avoid these phenomena design a strategy to manage the internal network in order to minimise the risk of overflow. To attain this objective, the most evident solution consists in enlarging the infrastructure in order to increase the drainage capacity of the network. In this way the network can transport water away from cities in a faster way and preventing flooding. However, this solution generally is invasive and expensive making it not always suitable. An alternative is to use a control approach, which optimises the state in the network through control structures in order to minimise the risk of flooding. This approach is less invasive in the environment and, in general, cheaper than an enlargement of the entire network. Figure 1.2 shows a summary di-

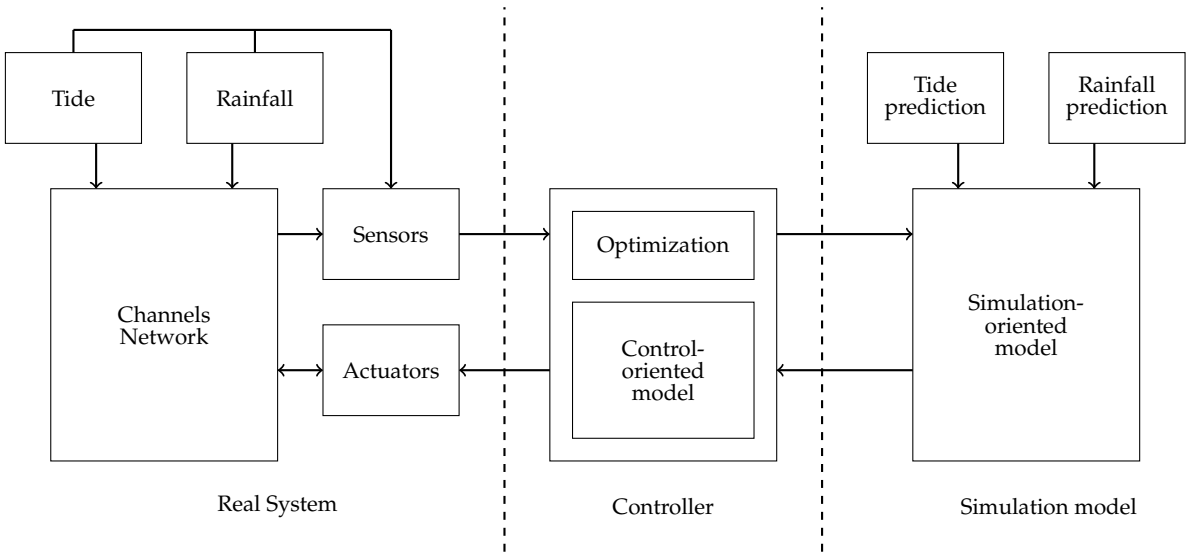

Figure 1.2: Diagram of the overall system.

agram of the control approach treated in this thesis. It is composed by three element: the real system, the control space and the simulation space. The real system is composed by transport network and the external environment such as rainfall and tide. Also, the real system is composed of the sensors which aim to measure the state of the network, such as the water height which is a fundamental variable to be monitored to prevent flooding. Also it is necessary to accurately measure the intensity of the rainfall and the tide in order to predict their effect on the network. Finally, the actuators (or control structures) are devices capable of modifying the natural water flow. They are distinguished into two groups. The first regards the gate that regulate the flow of water through a mobile bulkhead. While, the second group are the

water pumps, which are devices able to pump water contrasting the force of gravity. These devices are the tools available to manage the flow within the network. The controller is the core of the system: this element has the task of controlling the actuators in order to achieve a given task, which is often encoded through an optimisation problem. To support the controller a control-oriented model can be used. This model has the purpose of describing the main characteristics of the real system in the short term and can be used, for example, to predict the behaviour of the system. The controller is crucial to achieve the objective being pursued: numerous techniques have been developed to minimise the risk of flooding and in controlling the distribution to reduce waste. For these topics the reader is referred to [3] and [4] that review and discuss several techniques and strategies commonly used for the control of drainage network. The last element of the scheme is the simulation-oriented model. This type of model, unlike the control-oriented model, have the aim to describe in detail the real system shows in Fig.1.1. Also, it can be used for a preliminary study of the system to understand weaknesses and to dimension and test the control strategies. This category of models can achieve a high accuracy in estimating the system state; however, they have a high computational burden which makes them not suitable for real-time implementation. Lastly, a detailed prediction of precipitation and tide is a fundamental prerequisite to accurate assessment of urban rainfall-runoff response. In [5] the state of the art of rainfall measurement and prediction is discussed.

1.1 State of the art

In this section, the state of the art about network models is presented. In particular, the concerned networks are composed by open-channels, pipelines, junctions and other control elements, as gates and water pumps. These elements are generally modelled separately and then combined to create a model of the network. In this section, it is discussed the state of the art of open channels and junctions. However, models for pipelines are not taken into account, since they are not considered in this thesis. Also, models for gates are discus in a dedicated section of appendix A.5. The open-channels models can be classified into simulation-oriented models and control-oriented models. In both cases, they are based on the Saint-Venant Equations (SVEs): they describe the propagation of a wave in an open channel modeling accurately the flow in channels. Note that, a closed-form solution of the SVEs, in general, is complex to be obtained due to the presence of highly nonlinear terms.

Therefore, several models have been developed starting from Saint-Venant equations in order to describe the dynamics of open channels.

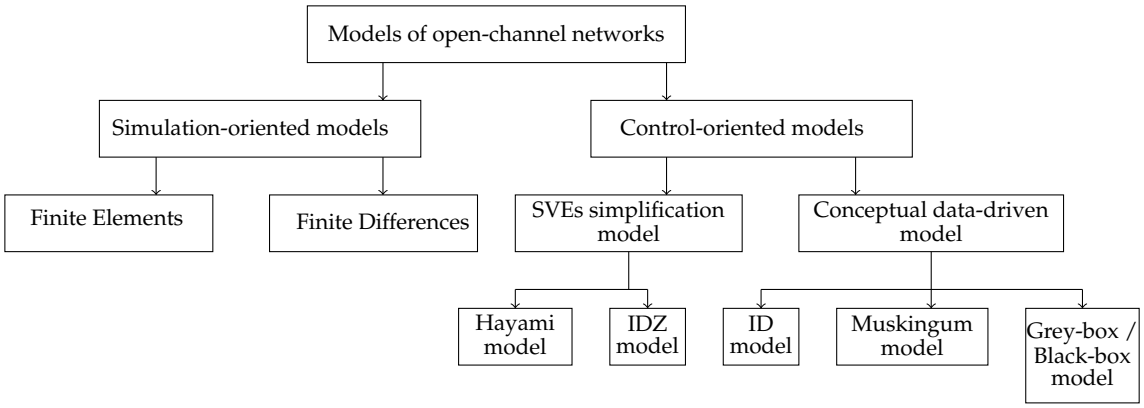

Figure 1.3: Summary of the state-of-art of open-water channels modeling.

Figure 1.3 shows a diagram that summarises the main models for open channels in the literature, it is structured on the basis of the review of the state of the art of open-channel models in [5] and [4]. The branch called simulation-oriented models includes numerical methods that use the discretisation tecnique to find the solution for SVEs. These methods are called finite differences and the finite elements. The first one approximates derivatives both in spatial and time domain with finite differences. These methods are used in the literature to simplify the SVEs in [6]- [7]. Note that, in general, the stability of the discretized models depends on the discretisation step size. However, there are some versions of this approach that overcome the problem. An example of such strategy is developed by Malaterre et al. [8] that employs an implicit Preissmman finite-difference obtaining a model whose stability does not depend on the discretisation step size. The finite elements is a numerical method for solving partial differential equations in two or three space variables. It subdivides a large system into smaller ones, that are simpler parts that are called finite elements. Several implicit finite-differences have been used for the analysis unsteady open-channel flows as [9]-[10]. In conclusion, this branch of models describe the actual system in detail, yet they have an high computational burden. Therefore, these techniques are more suitable for simulation-oriented models.

The second branch of models presented is the control-oriented models. This branch is separated into two groups: SVEs simplification models and Conceptual data-driven models. The SVEs simplification approach is based on the linearization of SVEs around a steady-state equilibrium. The first model obtained whit this tecnique was published by Hayami (1951) [11], which proposes the linearization of the SVEs to study the flow in rivers. Later Corriga et al. (1980) [12] proposes the

Laplace transformation of the linearized SVEs to describe the behavior of the level and flow along the channels. To this group also belongs Integral delay zero (IDZ) model published by Litrico and Fromion (2004) [13], which will be treated in this thesis in detail. The latter provides a linear model that describe the water height in a channel knowing the inflow and outflow considering the backwater effect. This model describes the state of the water using two parameters: an integrator and a delay. Also, unlike the others, this model includes a set of parameters to describe the high frequency behaviour of the water height. The second group of models are the Conceptual data-driven models: they are not derived with a rigorous approach from the SVEs, but using some basic physical observations. The main advantage of these models is the simplicity, indeed they are able to describe with a few parameters the part of the dynamics that is more interesting for the control design purpose. However, a large amount of data is required to carry out the identification and parameter estimation process. The Integral delay model was proposed by Schuurmans (1997) [14], it is very similar to the IDZ: it models the water height with two parameters, an integrator and a delay, but it does not describe high-frequency behaviours of water height. In addition, unlike the IDZ, this model is not able to estimate these parameters accurately as IDZ model and the backwater effect is modelled more roughly. The Muskingum model was proposed by McCarthy (1939) [15], it is based on mass balance principle, which is used to obtain a relation between the inflow and the outflow of a channel. However, this model does not provide any information on the upstream or downstream channel depth. The last method presented is the modelling by identification. This type of method is based on the collected data, in particular, the black-box model only describes the relationship between the measurement input and output data without using physical knowledge of the system. Instead, the gray-box model uses some physical knowledge of the system. An example is proposed by Weyer [16]: this model is based on the mass balance principle. It assumes that the water volume in the channel is proportional to the water level and includes the time delay which required the inflow to pass through the channel.

As far as junctions are concerned, the state of the art is mainly based on conservation principles of energy, momentum and mass. The work of Akan and Yen (1981) [17] proves that the energy equation can be approximated by the water stages equality, if the flow through the junction is subcritical. From this study it is concluded that modelling water level in a junction as constant has a solid foundation. In particular, this model called Equality model, it has the advantage to be linear and it can be applied for junctions with an arbitrary number of branches. However, this model

only performs well if the flow through junction has a sufficiently small Froude number. Indeed, in the study presented by Kesserwani et al. (2008) [18] shows that the Equality model has an acceptable error if the Froude number is smaller than 0.35. An other approach is introduced by Gurram et al. (1997) [19], which uses the momentum and mass conservation principle applied to the junction. In a more advance version, Hsu (1998) [20] also considers the energy losses in the junction. The advantage of these models is that they are not sensitive to Froude number as the Equality model. However, they have the disadvantage to be non-linear; also they are based on restrictive assumptions. Indeed the assume that the channel widths of inflow channel are equal and the height of inflow are equal.

A more advanced method is proposed by Shabayek et al(2002) [21]: this model is based on momentum principle and the conservation of mass as the Gurram model, but it is not based on restrictive assumptions of Hsu and Gurram model. However, the latter models are derived for a specific type of confluence, so it is not possible used them for junctions with an arbitrary shape and number of branches. An alternative method to the classical approach seen so far is based on the Riemann problem approach. The Riemann problem for a junction was proposed by Goudiaby et al. (2013) [22]: it solves a well-posed Riemann problem at the junction assuming a continuous bottom and symmetric configurations (e.g Y-shaped junction). Lastly, Elshobaki et al. (2018) [23] investigates this approach for general configurations taken into account asymmetric junction and discontinuous bottom.

1.2 Thesis contributions

This thesis deals with the analysis of the overflow risk in the network of open-channels presented in the previous section. For this purpose, a model is presented whose task is to describe the propagation of the flow through the network and the evolution of water height when the network is under stress, i.e. when its drainage capacity is low and there is a large amount of rainwater to drain out. The advantage of the presented approach is that, although this is based on typically control-oriented models, it describes the flow in a more advanced way, namely, by considering some important non-linearities as the backwater effect.

In addition, this thesis deals with the problem of sensors placement to monitor the network flow states. In particular, the objective is to find the optimal sensor placement in order to estimate the flow of each channel in the network, by minimising the inference error. Also, by means of the proposed strategies, it is possible

to achieve other objectives such as robustness against sensor malfunctions or data transmission failures. In particular, the state of the art for the sensor placement problem is dealt with in the dedicated chapter 5.

1.3 Thesis outline

The following chapters of this thesis are organised as follows. Chapter 2 presents the IDZ model. The latter is studied in detail analysing its continuous and discrete-time versions. In addition, the IDZ model is extended incorporating a model of a control structure. In chapter 3 are presented four models which aim is to describe the flow state in a three-branch open-channel junction. These models are tested and compared in order to study their performance. Finally, some considerations are made about the possibility to extended the models in order to describe junctions with an arbitrary number of branches. Chapter 4 deals with the sensor location problem. The aim is to estimate the flow in an open-channels networks. In particular, a strategy to solve it is presented and tested on a network that is a simplified version the *Cavallino* network shows in figure 1.1. In chapter 5 is proposed a model to describe the dynamics of water flow in a open-channels network with a particular regard on the propagation of the backwater effect through channels and junctions. Finally, this model is tested with a simplified version the *Cavallino* network.

CHAPTER 2

Modeling of Open Channel Flow

Open- channels are transport structures for liquids. They are characterised by a cross-section that is open on top so that the liquid surface is subject to atmospheric pressure. Liquids can be also transported through pipes characterised by closed cross-section. In this case, they are partially filled, the top surface of the liquid is subject to atmospheric pressure as in an open channel. The flow in an open channel or in a partially filled pipe is called free-surface flow or open-channel flow. If there is no free surface, thus the conduit is full, the liquid is subject to a bigger pressure and the flow is called pipe flow or pressurised flow. In this thesis will be treated only the open- channels.

2.1 Assumptions and notation

This section presents the main variables and notation used for open channel models. Figure 2.1.a shows a lateral section of a open channel with length L and the reference frame used for the flow variables. The axis x is defined as the versor perpendicular to the direction of gravity and it points to the direction of the channel (if it is straight). In general, this versor is not parallel to the channel bottom unless it is flat. The axis z is defined as the versor parallel to the direction of gravity force, while versor y is given by the cross product between the versors x and z. Finally, the variable t is the time variable.

Figure 2.1.b shown the cross-section of canal: it is defined as the surface normal to the direction of flow and delimited by the channel bed and the water surface; its unit of measurement is m^2. It is also called channel section area or wetted area and it is denoted by $A(x,t)$. In particular, the variable $A(x,t)$ represents the channel section area at the time instant t taken in the position x along the channel. The

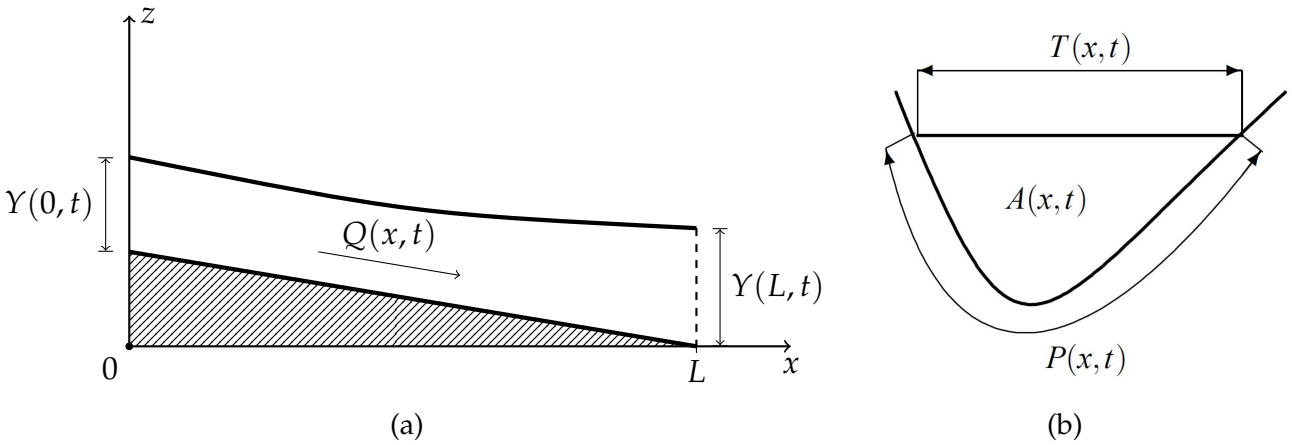

Figure 2.1: (a) Lateral section of an open-channel with the reference frame. (b) Example of an open-channel cross-section.

variable $Q(x,t)$ denotes the flow passing through the cross-section area $A(x,t)$, its unit of measurement is m^3/s and it can be calculated multiplying the cross-section area by the velocity of water flow $V(x,t)$:

$$Q(x,t) = A(x,t)V(x,t). \tag{2.1}$$

Note that this equation is valid only if the velocity is constant over the cross-section area. In practice, the velocity is non uniform, indeed, the water near to the channel bed is slower than in the middle due to frictional forces, so $V(x,t)$ is not constant over the cross-section. For the purposes of this thesis, the flow is considered as one-dimensional quantity constant over the cross-section; in particular, $V(x,t)$ is assumed scalar defined as the average of actual velocity over the cross-section. Also it is assumed that the direction of $Q(x,t)$ lies in the plane $y = 0$, so the velocity vector components along y-axis is null, while x-axis and z-axis component are not null in general. Another fundamental variable is the water height, also known as flow depth. In the literature are used two different definition: $D(x,t)$ is the depth of flow normal to the channel bed, whereas $Y(x,t)$ is the depth of the flow normal to the the x axis. In general, these two height variables are different, but they can be considered equal in the case where the channel is flat or its bed slope is small enough. In particular, the bed slope is defined as the incidence angle θ between axis x and the channel bottom. Often it is represented by the variable S_b which is defined as:

$$S_b = \tan(\theta). \tag{2.2}$$

Note that S_b and θ are assumed constant values which do not vary along the length

of the channel $x \in [0, L]$. In general, the bottom of a channel has a variable slope along its course, in this thesis it is assumed to be constant for simplicity. Therefore, $Y(x,t)$ is related to $D(x,t)$ by the following formula:

$$Y(x,t) = \cos(\theta) D(x,t) \tag{2.3}$$

From this last formula it can be seen that, if the slope of the bottom is small enough, i.e. $\theta \simeq 0$, it implies that $\cos(\theta) \simeq 1$ and therefore $Y(x,t) \simeq D(x,t)$. In this thesis, unless otherwise specified, the height used is always the vertical depth $Y(x,t)$. Figure 2.1.a shows two values of the water height: $Y(0,t)$ and $Y(L,t)$. The first variable is the height of the water at the channel inlet, so where the water flow enters; this end is called upstream end. While $Y(L,t)$ is the height of the water at the channel outlet called downstream, it is defined as the end where the channel flow exits. A fundamental assumption that is made in this thesis is that the water always enters from the upstream end where the channel bed height is higher (w.r.t the downstream side) and thanks to the force of gravity, the water moves towards the downstream end (i.e where the channel bed height is lower w.r.t the upstream side).

In figure 2.1.b, it is shown the width of the water surface $T(x,t)$ and the wetted perimeter $P(X,T)$ that is the perimeter of the cross-section area $A(x,t)$. Usually, open- channels are modeled through a known cross-section shape as rectangular or trapezoidal. Therefore, knowing the geometrical dimensions of the cross-section and the depth $D(x,t)$ of the water, it is possible to calculate wetted area, perimeters and top width using the formulas reported in appendix B.4.

2.2 Saint-Venant equations

The Saint-Venant equations (SVEs) are nonlinear equations that are used to studies the unsteady water flow. In order to derive them some assumption are made: the most important one is that flow $Q(x,t)$ for a given position x is considered as one-dimensional variables as described in the previous paragraph. Similarly, the height $Y(x,t)$, for a given position x, is considered as one-dimensional variables, so it is considered constant over the cross-section of channel. Also, the following assumptions are made:

- The pressure to which water is subject is hydrostatic, namely the pressure to which the water is subjected increases in proportion to the water depth. A detailed description of this type of pressure is given in appendix A.3;

- The effect of friction is modeled using Manning's equation reported in appendix A.1;
- Lateral inflow of channel is negligible, so the flow enters only from upstream end and exits only from downstream end;
- The channel bed slope is small (i.e $\theta \simeq 0$), so the depth of flow normal to the channel bed $D(x,t)$ and the depth of the flow normal to the the x-axis $Y(x,t)$ are approximately equal.
- The channel modeled by this equation is rectilinear with a known cross-section shape as rectangular or trapezoidal. Also the variations of the cross-section sizes, bottom width and lateral slope along x are small;

Note that the last assumption can be relaxed: if the dimensions of the channel are not constant, it is possible to divide the channel into several sections and to each of them is assigned constant dimensions given by the average of the actual values.

The Saint-Venant equations are two coupled equations: the first one is the mass conservation equation, second one is the momentum conservation equation. The two equations are reported below:

$$\frac{\partial A(x,t)}{\partial t} + \frac{\partial Q(x,t)}{\partial x} = 0; \tag{2.4}$$

$$\frac{\partial Q(x,t)}{\partial t} + \frac{\partial}{\partial x}\left[\frac{Q^2(x,t)}{A(x,t)}\right] + gA(x,t)\left(\frac{\partial Y(x,t)}{\partial x} + S_f(x,t) - S_b(x)\right) = 0. \tag{2.5}$$

In (2.4)-(2.5), symbols g, $S_b(x)$ and $S_f(x,t)$ represent respectively the gravity acceleration, the bed slope along the direction x and the friction slope modeled with the Manning formula. To complete the SVEs, initial and boundary conditions are needed. The initial conditions are yielded by $(Q(x,0), Y(x,0))$, for all $x \in [0,L]$, with L the length of the channel, whereas the boundary conditions are given by $Q(0,t)$, $Q(L,t)$, $Y(0,t)$ and $Y(L,t)$. Note that a closed-form solution of the SVEs, in general, is not available due to the presence of nonlinear terms. Therefore, several models have been developed starting from Saint-Venant equations in order to describe the dynamics of the open- channels. In the following the ID and the IDZ model are dealt with in detail.

2.3 Integral delay model

The Integrator Delay (ID) model was proposed for the first time by Schuurmans [14], it describes canal including the phenomenon known as backwater. In particular, the channel flow is approximated as uniform in the first segment, for $x \in [0, x_1]$. In this part the water depth is constant and it can be calculated in close-form using the inverse of Manning formula. In the second part, for $x \in [x_1, L]$, the flow is affected by the downstream boundary condition. In particular, if the outflow $Q(L,t)$ is small compared to the inlet flow, the water is slowed down and it is accumulated generating a rise of the level with respect to the normal depth, which is called backwater effect. In this part the water depth is assumed parallel to the x-axis, in contrast to the first part where water depth is parallel to the channel bed. The model equation is the following:

$$A_d \frac{\mathrm{d}Y_L(t)}{\mathrm{d}t} = Q\left(0, t - \tau_d\right) - Q(L,t). \tag{2.6}$$

where A_d is the integrator gain and τ_d is a delay, that is the time needed for upstream flow perturbation to reach the end of a channel. Looking (2.6), a simple interpretation of the model can be made. This model states that a downstream height variation is generated if inflow and outflow are different. For example, if there is an increment of input flow and the outflow does not adapt, this leads to an increase in the water level after a time delay of τ_d. Conversely, with a constant input, if the outflow increases the downstream water level is reduced. However, this model has some weaknesses: even if the parameters of ID model (2.6) can be calculated with closed-form equation, the original method proposed by Schuurmans may lead to a bad approximation of the system's dynamics. In the next paragraph, it is presented a model that gives a more accurate approximation of the open-channel dynamics preserving the simplicity of the ID model.

2.4 Integrator delay zero model

The ID model introduced above is extended by the so-called integrator delay zero (IDZ) model introduced by Litrico et al. [13]. The latter is able to capture the main physical behavior of the open-channel dynamics as the backwater effect and its parameters can be computed analytically from the physical parameters of the system. In addition, IDZ model overcomes some weaknesses of the ID model:

- It provides more accurate values of the delays and the integrator gains which are the key parameters describing the dynamics of the system;
- It adds a zero to the model transfer function to obtain a better fit in high frequencies;
- Improves the ID backwater profile approximation by modelling the water height in the backwater part as no longer parallel to the x-axis, but linearly variable along the direction of flow.

The first assumption done by this model is the backwater profile approximation: it is an approximation of the water depth along the entire length of the channel. In figure 2.2, a continuous line shows the real water height, while a dashed line represents the approximation made by the model. In particular, along the first part for $x \in [x_1, L]$, the height and flow are assumed constant. This type of flow is called uniform, its advantage is that the height, also called Y_n, can be calculated analytically from the flow $Q(0,t)$ (see paragraph A.1). The second portion the flow is characterised by the backwater effect: the height is no longer uniform, but grows linearly as x increases, in particular at the point $x = x_1$ takes value Y_n while for $x = L$ takes value Y_L. In addition, since the IDZ model is derived from the SVEs, it inherits the assumptions on which they are derived. These assumptions are reported in the list 2.2. In addition to these, it is assumed that the bed slope $S_b(x)$ is considered constant over the channel length, so $S_b(x) = S_b$.

The Integrator Delay Zero models describes how the levels $Y(L,t)$ and $Y(0,t)$ are related to the upstream and downstream discharge $Q(0,t)$ and $Q(L,t)$ using

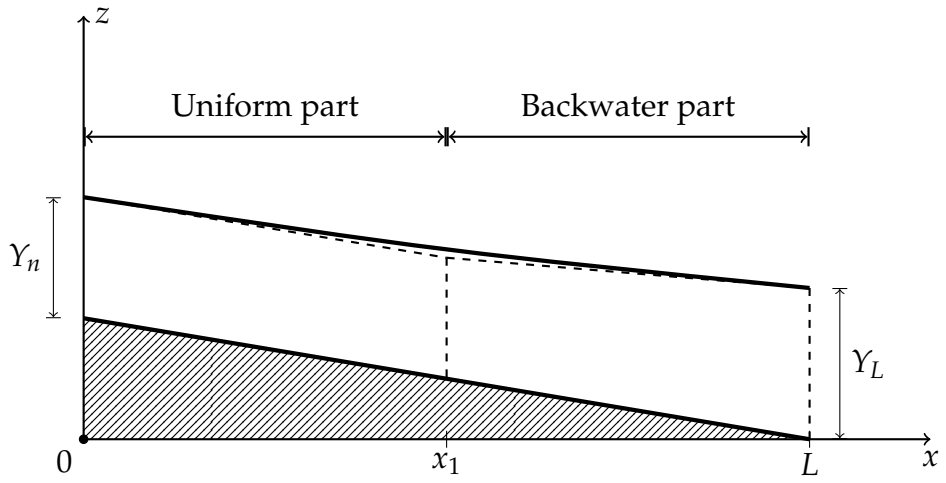

Figure 2.2: Lateral section of a open channel with it backwater profile $(-)$ and its approximation $(--)$.

two ordinary differential equations with input delays. This model considers small deviations of hydraulic variables from initial states of the system represented by the initial conditions. The deviations from these values are denoted with small letters:

- $q(0,t)$ and $q(L,t)$ stand for the deviations of upstream and downstream discharges respectively from $Q(0,0)$ and $Q(L,0)$;
- $y(0,t)$ and $y(L,t)$ stand for the deviations of upstream and downstream water depths respectively from $Y(0,0)$ and $Y(L,0)$;

The equations of IDZ model are reported below, the first one describes the dynamics of $y(L,t)$:

$$\begin{cases} A_d \frac{dh(t)}{dt} = q\,(0, t-\tau_d) - q(L,t) \\ y(L,t) = h_L(t) + p_{21}\, q\,(0, t-\tau_d) - p_{22}\, q(L,t). \end{cases} \tag{2.7}$$

where $h(t)$ is an auxiliar variable initialized as $h(0) = 0$, the delay τ_d acting on the upstream discharge $q(0,t)$ represents the time need to input flow to reach the downstream end of channel. The parameter A_d is called backwater area, while p_{12} and p_{12} are coefficients that approximate the high frequency behavior of the system. The second equation describes the dynamics of $y(0,t)$:

$$\begin{cases} A_u \frac{dh(t)}{dt} = q\,(0,t) - q(X, t-\tau_u) \\ y(0,t) = h(t) + p_{11}\, q\,(0,t) - p_{12}\, q(X, t-\tau_u), \end{cases} \tag{2.8}$$

Similarly to the previous equation, $h(t)$ is an auxiliar variable initialized as $h(0) = 0$, A_u is called upstream backwater area, while the delay τ_u is the time required for a perturbation $q(L,t)$ to travel from the downstream to the upstream end. Finally p_{21} and p_{22} are coefficient that represent the high-frequency behavior of the system. Note that the parameters A_u and A_d control how much of the model output ($[y(0,t),\ y(L,t)]$) is generated due to the accumulation of water ($q_{in} - q_{out}$), for this reason they are also called integrator gain. Note that these parameters are positive, to demonstrate this, consider as example A_d. If it was negative, with an accumulation of water in the channel (i.e. $q_{in} - q_{out} > 0$), it would have $\dot{h}(t) < 0$, that implies a reduction of the water level. This does not make physical sense, so A_u and A_d have to be positive coefficients. Also the delays τ_u and τ_d are positive coefficients, otherwise the state of the system at a certain time t would depend on future values of the input and therefore the model would not be causal.

To sum up, this model calculates the value of the heights $Y(0,t)$ and $Y(L,t)$ given $Q(0,t)$ and $Q(L,t)$. In particular, the model is able to calculate the variation of these heights (w.r.t the initial value) due to the accumulation of water. In addition, through the delay parameters τ_u and τ_d, the model considers that the flow takes time to propagate along the channel. The interpretation of τ_d is intuitive: it is defined as the time required for a perturbation of input flow to have an effect on the downstream height $Y(L,t)$. The parameter τ_u is defined as the time required for a perturbation $q(L,t)$ to travel from the downstream to the upstream end. For example, given a channel in equilibrium with a constant height over time and an input flow equal to the output flow, if the outflow is increased (i.e. $q(L,t) > 0$), the IDZ model predict that the level $Y(L,t)$ starts to decrease instantaneously. Consequently the decrease of water depth propagates backwards along the channel until, after a time τ_u, also $Y(0,t)$ is affected by the perturbation. In addition, the IDZ has four parameters called $[p_{11}, p_{12}, p_{21}, p_{22}]$ that represent the high-frequency behaviour of the actual system. Note that IDZ model can be represented in the Laplace domain with a 2×2 transfer matrix $P(s)$:

$$\begin{bmatrix} y(0,s) \\ \\ y(X,s) \end{bmatrix} = \underbrace{\begin{bmatrix} \left(\frac{1}{A_u s} + p_{11}\right) & -\left(\frac{1}{A_u s} + p_{12}\right) e^{-\tau_u s} \\ \\ \left(\frac{1}{A_d s} + p_{21}\right) e^{-\tau_d s} & -\left(\frac{1}{A_d S} + p_{22}\right) \end{bmatrix}}_{\boldsymbol{P}(s)} \begin{bmatrix} q(0,s) \\ \\ q(X,s) \end{bmatrix} \tag{2.9}$$

Note that for low frequency ($s \to 0$), the behavior of the transfer matrix is dominated by the integrator and the delays. For high frequencies ($s \to \infty$), the delay and the constant gains $[p_{11}, p_{12}, p_{21}, p_{22}]$ are predominant in the transfer matrix elements. To summarise, all model parameters are shown in the table 2.1 with the respective units of measurement. To complete the IDZ model, initial and boundary conditions are

Acronym	Description
A_d $[m^2]$	Downstream equivalent backwater area
A_u $[m^2]$	Upstream equivalent backwater area
τ_d $[s]$	Downstream propagation delay time
τ_u $[s]$	Upstream propagation delay time
$[p_{11}, p_{12}, p_{21}, p_{22}]$ $[s/m^2]$	High frequency gains

Table 2.1: List of IDZ model parameters with their units of measurement.

needed. In general, the initial conditions are the values of the flow depth $Y(x,0)$ for

each $x \in [0, L]$ and the flow $Q(x, 0)$ for each $x \in [0, L]$. However, it is sufficient to know only the boundary conditions $Y(0, 0)$ and $Y(L, 0)$ from which $Y(x, 0)$ can be calculated for each x thanks to the backwater profile approximation introduced in figure B.2. In addition, it is assumed that, at initial time, the flow in the channel is steady and constant along the entire length of the channel, so $Q(x, 0) = Q_0$, $\forall x \in [0, L]$. Note that, given Q_0, the upstream water height can be calculated in closed form as $Y(0, 0) = Y_n$, where Y_n is the normal depth of the flow Q_0. So, in conclusion, the initial conditions are characterised only by the two quantities $[Q_0, Y(0, L)]$ that has to be known a priori.

Note that for the IDZ model, the initial conditions are not used only to solve the model equations, but also for the calculation of its parameters. The calculation of the model parameters starts from the SVEs, in this thesis the complete procedure is reported in appendix B.3; whereas, in the following list, it will be described briefly underlining the fundamental aspects that must be taken into account when the model is used.

1. The SVEs are linearised on the initial conditions of the system $[Q_0, Y(0, L)]$;
2. The channel is considered as union of two channel: one with uniform flow and the another one with backwater flow (i.e subject to the backwater effect), the model parameters are calculated separately for both channels;
3. The global IDZ model is obtained merging the parameters of both channels with a interconnection rules.

Note that, since the parameters of IDZ model are calculated by linearising the SVEs at a given steady flow regime, it can be assumed that the model is a good approximation of the real system as long as the state does not deviate too much from the initial state $[Q_0, Y(0, L)]$. In long-term simulations the variables can have large variations, so it is necessary to repeat the linearisation periodically to maintain a reasonable approximation error.

The others quantities needed to complete the IDZ model are the boundary conditions. In particular, it has been seen that the IDZ model calculate $Y(0, t)$ and $Y(L, t)$ (i.e the boundaries condition of water depth). To do that it has to know the inflow $Q(0, t)$ and outflow $Q(L, t)$ for each t , i.e the boundary conditions of flow. The value of $Q(0, t)$ has to be known a priori, for example it can be set equal to the outflow of a upstream channel connected to the inlet of the current channel. For $Q(L, t)$ there are two possibilities:

- Similarly to the inflow, it is a value known a priory. This is the case when the outflow is regulated by a water pump which imposes a fixed discharge flow.
- The output flow can be regulated by a hydraulic structure such as a gate or weir. In this case, the outflow can be calculated as a function of $Y(L,t)$.

For the latter case, it is possible to calculates the relationship between $Q(L,t)$ and $Y(L,t)$. In general, these structures are modeled by static non-linear equations that provides a the relation between $Q(L,t)$ and $Y(L,t)$. In order to include these equations in the IDZ model, they have to approximates as local linear relations between $Q(L,t)$ and $Y(L,t)$. These relations are obtained by linearizing the hydraulic equations around a given working point obtaining the following equation:

$$Q(L,t) = f\left(Y(L,t), Y_2(0,t), H\right) \simeq K_v Y(L,t), \tag{2.10}$$

where $Y(L,t)$ and $Q(L,t)$are the flow state of the channel at the upstream side of the structure and $Y_2(0,t)$ is the upstream water height of a channel at the downstream side of the structure. The parameter H represents, for the gate, the height of the hole or, for the weir, the height of the barrier. A more detailed description of this quantities and the equations that model this structures are reported in appendix A.5. As a consequence, the IDZ model with the linearised hydraulic structure equation is given by

$$\begin{cases} A_d \frac{dh(t)}{dt} = q\left(0, t-\tau_d\right) - K_v y(L,t) \\ y(L,t) = h_L(t) + p_{21} q\left(0, t-\tau_d\right) - p_{22} q(L,t). \end{cases} \tag{2.11}$$

From this approximated model, it is possible to study the effect of the hydraulic structure on the IDZ model dynamics. In order to that, it is assumed also that $p_{21} = p_{22} = 0\ s/m^2$, hence the model becomes:

$$A_d \frac{dy(L,t)}{dt} = q\left(0, t-\tau_d\right) - K_v y(L,t). \tag{2.12}$$

This simplification does not lead to a radical change of the IDZ model dynamics, indeed the parameters p_{21} and p_{22} give a small contribution compared to the integrator effect, which is the core of the model. The resulting differential equation can be written in state-space form as:

$$\dot{y}(L,t) = -\frac{K_v}{A_d} y(L,t) + \frac{1}{A_d} q\left(0, t-\tau_d\right). \tag{2.13}$$

In this form, it can be seen that the eigenvalue of the system is $\lambda = -\frac{K_v}{A_d}$. It is also the pole of the corresponding transfer functions, since the latter does not have zeros, so there cannot be zero-pole cancellations. Note that λ depends on the parameter K_v which is a function of the geometrical parameters of the gate, hence the dynamics of the system depends on the gate state. In particular, it is interesting to study the BIBO stability of the system. This form of stability is sufficient because the target of this study is to analyse the drainage capacity of a open channel network in the case of inflow increase generated by a water storm. Even if these events are intense and the volume of the dropped water can be large, it is reasonable to assume that the flow generated is bounded in amplitude and in time. Therefore, it can be said that the system is subject to a bounded input. Furthermore, under stress conditions, it is expected that the water height in the channel grows inevitably. The important aspect is that this growth is bounded below the maximum height of channel banks in order to avoid an overflow. From the point of view of the IDZ model, this objective is equivalent to require a bounded output (bounded water height) given a bounded input (bounded waters flow). In other words, it is required the BIBO stability of the system (2.13). Recall that, if all poles with positive or null real part are crossed out by the zeros of the transfer function and the remaining ones have strictly negative real part, then the system is BIBO stable. The systems (2.13) has a single eigenvalue that corresponds to the pole of its transfer functions, since there are no zero-pole cancellations. Therefore the system is BIBO stable if the pole have negative real part. In this case, the pole depends on the parameter A_d, which is strictly positive by definition, and on the parameter K_v. If it is considered a channel with an undershot gate in free flow condiction at the downstream end, the parameter K_v is:

$$K_v = \frac{gC_dWH}{\sqrt{2gY_1}}, \tag{2.14}$$

where W is the gate width which is fixed, while H is the height of the gate hole which can be controlled. Note that this parameter is always positive since all the variables on which it depends are positive. The only exception is for $H = 0\ m$, in this case $K_v = 0$ and it is the only case in which the system is not BIBO stable since $\lambda = 0$. For $H > 0$ the system 2.12 is BIBO stable. In particular, increasing the gate opening H the negative pole becomes larger in absolute value and thus the system converges faster to the final state.

2.5 Numerical results

In this section, the continuous and discrete time versions of the IDZ model are validated, also the effect of an hydraulic structure on the system dynamic is tested. The discrete IDZ model is introduced because it will be used later in the model of the open-channels network. This model cannot be implemented in continuous time because it include non-linearities as the backwater effect and hydraulic structures models, so, it is necessary to discretize all its components including the IDZ model. In order to test the model, two canals are used: both present a trapezoidal cross-section and their parameters are reported in the table 2.2. Also it is reported the quantity Y_{max}, i.e the maximum value of that the water height can reach after which an overflow occurs. The parameters of the channel 1 are chosen to represent

	$L[m]$	$m[\,]$	$B[m]$	$Y_{max}\ [m]$	$S_b[\,]$	$n\ [m^{1/3}/s]$
Canal 1	500	1.5	2	2.5	0.001	0.02
Canal 2	500	1.5	2	2.5	0.0001	0.05

Table 2.2: List of the channels parameters used in the simulation.

an artificial channel: its bed is made of concrete (i.e. with a Manning's number of $n = 0.02\ m^{1/3}/s$) and a bed slope $S_b = 0.001$. This means that there is a vertical drop of 1 m on a channel of length 1 km.The second channel represents a natural watercourse with the presence of vegetation. This channel is considered flat because, in natural watercourses, the transport of debris is frequent and it is possible that there is an accumulation of material which may reduce original bed slope. Indeed the second canal has a bed slope $S_b = 0.0001$. This means that its bed has a vertical drop of 1 m every 10 km. On other words, on a channel with a length of $L = 500\ m$ there is a vertical drop of 5 cm. Such value is, in practice, negligible, but it is used for channels that is considered flat in order to avoid simulation errors due to division by zero. Finally, the parameter B is the bottom width of the trapezoidal cross-section, while m is a parameter that describes the slope of the the cross-section. For more information the reader is referred to the appendix B.4. In this section, some assumptions are made in addition to those presented in section 2.4. For completeness all assumptions done for these simulations are listed below:

- The input flow at the initial instant is $Q(0,0) = Q_0 = 2\ m^3/s$, while for $t \neq 0\ s$, $Q(0,t) = Q_0 + \Delta Q$, with $\Delta Q = 1\ m^3/s$, in this way the input is a step signal;

- The outflow at the initial instant is $Q(L,0) = Q_0$. For $t \neq 0\ s$, $Q(L,t)$ is equal to Q_0 in the first experiment and it is regulated by a hydraulic structure for the others simulation;
- In section 2.4 it is assumed that $Y(0,0) = Y_n$, while $Y(L,0)$ is known a priori. In this case, the channel height at the beginning of simulation is assumed constant, so $Y(0,0) = Y(L,0) = Y_n$. In general, for the IDZ model, it hold that $Y(L,0) \neq Y_n$;
- The bed slope $S_b(x)$ is considered constant over the channel, so $S_b(x) = S_b$;
- To perform tests with an hydraulic structure, a submerged gate is used, which has a width $W = 1.5\ m$ and height of the stream aperture H with variable dimension ($0 < H < 2\ m$);
- It is assumed that at downstream end of the channel, beyond the hydraulic structure, there is a tank with infinite capacity and with constant water height. This assumption is made to avoid that $Q(L,t)$ is influenced by the state of the tank which, if it fills up, it affects the dynamics of the channel under analysis. In particular, the height of the water in the tank is called $Y_2(0,t)$ and it is assumed constant in time , i.e $Y_2(0,t) = Y_2$.

To calculate the parameters of the IDZ model, it is used the function provided in the multimedia material available in the book [24]. This function calculates the parameters of the model in the following way:

1. It receives as input the initial condiction and the channel parameters reported in table 2.2;
2. It calculates the normal depth solving the inverse Manning's formula A.3 and the other parameters that describe the backwater profile;
3. It calculates the parameters of IDZ model using formulas reported in appendix B.3.

Note that, in the simulations presented in this section, the model parameters are calculated only at the initial instant and they are not updated periodically during simulation time. This procedure is not entirely correct because IDZ model are calculated by linearising the SVEs at a given steady flow regime, so the model can be considered a good approximation of the real system as long as the state does not deviate too much from the initial work point. Otherwise, it is necessary to re-compute

the parameters periodically during the simulation to ensure a reasonable approximation. Also recall that the parameters can be calculated only when the system is in steady state conditions, so when the flow and heights are constant over time. This implies that it is not possible to recalculate the parameters periodically, but it is necessary to wait until the system reach a new steady state after a transient phase generated by flow perturbation.

2.5.1 Continuous-time IDZ model

In this simulation, the continuous-time IDZ model is tested. In particular, it is assumed that the input flow is $Q_0 = 2\ m^3/s$ and the flow perturbation is $\Delta Q = 1\ m^3/s$ for both channels. The outflow $Q(L,t)$ is constant and equal to Q_0 for each t, so that, at the initial time, the channel is in at the equilibrium state with the inflow equal to the outflow and with a uniform height over its length. However, the outflow does not adapt to the perturbation ΔQ; therefore, it is expected an accumulation of water over time and a consequent increases of the water depth.

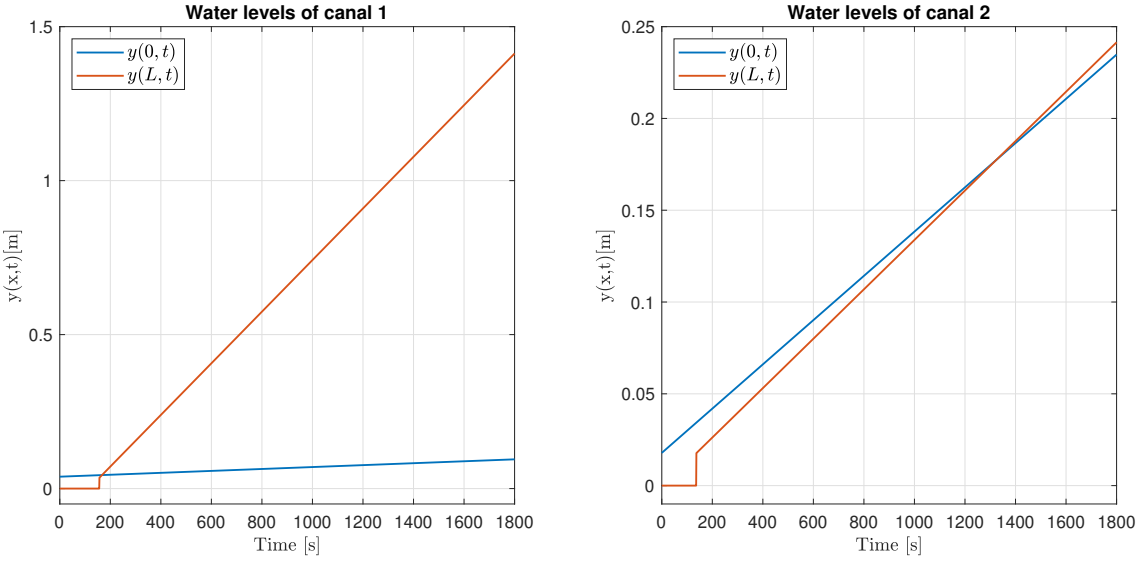

(a) (b)

Figure 2.3: Step responses of continuous-time model with fixed outflow Q_0: (a) Step responce for channel 1 , (b) Step responce for channel 2.

In figure 2.3, the variables $y(L,t)$ and $y(0,t)$ are plotted for both tested channels. Note that, for a first period of the simulation, $y(L,t)$ does not change. This is due to the propagation time delay of the water flow τ_d; indeed, the perturbation ΔQ takes time to propagate along the channel and thus its effect on $y(L,t)$ is not immediate.

The values of these parameters are reported in the table 2.3 along with the other IDZ parameters. After this period of time, $y(L,t)$ value grows linearly. This growth is due to integration effect modeled by the IDZ model: for both channels, the outflow is constant in time over the entire simulation, so it does not adapt to the increase of inflow and, hence, there is an accumulation of water in the channel. Figure 2.3 also shows the variable $y(0,t)$. Note that it starts to increase immediately from $t = 0$; indeed, according to the IDZ model, the perturbation $q(0,t)$ acts on $y(0,t)$ without delay. Note that in this figures the effect of $q(L, t-\tau_u)$ is not visible because the outflow is constant in time, so its perturbation is $q(L,t) = 0\ m^3/s$. An important aspect to note is that, in channel 1, $y(0,t)$ grows more slowly than $y(L,t)$, instead, in channel 2, the two heights grow almost equally. This is due to the slope of the channel; in particular, the second channel is flat, so the water grows uniformly along it. Furthermore, since the growth is distributed, it leads to smaller increase of water depth, indeed, for the channel 2, at the end of simulation, one has $y(L,t) = 0.24\ m$. In channel 1, since the bed slope is greater, the water tends to accumulate towards the downstream end of the channel, then $y(L,t)$ grows more than channel 2; indeed, at the end of simulation one has $y(L,t) = 1.4\ m$. In addition to slope, also the friction force influences the dynamics. Its effect is smaller for the channel 1 w.r.t the channel 2 because the channels beds are made of different material. In particular, channel 1 has a concrete bottom which, according to the Manning formula, produces less friction than channel 2 that has a more irregular bottom and then has a bigger friction effect. This difference in friction affects the height of the water in the two channels. In particular, due to the higher friction force, the water flow in the channel 2 is slower to propagate than channel 1. This leads to a bigger propagation time in the channel 2 and it reduces the water accumulation at the downstream end.

	$Y_n\ [m]$	$A_d\ [m^2]$	$A_u\ [m^2]$	$\tau_d\ [s]$	$\tau_u\ [s]$	$[p_{11}, p_{12}, p_{21}, p_{22}]\ [s/m^2]$
Channel 1	0.69	596	$1.59\ 10^4$	156	358	[0.077, 0.003, 0.069, 0.19]
Channel 2	1.95	$3.71\ 10^3$	$4.18\ 10^3$	136	153	[0.032, 0.027, 0.029, 0.034]

Table 2.3: Parameters of the IDZ model for the two analysed channels.

In table 2.3, the parameters of the IDZ model for the two channels analysed in this section are reported. In the following, such a models will be discussed and compared with the observations made previously. The parameters A_d and A_u regulate the derivative of the output ($[y(0,t),\ y(L,t)]$). From the equations (2.8)-(2.7), it is observed that as these parameters increase, the derivative of the heights is smaller and therefore heights grow more slowly. For channel 1, A_u and A_d have different

values, indeed, from the figure 2.3, it can be observed that the $y(L,t)$ grows faster than $y(0,t)$. For channel 2, A_d and A_u have similar value, indeed, from the figure 2.3 it can be observed that $y(0,t)$ and $y(L,t)$ grows in the same way.

Furthermore, the parameters τ_d and τ_u describe the propagation time of the flow perturbation inside the channel. The parameter τ_d is defined as the time required for an inlet flow disturbance to have an effect on the downstream height $Y(L,t)$. The parameter τ_u is the time required for a perturbation $q(L,t)$ to travel from downstream to upstream and to affect the downstream height $Y(0,t)$. A remarkable aspect is that the two channels have a similar τ_d even though the two channels have different slope. Indeed, channel 1 has a slope ten times greater than channel 2 and also it has a smaller friction effect. Therefore, it is expected that the flow is much faster in channel 1 than in channel 2. However, the parameters τ_d and τ_u describe respectively the propagation time of the flow perturbation $q(0,t)$ and $q(L,t)$. As shown in the appendix B.3, τ_d is derived from the velocity of the perturbation that is $V_0 + C_0$, where V_0 is the velocity of flow Q_0, while C_0 is the celerity defined as the relative velocity of the perturbation respect to the flow Q_0. Therefore is the velocity of the perturbation w.r.t a reference frame moving with the same speed and direction as the flow Q_0. In particular, C_0 increases as the height Y_n of flow Q_0 increases. Therefore, even if flow Q_0 is faster in channel 1 than that in channel 2, C_0 is bigger in channel 2 than that in channel 1. This leads to similar delays in the two channels. Instead, the parameter τ_u depends on $V_0 - C_0$, because it represents the propagation time of the perturbation $q(L,t)$ moving in the opposite direction to the flow Q_0. In this case, the two channels have a different value of τ_u, indeed channel 1 has a steeper slope than channel 2. This implies that the flow velocity V_0 is greater in the channel 1 than in the channel 2. Therefore the perturbation $q(L,t)$, that moves in the opposite direction to the flow Q_0, takes a longer time to propagate towards the upstream end in channel 1 w.r.t channel 2 because it has to oppose to a faster flow.

2.5.2 Discrete-time IDZ model

In this simulation, the discrete-time version of IDZ model is used. This version is introduced because it will be used for the channel network model. Indeed due to the non-linearities introduced by the presence of channel junctions, it is necessary to implement the network model with a discrete approach. The IDZ model will be used to model each single straight channel of the network, consequently, it will also have to be discretized. In order to discretize the IDZ model, the backward Euler

approximation is used, in particular the derivative is approximated as:

$$T_s \frac{\partial h(x,t)}{\partial t} = h(x, t + T_s) - h(x, t); \tag{2.15}$$

where T_s is the sampling time. This method is used because, once applied to the IDZ model (2.7) -(2.8), the discrete state-space representation of the model is obtained. These equations are reported below:

$$\begin{cases} h(L, t + T_s) = h(L, t) + \frac{T_s}{\hat{A}_d}(q\,(0, t - \tau_d) - q(L, t)) \\ y(L, t) = h(t) + p_{21} q\,(0, t - \tau_d) - p_{22} q(L, t); \end{cases} \tag{2.16}$$

$$\begin{cases} h(0, t + T_s) = h(0, t) + \frac{T_s}{\hat{A}_u}(q\,(0, t) - q(L, t - \tau_u)) \\ y(0, t) = h(t) + p_{11} q\,(0, t) - p_{12} q(L, t - \tau_u). \end{cases} \tag{2.17}$$

Also, it is assumed that the output flow of the channel is regulated by an undershoot gate. Assuming that the gate is under submerged-flow conditions for the entire simulation (i.e. the downstream flow of the gate is subcritical), the equation that models its behaviour is:

$$Q(L, t) = C_d W H \sqrt{2g(Y(L, t) - Y_2(0, t))}; \tag{2.18}$$

where W is the width of gate hole and C_d is the discharge coefficient that is set to 0.6. These variables are constants over time, while $Y(L, t)$ and H can vary. In particular, H is the height of the gate hole, it can vary because the gate bulkhead is usually movable and it is used to regulate the flow. In this case, H is considered constant during each single simulation, but it is changed for different simulations. Finally, $Y_2(0, t)$ is the height of water of the reservoir at the downstream side of the gate, as already introduced, it is considered constant over time. Note that the input of IDZ model is $[q(0, t),\ q(L, t)]$: it is the variation of flows w.r.t. the initial value Q_0. The value of $q(0, t)$ is know, while $q(L, t)$ is regulated by an undershoot gate and can be calculated as:

$$q(L, t) = Q(L, t) - Q(L, 0), \tag{2.19}$$

where both $Q(L, t)$ and $Q(L, 0)$ can be calculated with (2.18). Note that the IDZ model assumes that $Q(L, 0) = Q_0$. With the implementation of the gate, it is necessary that this assumption remains verified. In particular, it is necessary that:

$$Q(L, t) = C_d W H \sqrt{2g(Y(L, t) - Y_2(0, t))} = Q_0. \tag{2.20}$$

To do this, Y_2 is used. Its value is chosen so that (2.20) is verified, i.e. $Q(L,0) = Q_0$. This is necessary because the data used are chosen to be plausible, but they are not derived from a measurement of a real system. Then to couple channel and junction, it is necessary to have a degree of freedom, in this case Y_2, to guarantee continuity of the system state. In this simulation, the sampling time used is $T_s = 1[s]$. This value is chosen because it does not alter the dynamics of the system. If a bigger value of T_s is choosen then the step response of the discrete IDZ model can be dramatically different from the continuous one even to the point of losing physical meaning. Later, the effect of T_s on the model is studied.

In the simulation, channel 1 and 2 are tested with an initial input flow $Q_0 = 2\ m^3/s$ and a flow perturbation of $\Delta Q = 1\ m^3/s$. Furthermore, it is assumed that the outflow is regulated by a submerged gate with a constant width $W = 1.5\ m$. The heights of the gate hole are different for each channel because the water depth at the initial instant are different. In particular, for the channel 1, $Y(0,t) = Y_n = 0.69\ m$, while for channel 2 $Y(x,t) = Y_n = 1.95\ m$. Note that if the heights of the gate hole H is greater than the water level, the flow dynamics is not influenced by the hydraulic structure, so, for each channel, the value of H used in the simulation has to be smaller than that Y_n. In particular, for channel 1, $H = [0.75, 1, 1.5, 2]\ m$, while for channel 2 one has $H = [0.2, 0.3, 0.5, 0.7]\ m$.

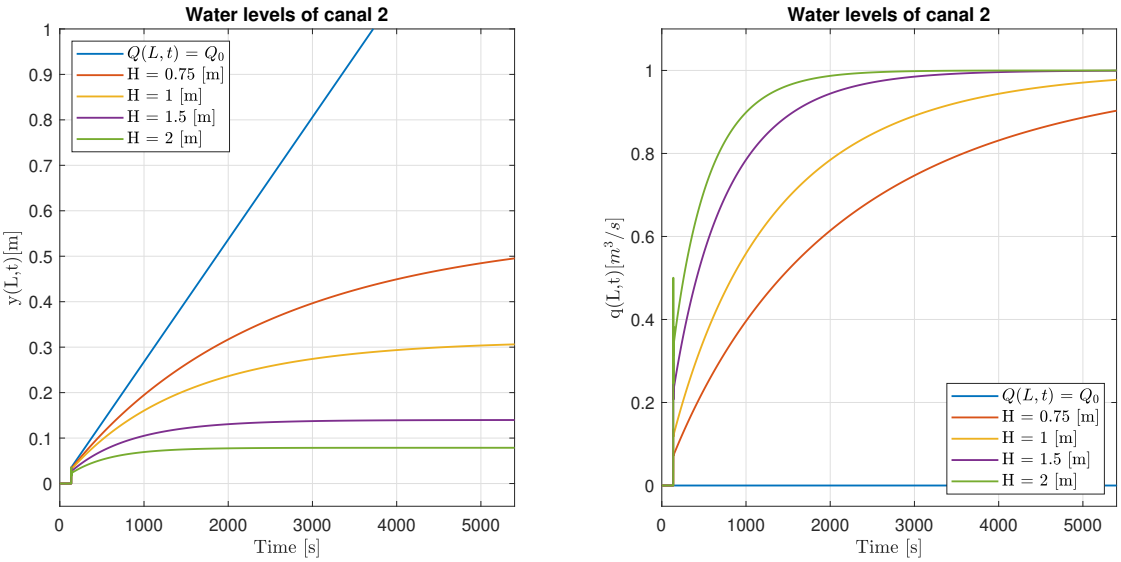

(a) (b)

Figure 2.4: Step responses of discrete-time model simulation for channel 2 for each value of H: (a) Plot the value of $y(L,t)$; (b) Plot the value of $q(L,t)$.

Figure 2.4.a shows the values of $y(L,t)$ of the channel 2 for each value of H. It is

also shown the case in which the outflow $q(L,t) = 0$, i.e. when the outflow remains constant at its initial value $Q(L,t) = Q_0$. Note that the flow depth $y(L,t)$ increase linearly while, in the case the output flows is controlled by the gate, for any value of H, $y(L,t)$ stabilise at a steady state value. This result has already been presented in the previous paragraph. In particular, it has been shown that the IDZ model integrated with the linearised gate model always had a negative pole if $H > 0$. However, in practice, even if the system stabilises, before $y(L,t)$ stabilises at a steady state, its step responce may take a long time and it may rise above the maximum level Y_{max} causing an overflow. Table 2.4 shows values at which the step response converge and their settling time with a tolerance of 2%.

Channel 1			Channel 2		
H	y_{max} [m]	$t_{s,2\%}$ [min]	H	y_{max} [m]	$t_{s,2\%}$ [min]
$Q(L,t) = Q_0$	-	> 120	$Q(L,t) = Q_0$	-	> 120
0.2	-	> 120	0.75	0.54	> 120
0.3	3.38	107	1	0.31	97
0.5	1.26	65	1.5	0.14	48
0.7	0.64	38	2	0.07	31

Table 2.4: Collection of step responses parameters of discrete-time model simulation.

Note that as H increases, $y(L,t)$ converges to a smaller value. In particular, for $H = [1, 1.5, 2]\ m$, the final height is smaller than Y_{max}. For $H = 0.75\ m$ the height fails to converge within the length of the simulation, which is 2 hours. In this latter case, according to the theory, the system converges, however it is not able to do so during the simulation and in any case the water level exceeds the maximum allowed generating an overflow. From the table 2.4 it is also observed that as H increases, $t_{s,2\%}$ decreases until arriving for $H = 2\ m$ at $t_{s,min} = 31\ min$. Note that, since in practice H has a maximum value, consequently the settling time has a minimum value. In Figure 2.4.b, it is shown the output flow $q(L,t)$: note that for every value of H (except for the first case $Q(L,t) = Q_0$), it stabilises at 1 m^3/s, which is the exact value of the perturbation ΔQ. This is a further confirmation of the previous statement, i.e. thanks to the gate, if the system is subject to an increase of the inflow it stabilises at a new equilibrium point in which inflow and outflow are equal, therefore water depth $y(x,t)$ becomes constant over time. Note that for each simulation the height of the gate hole H is constant, but the output flow increases over time. This may seem counter intuitive, but it is due to water pressure. Indeed, it can be seen in figure 2.4.a that $y(L,t)$ increases over time and this leads to an increase of upstream

pressure of the gate and therefore an increase of the inflow. Figure 2.5 shows the values of $y(L,t)$ and $q(L,t)$ of channel 1. Note that the responses are similar to those obtained with the 2 channel, but they are obtained with different value of H. This is due to the fact that in channel 1 has a greater slope the water tends to accumulate towards the downstream part faster respect to channel 2. This also means that the upstream pressure of the gate increases faster than in the channel 2, which is flat and ,therefore, the water height increases more slowly. This generates bigger outflow in channel 1 w.r.t channel 2 with the same value of H.

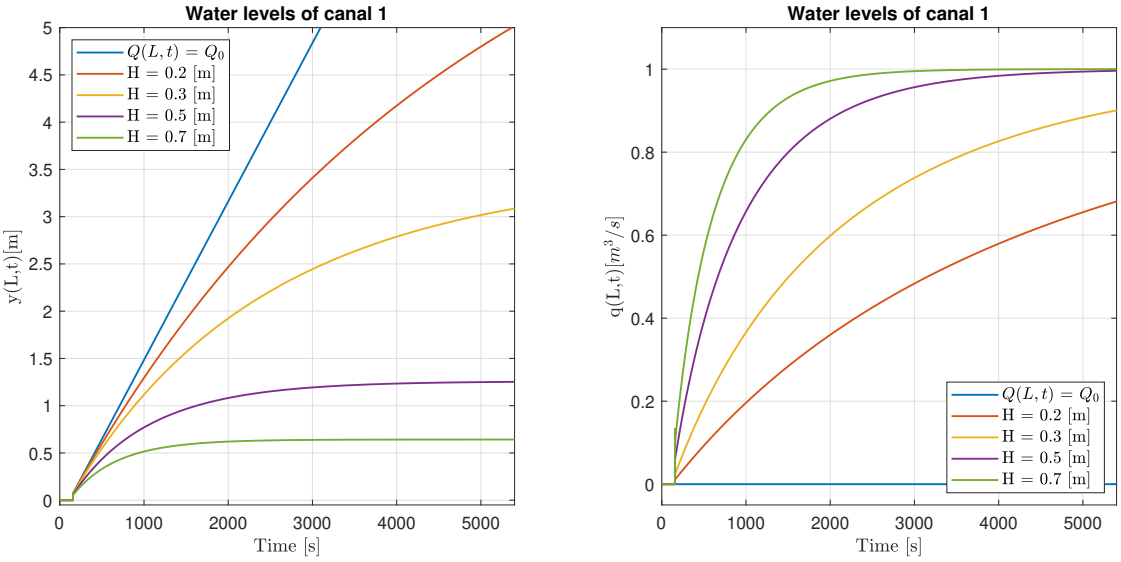

(a) (b)

Figure 2.5: Step responses of discrete-time model simulation for channel 1: (a) Plot the value of $y(L,t)$ for $H \in [0.2, 0.3, 0.5, 0.7]$ m; (b) Plot the value of $q(L,t)$ for $H \in [0.75, 1, 1.5, 2]$ m.

So far, it is discussed only the the dynamics of $Y(L,t)$ and not of $Y(0,t)$. This is due to the fact that the water tends to accumulate towards the downstream end of the channel because it is sloped, so in general, $Y(L,t) \geq Y(0,t)$. Since the objective of this thesis is to study the ability of the system to avoid overflow events, it is necessary to study the points in the channels where the water level is higher, so it is more interesting to study $Y(L,t)$ than $Y(0,t)$. For completeness, in figure 2.6 is shown the variable $y(0,t)$ for both channels. Note that $y(0,t)$ stabilises as $y(L,t)$. This is due to the fact that both depend on the difference between $q(0,t)$ and $q(L,t)$ with the appropriate delays. Consequently, given a constant inflow, the stability of $Y(L,t)$ and $Y(0,t)$ is depends on $Q(L,t)$, so in general, it is possible to say that if $y(L,t)$ is stabilized then $y(0,t)$ is also stabilized.

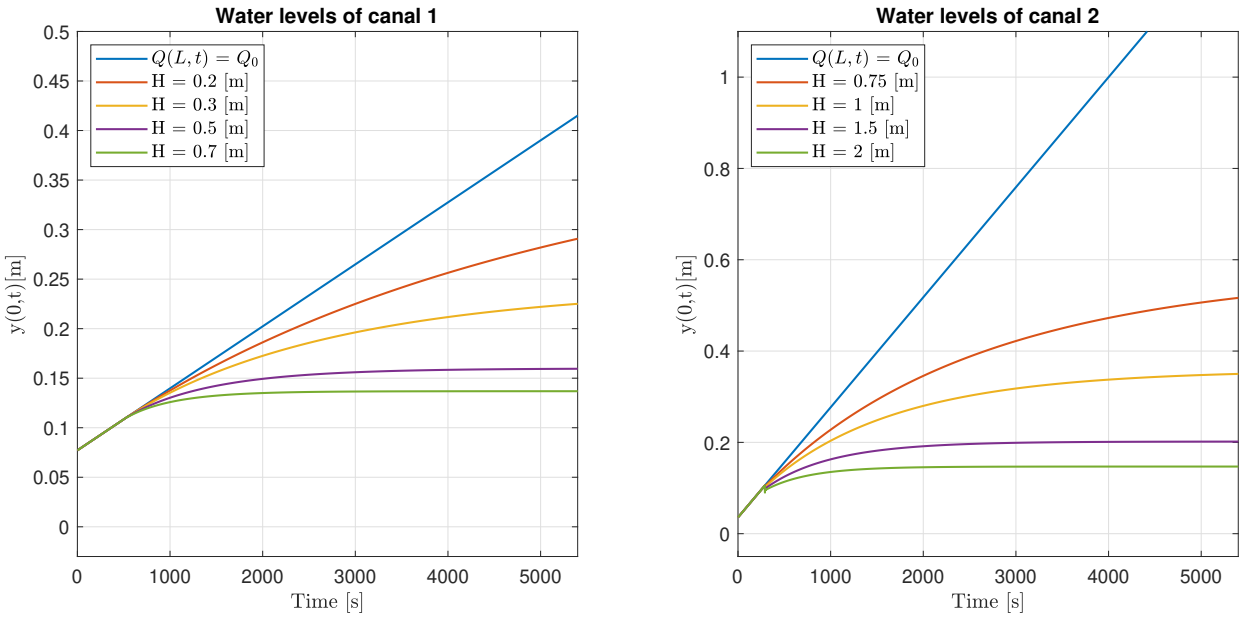

(a) (b)

Figure 2.6: Step responses of discrete-time model simulation (a) Plot the value of $y(0,t)$ for channel 1 (b) $y(0,t)$ for channel 2.

2.5.3 Sampling time study

In the following paragraph, the effect of sampling time on system dynamics is studied. To do that, it is assumed that the output flow of the channel is regulated by an undershoot gate in submerged flow condition. To analyse the effects of discretisation on the IDZ model, one may consider the equation of IDZ model (2.7) that describes the downstream flow depth $y(L,t)$ neglecting the high frequency behaviour of the model, i.e $p_{12} = 0$ and $p_{22} = 0$. To include the gate model (2.18) in this equation, it is linearized over the initial conditions $Y(L,0) = Y_n$. Then (2.18) can be approximated with:

$$q(L,t) \simeq K_v y(L,t), \text{ with } K_v = \frac{gC_dHW}{\sqrt{2g(Y_n - Y_2)}}. \tag{2.21}$$

Applying the discretisation rule and (2.21), the the simplified IDZ model equation (2.7) becomes:

$$y(L,t+T_S) = (1 - \frac{T_s K_v}{A_d}) y(L,t) + \frac{T_s}{A_d} q\left(0, t - \tau_d\right). \tag{2.22}$$

Note that the eigenvalue of this equation depends on the sampling time T_s. In particular, it is possible to calculate an upper bound for this parameter in order to guarantee the BIBO stability of the system. To do this, it is necessary that the pole of the system transfer function has a magnitude less than one (i.e it has to be inside the unit circle). For the system (2.22) this inequality can be written as:

$$|1 - \frac{T_s K_v}{A_d}| < 1 \quad \Rightarrow \quad 0 < T_s < \frac{2A_d}{K_v} = T_{s,MAX}. \tag{2.23}$$

Note that this upper bound is indicative because it is calculated using the parameter K_v. The latter is derived from the linearisation of equation (2.18) around the initial condiction of simulation and, therefore it is an approximation of the gate model. Furthermore, K_v depends on gate parameters that may vary over time. In particular, the height of the gate hole H can be modified to control the flow of the gate. In practice, this variable is limited within a range $H_{min} < H < H_{max}$, so, in order to have an upper bound of T_s robust to changes in H, it is possible to calculate it using the maximum value $H = H_{max} = 2\ m$. However, this upper bound is only able to guarantee the stability of the system and this is not sufficient. Indeed, the goal is to find a sampling time such that the discrete IDZ model reasonably approximates the continuous one. In order to do this, it is necessary to test the model with different T_s values and choose the most suitable one. In particular, its value it should not be too high since it distorts the system dynamics but, at the same time, it does not have to be too low, since it increases the computational time of the simulation that can be a problem, especially if many channels are simulated simultaneously as in the case of the network model.

As an example, in this paragraph, the IDZ model (2.16)-(2.17) is tested using channel 2 with the same setting of previous simulations, so with an input flow being $Q_0 = 2\ m^3/s$ and the flow perturbation being $\Delta Q = 1\ m^3/s$. At the channel end, there is a gate in submerged flow condiction that regulates the outflow $Q(L,t)$. For this experiment H is fixed to 2 m.

Figure 2.7 shows the variable $y(L,t)$ obtained with the discrete IDZ model for different sampling times $T_s = [1, 60, 120, 360, 480]\ s$. From 2.7, two important phenomena can be observed: the first is that the delay τ_d varies as the sampling time varies. This is due to the fact that, in the implementation of the discrete model, the delays τ_d and τ_u are approximated as multiples of the sampling time T_s. In the case where T_s smaller or similar to τ the approximation error is small. If the sampling time is larger than the delay, i.e $T_s > \tau$, the delay is approximated to 1 discrete time

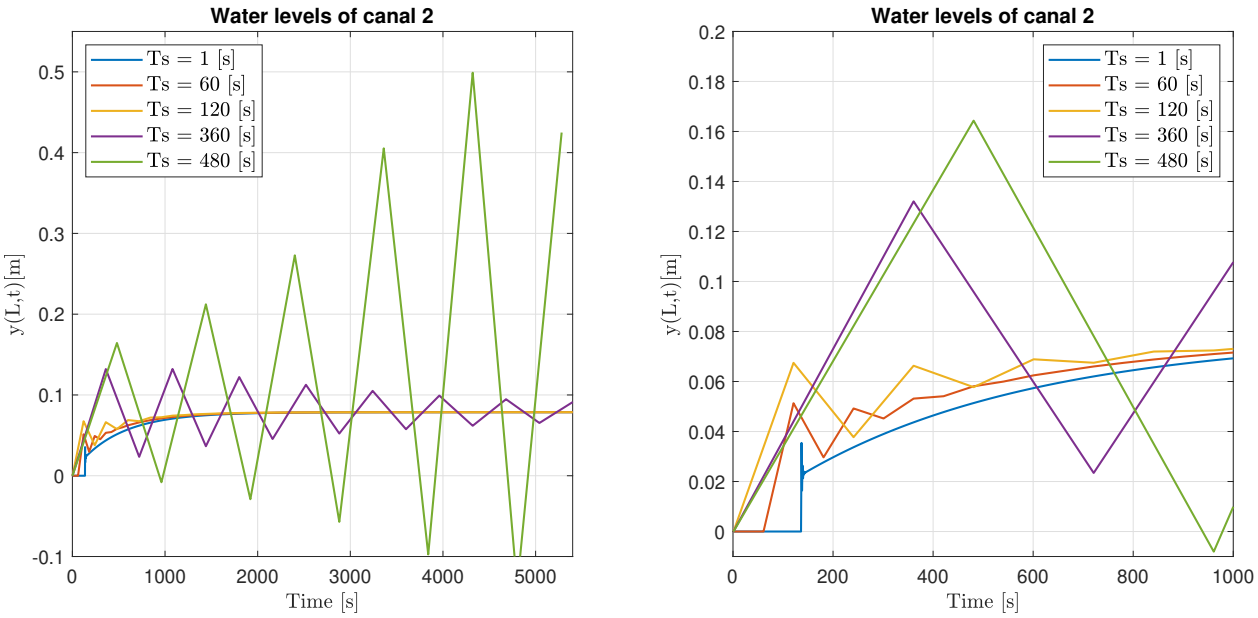

(a) (b)

Figure 2.7: Step responses of discrete-time model simulation with different sampling time with H = 2 m . (a) Plot the value of $y(L,t)$ for channel 2. (b) Zoom of the $y(0,t)$ for channel 2.

step independently of the value of τ (that can be much smaller), so the approximation may not be accurate. This phenomenon can be seen in figure 2.7.b for $T_s = 360\ s$ where τ_d is approximated to the time step 1, so $\tau_d = 360$ even though its original value is 136 s.

Also, figure 2.7 shows that for $T_s = 1, 60, 120, 360\ s$ the step response presents oscillatory behaviour, but it converges to the same value of continuous time model response. These oscillations do not describe a behaviour of the physical system, they are due to the effect of the sampling time on the pole of the IDZ model. Indeed, by increasing the sampling time, the magnitude of the pole tends to move towards the unit circle and therefore the oscillations are damped more slowly. For $T_s = 480\ s$ the system is unstable, indeed bound of sampling time that should ensure stability is experimentally determined around $T_s \simeq 470\ s$.

Note that instability issues occurs only for channels whose flow is controlled by an hydraulic structure. In the case where the output flow is constant or, in general, it does not depend on $Y(L,t)$, the discrete IDZ model is a delayed integrator, thus with a pole p equal to 1 independently of the value of T_s. In this case, the sampling time has to be chosen only to guarantee a reasonable approximation of the delays τ_u and τ_d. In conclusion, this study analyses the main issues generated by the discretisation

of the IDZ model. The next step is to extend the design of sampling time for the network model. In this case, the design is more complex because there are channels with different characteristics. However, it is possible to exploit what has been seen so far. In particular, it is necessary to design T_s considering the worst cases, so the channels that are more sensitive to the effect of discretisation. For example, it is necessary to pay attention to channels with hydraulic structure, since their dynamics may be unstable, if T_s is too high.

CHAPTER 3

Junction model

As mentioned in the introduction, the main objective of this thesis is to develop a model for open channel networks. The network can be seen as a set of channels interconnected by junctions. In the previous sections, the modelling of the channels was studied but, in order to model the network, it is also necessary to model its junctions. This topic is dealt with in this chapter: the aim is to obtain a model that describes the behaviour of water depths and the flows on the junctions. In particular, for the purpose of the network model, it is important to obtain a junction model that describes the dynamics of flows at the boundaries of the junction. Then the detailed behaviours of the flow within the junction can be neglected. Furthermore, it is necessary to obtain models that can be applied to junctions with an arbitrary number of branches. As a reference for this chapter, it is considered the simplest junction: it consists in a main channel to which a second channel is connected generating a junction with three branches. For each branch i the water flow state is defined by two scalar quantities $Q_i(t)$ and $Y_i(t)$. $Q_i(t)$ is defined as the flow passing through the branch i while $Y_i(t)$ is defined as the height of water. Both quantities are taken at the boundaries between channels and junction, these positions are marked by a dotted line in figure 3.1. These variables are scalar because, similarly to SVEs, the flow is assumed to be uniform over the channel cross-section. Also, the height is considered constant over the channel cross-section. Then for a given position x the water flow state it can be described using two scalar scalar variable.

These quantities coincide with those of the adjacent channels: for example, with reference to figure 3.1, $Y_1(t)$ coincides with $Y_1(L_1, t)$, i.e. the height of the water flow at the downstream end of the channel connected to branch 1 of the junction. Similarly, $Y_3(t)$ coincides with $Y_3(0, t)$, i.e. the height of the water flow at the upstream end of the channel connected to branch 3. Then the i-th state of the junction

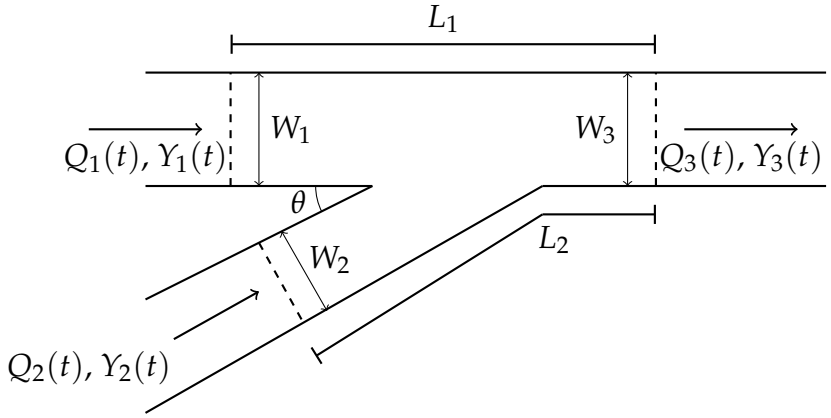

Figure 3.1: Diagram of the reference junction with its geometric variables.

$[Q_i(t), Y_i(t)], \forall i$ describes the flow state at the boundaries of it.

Figure 3.1 shows the three junction branches just described. The parameters of the junction are also shown and these are introduced in the following list:

- W_i is the width of the i-th branch. Note that, for simplicity, the channels of junctions are assumed rectangular. This assumption differs from that made for channels but it is useful for simplifying models. Indeed, in this way, the cross section geometry is defined by less parameters with respect to the trapezoidal cross section;

- L_1 and L_2 is the lengths of junction: L_1 is defined as the distance between the inlet of stream $Q_1(t)$ and the outlet of stream $Q_3(t)$. Similarly, L_2 is defined as the distance between the inlet of stream $Q_2(t)$ and the outlet of stream Q_3;

- θ is the incidence angle of branch 2 on the main channel.

As introduced above, the flow state of a junction is described by the variables $Q_i(t)$ and $Y_i(t)$. In the case of junction with three branches, there are six variables. The purpose of the model is to provide relationships between these variables. In this way, it is possible to measure some of them and estimate the others using the models. In the following lines, a series of models are presented. The aim is to find a model that allows to estimate as many state variables as possible by means of as fewer measurements as possible. Furthermore, it is necessary to identify models that are suitable for describing joints with a generic number of branches. All the models presented in this section are derived w.r.t. the subcritical flow condition, which is typical conditions in natural watercourses. Furthermore, these models describe the flow state of a junction under the assumptions that it is steady, i.e. $Q_i(t)$

and $Y_i(t)$ do not vary in time. Hence, in the following paragraphs the flow variables are written without indicating the time dependency.

3.1 Flow model

The fundamental principle used to model the flow is the conservation of mass, which can be written as:

$$Q_3 = Q_1 + Q_2. \tag{3.1}$$

This relationship is coupled with all the models presented below. In addition, it is valid under the assumption that there is no unexpected leak or inflow in the junction, otherwise it is necessary to estimate and include them in the equation by accounting for an additional term denoted as Q_L. Note also that the flow variables in equation (3.1) are not time dependent. This is due to the fact that (3.1) is derived from the conservation of mass under the assumption that the flows are steady, i.e. they are constant in time. This assumption is restrictive, indeed it implies that is not possible to use (3.1) in transient situations but only when the state reaches a steady equilibrium. However, in cases the flows vary slowly over time, it is possible to adopt this model and obtaining an acceptable approximation. Note that (3.1) allows to estimate a single flow, so it is necessary to measure the value of the other two flows. Moreover, the general version of this formula is valid for a joint with n branches is:

$$\sum_{1=1}^{n} Q_i = 0. \tag{3.2}$$

where the value Q_i is positive, if the flow enters in the junction; otherwise it is negative, if the flow exits the junction. Note that, for any n, (3.2) provides one constraint, so it is possible to estimate one flow from $n - 1$ flows that have to be measured. Furthermore, it can be observed that (3.1)-(3.2) does not consider any delay in the propagation of the flow, unlike the IDZ model in which the input flow takes a time τ_d to have an effect on the downstream end. However, in junctions it is possible to assume that the flow propagation is instantaneous, since their lengths, represented by parameters L_1 and L_2, are small compared to the channel lengths. Thus, the propagation time of flows in the junction can be neglected, since, in general, it is much smaller than the length of channels.

3.2 Equality model

In addition to the flow estimation, it is necessary to understand the behaviour of the heights $Y_i, \forall i \in [0, n]$. The easiest model that can be used is the *Equality model*. The latter leverages the assumption that the water levels of the three branches junctions are equal, namely:

$$\begin{cases} Y_1 = Y_3 \\ Y_2 = Y_3. \end{cases} \tag{3.3}$$

This model has the advantage to be linear; moreover, it can be easily extended to a junction with arbitrary number of branches. In all cases, it provides enough equations to estimate all water heights from a single water depth that has to be measured. However, the model may be too approximative: if the water is stagnant (i.e $Q \simeq 0$), it is intuitive that the water level tends to be constant throughout the junction. In this case, the model well describes the water height trough the junction; however, if the velocity of flows is not null then its performance decreases because the union of different water flows may slow down the water creating local differences in height. To model a junction more accurately, more complex models can be used. Two of them are presented in this theses: the first is called *Gurram* model and the second is called *Shabayek* model.

3.3 Gurram models

Gurram model is based on the conservation of translational momentum. Exploiting it together with equation (3.1), this model allows to estimate the whole state of a three-way junction measuring Q_3, Y_3 and one of the input flows. The equations derived by Gurram et al. [19] are the following:

$$\begin{cases} y_1 = y_2 \\ y_1^3 - y_1\left(1 + 2F_{\mathrm{d}}^2\right) + 2F_{\mathrm{d}}^2\left[q_1^2 + q_2\cos(\alpha\theta)\right] = 0; \end{cases} \tag{3.4}$$

where $\alpha = 8/9$, θ is the incidence angle of lateral branch measured in radiant and F_d is the Froude number at the downstream of the junction, i.e calculated with Q_3 and Y_3. Note that in the models state variables are not time-dependent because the model is derived under the assumption of steady flow with constant height and velocity over time. For both the Gurram and Shabayek models, the variable q_1 and q_2 are defined as the rate between inflows and outflow, i.e $q_1 = Q_1/Q_3$ and $q_2 = Q_2/Q_3$. However, quantities y_1, y_2 are the heights Y_1 and Y_2 normalised

by Y_3, i.e. $y_1 = Y_1/Y_3$ and $y_2 = Y_2/Y_3$. This notation is used so that the model equations be slightly readable. Indeed, the second equation of (3.4) is written using the normalized depth and it is clearly visible that it is a third order polynomial in y_1. Notwithstanding, using normalised variables, it does not lead to any issue in solving system (3.4) because Y_3 and Q_3 are known quantities. Then, it is possible to switch from q_i and y_i to Q_i and Y_i, or vice versa, dividing or multiplying by a known constant. Note that this model provides two constraints, so it allows to estimate two heights Y_1 and Y_2 while Y_3 has to be measured. This model is based on the following assumptions:

- The flows Q_i are steady, i.e they are constant over time;
- The width of the inflow branches are equal, i.e $W1 = W2$;
- Bed slope and friction forces are negligible.

These assumptions are actually quite restrictive: the first one states that this model cannot be used in transient situations, but only when the state reaches a steady equilibrium. The second assumption states that inflow branches have the same width. In practice the assumption is not always verified, which leads to a strict limitation in the implementation of the model since it can only be used for a particular case. The third assumption states that the bed slope and the frictions are negligible, so the model does not include them. This assumption is reasonable since, for short distances and for small values of the slope, the acceleration of gravity has a negligible effect on the flow. Furthermore, it can be assumed that the force generated by small bed slope is similar to the friction forces generated between the bed of channel and the water mass. Since the latter have opposite direction w.r.t. to the former but same intensity, they cancel out each others.

3.4 Shabayek model

This model is proposed by Shabayek et al. [21], it is composed of two nonlinear equations and, as the *Gurram model*, allows to estimate the whole state of a three-branch junction measuring Q_3, Y_3 and one of the input flows. Moreover, compared to the *Gurram model*, it is based on less strict assumptions. Indeed, the Shabayek model considers the bed slope, the friction force and it does not impose that $W_1 = W_2$. The only assumption on which it is based is that the flows are steady.

The *Shabayek model* is represented by the the following system of equations based on momentum principle and mass continuity:

$$\begin{cases} q_1 - \frac{q_1^2}{w_1 y_1} - \frac{1}{8F_d^2}\left[w_1\left(3y_1^2 - 2y_1y_2 - y_2^2\right) + q_1\left(y_1^2 + 2y_1y_2 + y_2^2 - 4\right)\right] \\ -\frac{1}{2F_d^2}\left(\frac{L_1 S_b}{Y_3}\right)(w_1 y_1 + q_1) + K^*\left(\left[\frac{q_1}{w_1 y_1}\right]^2 - \left[\frac{q_2}{w_2 y_2}\right]^2\right)(y_1 + y_2)\left[2q_2 q_1\right] \\ +\frac{L_1}{W_3 C^2}\left(1 + \frac{W_3}{Y_3} q_1\right) = 0 \\ \\ q_2 - \frac{q_2^2}{w_2 y_2} - \frac{1}{8F_d^2}\left[w_2\left(3y_2^2 - 2y_1y_2 - y_1^2\right) + q_2\left(y_2^2 + 2y_1y_2 + y_1^2 - 4\right)\right] \\ -\frac{1}{2F_d^2}\left(\frac{L_2 S_b}{h_d}\right)(w_2 y_2 + q_2) - K^*\left(\left[\frac{q_1}{w_1 y_1}\right]^2 - \left[\frac{q_2}{w_2 y_2}\right]^2\right)(y_1 + y_2)\left[2q_2 q_1\right] \\ +\frac{L_2}{W_3 C^2}\left(1 + \frac{W_3}{Y_3} q_2\right) + K\frac{q_2^3}{w_2^2 y_2} = 0; \end{cases} \tag{3.5}$$

where:

- q_1 and q_2 are the input flows normalized by output flow Q_3, so they correspond respectively to $q_1 = Q_1/Q_3$ and $q_2 = Q_2/Q_3$;
- y_1 and y_2 are the input flow depths normalized by Y_3, so they correspond respectively $y_1 = Y_1/Y_3$ and $y_2 = Y_2/Y_3$;
- w_1 and w_2 denote the width ratios $w_1 = W_1/W_3$ and $w_2 = W_2/W_3$;
- F_d denotes the Froude number of downstream flow (Q_3, Y_3);
- C denotes the Chezy non-dimensional coefficient that quantifies the friction effect. It is analogous to the Manning's coefficient, indeed exists a relation (A.4) that provides a relationship between them;
- S_b denotes the bed slope of the branches of the junction, which is considered null, for sake of simplicity;
- K^* is called interfacial shear coefficient and K is called separation zone coefficient.

Note that coefficient K^* is used to model the shear force, a force generated by the collision of the two water masses coming from the two inflow branches. Coefficient K models the separation zone shear force, which is generated by the recirculating of flow at downstream end of the lateral channel entrance. These coefficients are estimated for each individual joint under analysis via experimental data. In [21], an

attempt is made to estimate coefficients K and K^* by using data from several experiments, including those used in this thesis. The study states that these coefficients are linearly dependent on the incidence angle θ and it provides an estimate of their relation. The latter is reported below:

$$\begin{aligned} K^* &= -0.0015\,\theta + 0.3; \\ K &= 0.0092\,\theta - 0.1855; \end{aligned} \tag{3.6}$$

where θ is the incidence angle of branch 2 on the main channel measured in degrees.

Note that, all models presented are based on the assumption that junction flows are steady, i.e. they are constant in time. This assumption is quite restrictive: it states that models cannot be used in transient situations, but only when their state reaches a steady equilibrium. However, it can be assumed that if the flows vary slowly over time, in a short period Δt, they can be approximated as steady since their variation over time is small and then it can be neglected. Therefore, in this period, the models presented so far can be used.

For example, it is considered the junction with three branches shown in figure 3.1 where $Q_1(t)$ and $Q_3(t)$ are measured $\forall t$. To estimate $Q_2(t)$ can be used 3.1 only if $Q_1(t)$ and $Q_3(t)$ are steady. In this way:

$$Q_2(t) = Q_3(t) - Q_2(t). \tag{3.7}$$

If $Q_1(t)$ and $Q_3(t)$ vary slowly over time, in a short period $[t_1, t_1 + \Delta t]$, the flows can be approximated as steady, hence:

$$Q_1(t_1 + i) = Q_1(t_1), \quad Q_3(t_1 + i) = Q_3(t_1),\ \forall i \in [0, \Delta t]. \tag{3.8}$$

with $Q_1(t_1)$ and $Q_3(t_1)$ are the measured value of $Q_1(t)$ and $Q_3(t)$ at time $t = t_1$. In this period of time can be used 3.7 and it gives

$$Q_2(t_1 + i) = Q_3(t_1) - Q_3(t_1),\ \forall i \in [0, \Delta t] \tag{3.9}$$

where $Q_1(t_1)$ $Q_3(t_1)$ are the flow measured at time t. The latter equation provides an estimate of $Q_2(t)$ only in the period $[t_1, t_1 + \Delta t]$. In order to obtain an estimate of the flow for each t it is possible to repeat periodically the same procedure. Therefore, at time $t_2 = t_1 + \Delta t$, the $Q_1(t_2)$ and $Q_3(t_2)$ measured again. To estimate $Q_2(t)$ in the interval $[t_2, t_2 + \Delta t]$ (3.8) and (3.9) can be used. In this way the estimated flow $Q_2(t)$ is approximated as piecewise constant in time.

$L_1\ [m]$	$L_2\ [m]$	$W_1\ [m]$	$W_2\ [m]$	$W_3\ [m]$	$C\ []$	$S_b\ [\,]$
0.31	0.31	0.155	0.155	0.155	17	0

Table 3.1: Summary of the parameters of the junction used in the simulation 3.5.

3.5 Numerical results

In this section the three models presented above are compared and validated through real data. The main objective is to understand how the *Equality model* performs with respect to other models. This aspect is important because this model will be used to create the proposed network model and, therefore, its performance will influence the network model. In particular, the models will be tested on a junction whose geometrical parameters are shown in Table 3.1. The latter are chosen because they are used in [20] -[25], which also provide dataset of the state of the junction. In particular, some measurements of the junction state are provided for different values of angle $\theta = [30, 45, 60, 90]\ [deg]$. These data are given Table 3.4. In the sequel, all models are compared with available experimental data. As a metric of comparison, it is used the percent relative error between the predicted and available data calculated according to the following formula:

$$\text{Error } [\%] \ = \frac{\left| Y_{\text{experiment}} - Y_{\text{predicted}} \right|}{\left| Y_{\text{experiment}} \right|} \cdot 100. \tag{3.10}$$

In particular, the three models are tested feeding them with the measured values of Q_2, Q_3 and Y_3. The models return the predictions of Y_1 and Y_2 which are compared with the respective measured values using (3.10). Note that (3.4)-(3.5) contain nonlinearities; hence, in the simulation, it is useful to exploit the Matlab function `fsolve()` to solve it. Note that the systems (3.4)-(3.5) have more than one solution for y_1 and y_2, since their equations are second and third order polynomials. This aspect has to be considered in the implementation. In particular, it is necessary to find a strategy for choosing the correct solution. A basic strategy consists to discard negative solutions, since they have no physical meaning. In addition to this, the behaviour of algorithm implemented via function `fsolve()` can be exploited. The latter is an iterative algorithm that starts from an initial value of the solution. This value is progressively updated until it converges to a reliable estimate of the actual solution. In order to guarantee convergence toward the right solution, initial value Y_0 can be choosen using prior information, in particular it is used the Equality model that provides, in general, an approximate solution that is a good starting

point. Specifically, as initial value, it is set $y_1 = 1$ and $y_2 = 1$ that is an equivalent expression of the Equality model $Y_1 = Y_2 = Y_3$. In the first simulation, it is studied how the performance of the models are affected by the incidence angle of the lateral branch. Tables (3.2) - (3.3) show the mean prediction error for each model as the angle θ varies. Note that the mean prediction error is used since, for each value of θ, a set of measures $D(\theta)$ is available. Each element $i \in D(\theta)$ consists of a measurement of the junction flows state $[Q_{1,i}, Q_{2,i}, Q_{3,i}, Y_{1,i}, Y_{2,i}, Y_{3,i}]$. Thus it is possible to average the error (3.10) calculated for each measure in $i \in D(\theta)$. Therefore the mean prediction error for Y_1 is define as:

$$ME[\%] = \frac{1}{|D(\theta)|} \sum_{i \in D(\theta)} \frac{\left|Y_{1,i} - \hat{Y}_{1,i}\right|}{|Y_{1,i}|} \cdot 100. \tag{3.11}$$

where $D(\theta)$ is the dataset of the junction state for a given value of θ. $Y_{1,i}$ is the measure of the height Y_1 of $i \in D(\theta)$, while $\hat{Y}_{1,i}$ is the corresponding estimate provided by the models. The mean prediction error for Y_2 is calculated with (3.11) substituting $Y_{1,i}$ and $\hat{Y}_{1,i}$ with $Y_{2,i}$ and $\hat{Y}_{2,i}$.

ME [%]	Equality	Gurram	Shabayek
θ			
30°	10.6	3.5	0.67
45°	11.6	2.9	0.39
60°	13.0	2.8	1.2
90°	17.8	1.5	2

Table 3.2: Relative mean errors between the predicted and the available data of Y_1.

ME [%]	Equality	Gurram	Shabayek
θ			
30°	10.9	3.9	0.6
45°	12.3	3.6	0.4
60°	12.6	2.4	0.3
90°	17.9	2.6	1.7

Table 3.3: Relative mean errors between the predicted and the available data of Y_2.

From Tables (3.2) - (3.3), it can be seen that the model with the lowest error is the *Shabayek* followed by the *Gurram* which has similar error (3.11). It can be said that the *Shabayek model* is the best model among those considered in this section, since

its prediction error is the lowest and it is based on less restrictive assumptions w.r.t. the *Gurram* model, though, it has complex non-linear equations. The *Gurram* model also performs very well with the advantage of having simpler equations and with the disadvantage that it can only be used in the case where $W_1 = W_2$. The worst performing model is the *Equality model*, having an error ranging from 10% to 20%. Note that the error of all models increases as the incidence angle increases, with the exception of the *Gurram model* which performs better for $\theta = 90$. This is due to the parameter $\gamma = \alpha\theta$ of model(3.4). The latter represents the average inflow direction of lateral inlet branch. This direction in general not coincides with angle θ. In this thesis α is set to $8/9$. This value is tuned for junction with $\theta = 90\ deg$. However, it is still used with other values of θ since the mean error (3.11) remains at an acceptable value, (i.e less than 5%).

Figure 3.2 shows the comparison of the junction models prediction of y_1 with respect to the experimental data. The equivalent comparison for y_2 is reported in 3.5 at the end of this chapter for completeness. Furthermore, from Tables 3.2-3.3, the behaviour of the predicted y_2 is similar to y_1, indeed, it can be seen that the mean prediction error (3.11) of y_1 and y_2 are similar for all values of θ. Note that the result in Figure 3.2 is congruent with what shown in Table 3.2, in particular the *Shabayek model* is the best performing model followed by *Gurram* and finally by the *Equality model* which differs significantly from the measurements. However, some remarkable aspects can be seen in these figures: the *Equality model* and *Gurram model* underestimate the heights for all tested values of θ. This is due to the fact that, unlike the *Shabayek model*, they do not consider the interaction forces between the Q_1 and Q_2, which slow down the flow increasing the water depth locally. In particular, the underestimation of heights is a significant problem for the purposes of the thesis. Indeed, the aim is to design a network model able to predict flooding due to the overflow of channels and junctions. If the height is underestimate respect the reality, the model may classify a certain scenario as not dangerous, even if the risk of overflow is real. The second aspects is that the mean error (3.11) is not uniform, some predictions are closer to the corresponding measured sample especially for the *Equality model*. This suggests that there are some conditions of flow under which the models perform better: looking at the individual measurements, it can be seen that the error is lower when the Froude number is smaller. The Froude number (A.5) of downstream flow is used rather than those of upstream branches because, to calculate it, flow and height is needed. In this case, the only branch, whose these quantities are measured directly, is the downstream branch, so it is the only one for which it can be calculated.

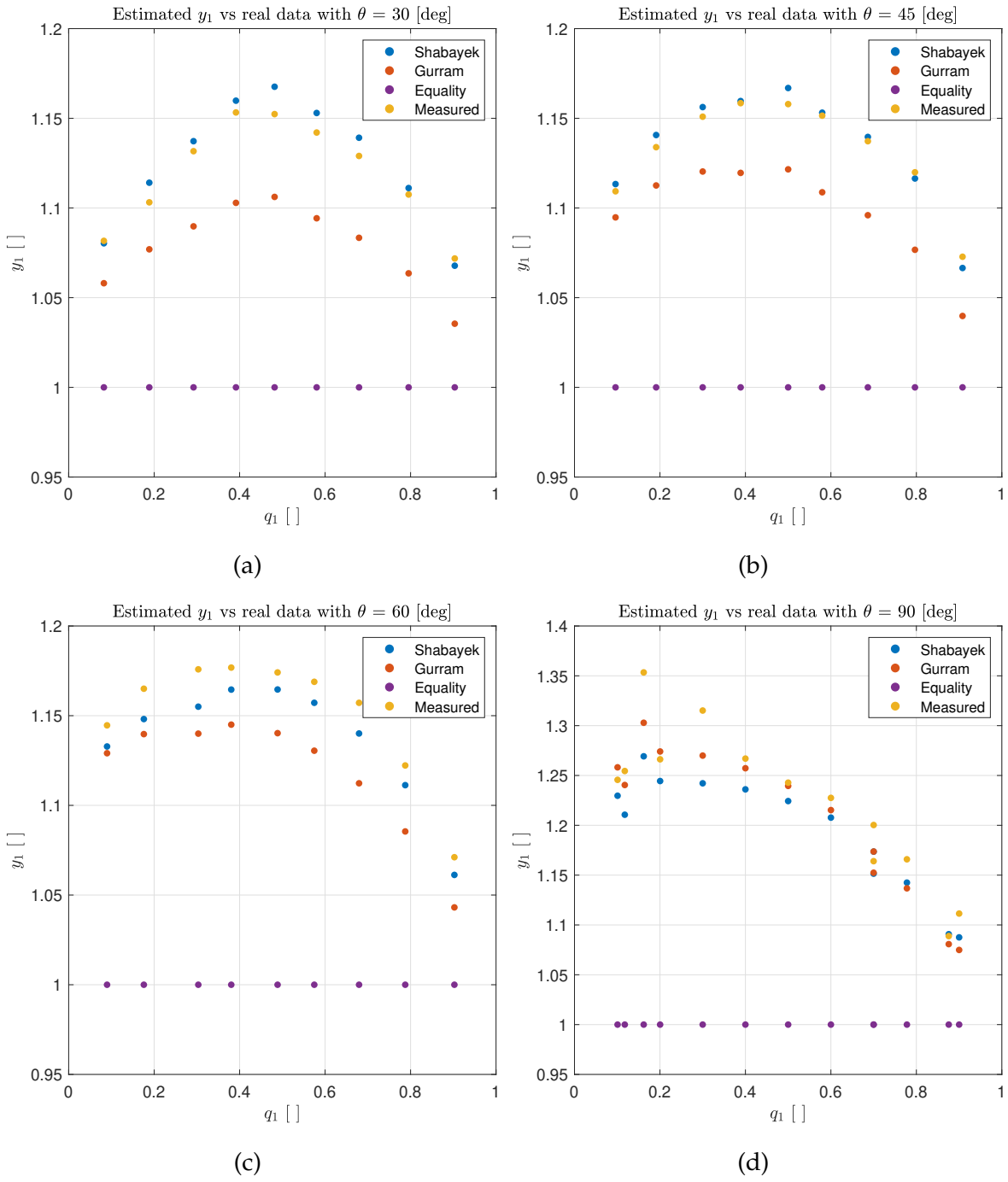

Figure 3.2: Comparison between the measured heights y_1 and those predicted for the junction with: (a) $\theta = 30$ *deg* (b) $\theta = 45$ *deg* (c) $\theta = 60$ *deg* (d) $\theta = 90$ *deg*.

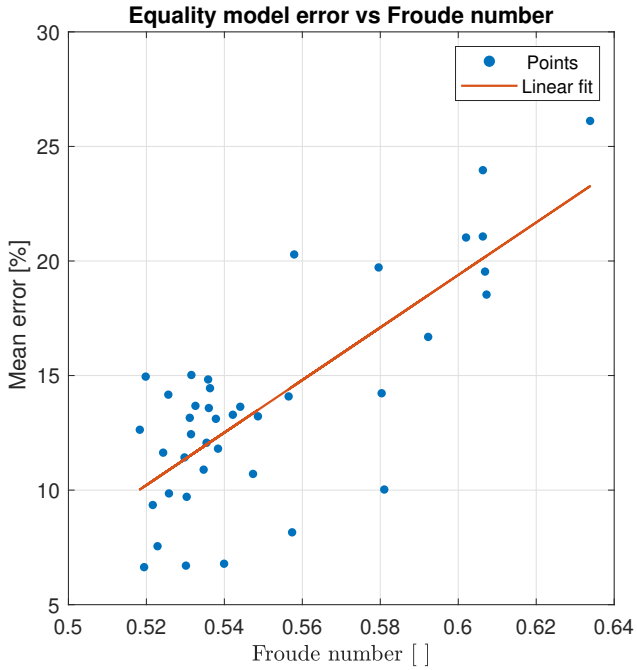

Figure 3.3: Comparison between the estimation error and the Froude number of each measurement in the dataset.

To validate this hypothesis, the relation between Froude number and error (3.10) is plotted in figure 3.3 for all available measurements. In particular, it is associated to each measurement $i \in D$ a point whose abscissa x is the Froude number of the junction outflow and the ordinate y is the relative error (3.10) between measurements Y_1 and the estimates obtained with the *Equality model*. The set D is define as the union of sets $D(\theta), \forall \theta \in [30, 45, 60, 90]$. Also, in Figure 3.3 it is plotted the linear regression line of the points; its equation is:

$$\hat{f}(x) = \hat{m}\, x + \hat{q}, \quad \text{with} \quad \hat{m} = 114.64\ \%,\ \hat{q} = -49.39\ \% \tag{3.12}$$

For completeness, it is reported the root mean squared error (RMSE) calculated between linear fit and the data points:

$$RMSE = \frac{1}{|D|} \sum_{i \in D} (y_i - \hat{f}(x_i))^2 = 2.92\ \%; \tag{3.13}$$

where (x_i, y_i) are the coordinates of the i-th element of set D, while $\hat{f}(x)$ is the estimate of y_i provided by (3.12). In order to verify that (3.12) is a suitable the model to describe the relationship between the error (3.10) and Froude number, a graphical analysis of the residuals is carried out. Figure 3.4 shows the residuals

$r_i = y_i - \hat{f}(x_i) \forall i \in D$. The figure shows that the residuals are randomly distributed around the line $y = 0$ without showing any trends or systematic behaviour. These observations allow to state that the chosen model is suitable. Therefore can be state that the relative error increases as the Froude number increases.

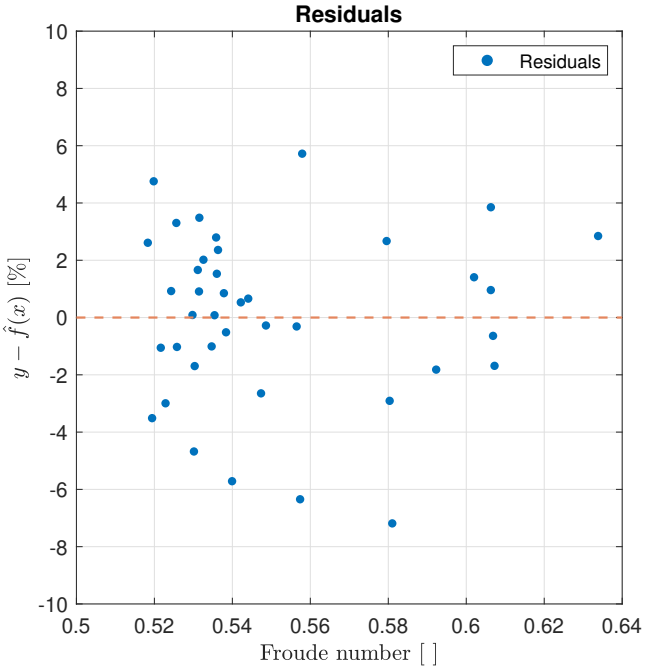

Figure 3.4: Residuals of the linear regression 3.12.

A further experiment to support this thesis is reported in [18]. In this case, it is used a dataset of a junction having the same shape of that one in Figure 3.1. In particular, the flows of this dataset has a Froude number ranging from 0.2 to 0.6. This experiment establishes that the *Equality model* has estimation error (3.10) of 2.5% for $F_d = 0.24$, 7% for $F_d = 0.38$ and of 15% for $F_d = 0.6$. This result is in agreement with what deduced from the figure 3.3, where for $F_d = 0.6$ a similar error is obtained (around 15%). Consequently, it is possible to state that the *Equality model* has good performance if the downstream flow has a low F_d, i.e. if it is a flow characterised by low speed and high depth. In conclusion, according to the result reported in this section, the *Shabayek model* attains the best agreement with the experimental data while the *Equality model* has generated the greatest errors among all. However, *Shabayek model* and *Gurram models* use non-linear equations calculated for the sole junction discussed in this section, so they are of difficult application. For this reason, in the network model implemented later, it is adopted the *Equality model*. Indeed, even if

in the comparison with the other models it is the worst, it can be easily generalised and it has acceptable performance with a low Froude numbers.

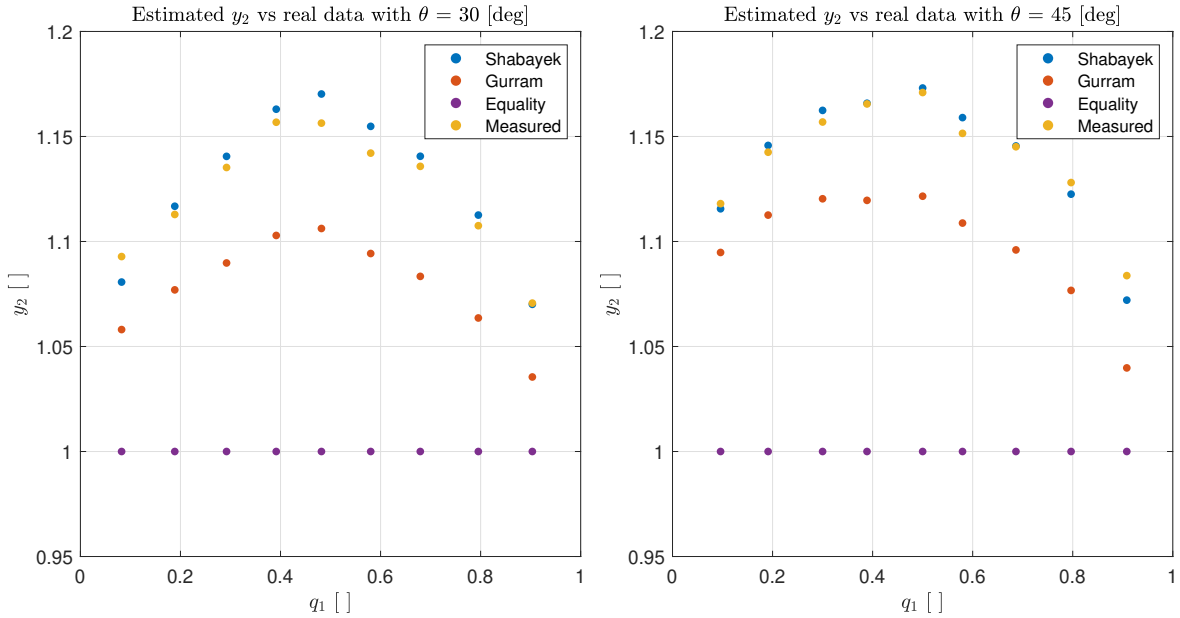

(a)

(b)

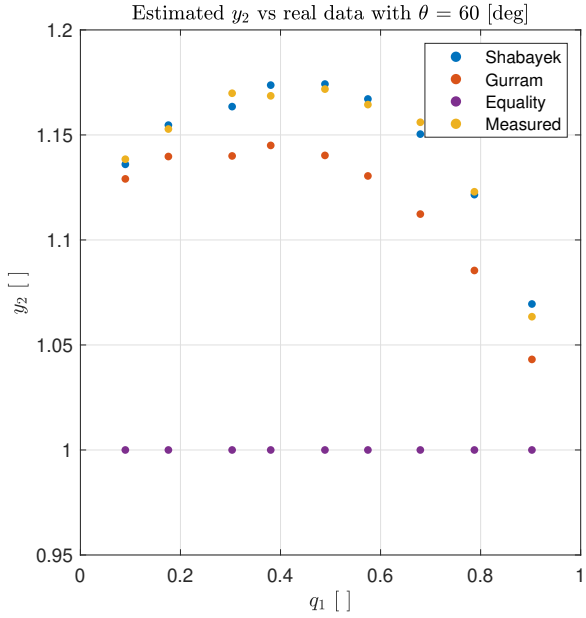

(c)

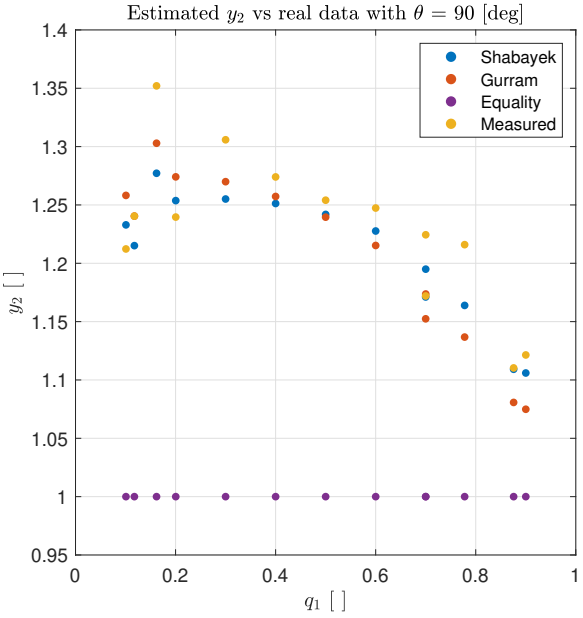

(d)

Figure 3.5: Comparison between the measured heights y_2 and those predicted for the junction with: (a) $\theta = 30$ *deg* (b) $\theta = 45$ *deg* (c) $\theta = 60$ *deg* (d) $\theta = 90$ *deg*.

3.6 Dataset

$Q_1[l/s]$	$Q_2\ [l/s]$	$Q_3\ [l/s]$	$Y_1\ [cm]$	$Y_2\ [cm]$	$Y_3\ [cm]$	$Q_1[l/s]$	$Q_2\ [l/s]$	$Q_3\ [l/s]$	$Y_1\ [cm]$	$Y_2\ [cm]$	$Y_3\ [cm]$
$\theta = 30\ deg$						$\theta = 60\ deg$					
0.48	5.35	5.83	8.74	8.83	8.08	0.52	5.27	5.79	9.26	9.21	8.09
1.13	4.86	5.99	9.09	9.17	8.24	1.05	4.92	5.97	9.53	9.43	8.18
1.82	4.41	6.23	9.54	9.57	8.43	1.85	4.25	6.1	9.83	9.78	8.36
2.56	3.98	6.54	9.82	9.85	8.515	2.45	3.99	6.44	10.05	9.98	8.54
3.31	3.56	6.87	10.06	10.095	8.73	3.28	3.43	6.71	10.25	10.23	8.73
4.12	2.98	7.1	10.41	10.41	9.115	4.04	2.99	7.03	10.52	10.48	9
4.62	2.18	6.8	10.02	10.08	8.875	4.6	2.17	6.77	10.16	10.15	8.78
5.21	1.34	6.55	9.58	9.58	8.65	5.19	1.4	6.59	9.694	9.7	8.638
5.61	0.6	6.21	8.95	8.94	8.35	5.65	0.61	6.26	9.115	9.05	8.51
$\theta = 45\ deg$						$\theta = 90\ deg$					
0.56	5.27	5.83	8.93	9	8.05	0.386	3.443	3.829	7.1	6.91	5.7
1.16	4.91	6.07	9.23	9.3	8.14	0.697	5.226	5.923	9.81	9.7	7.82
1.89	4.41	6.3	9.61	9.66	8.35	0.983	5.086	6.069	9.88	9.87	7.3
2.5	3.93	6.43	9.87	9.93	8.52	0.863	3.444	4.306	7.61	7.45	6.01
3.43	3.43	6.86	10.155	10.269	8.77	1.821	4.249	6.07	9.89	9.82	7.52
4.11	2.98	7.09	10.49	10.49	9.11	2.218	3.327	5.545	8.97	9.02	7.08
4.73	2.16	6.89	10.11	10.18	8.89	3.327	3.327	6.654	9.93	10.02	7.99
5.33	1.36	6.69	9.62	9.69	8.59	3.677	2.451	6.128	9.28	9.43	7.56
5.63	0.57	6.2	8.84	8.93	8.24	3.884	1.665	5.549	8.73	8.79	7.5
						3.76	1.611	5.371	8.45	8.62	7.04
						3.54	1.011	4.551	7.45	7.77	6.39
						4.37	0.62	4.99	7.6	7.75	6.98
						4.702	0.522	5.224	7.78	7.85	7

Table 3.4: Datasets $D(\theta)$ used to evaluate the performances of the junction models with $\theta = [30, 45, 60, 90]$.

CHAPTER 4

Sensor location problem

The link flow measurement for hydraulic network analysis is fundamental to predict the state of the network to prevent flooding. The IDZ model used in this thesis to model the channel is able to estimate the water heights over its entire length. However, the IDZ model requires the knowledge of inflow and outflow. These flows can be estimated in different ways: one possibility is to exploit the models of the hydraulic structure which are able to provide the value of the flow passing through them from the heights of water. However, in general, there is no hydraulic structure at the upstream and downstream ends of each channel in the network. Also they are able to provide an only approximation of the actual flow. Therefore, these models are not sufficient to estimate every flow in the network.

Another way to estimate flows is to exploit junction constraints in the network. These constraints are derived from the principle of mass conservation and state that, in a junction, inflows are equal to the outflows. Each junction provides only one constraint that can be used to estimate the flow of a single channel; the others have to be measured or estimated in other ways. However, in a graph, the number of junctions is smaller than the number of links, so also these models are not sufficient to estimate every flow in the network. At the light of these observations, it can be deduced that it is not possible to estimate all flows of the network using only these models, but it is necessary to integrate them with measurements. A further reason why flows have to be measured is that the IDZ model calculates its parameters using the linearisation of SVEs around a steady state working point. If the working point at which the parameters are calculated is not accurate, the capability of the model to fit the actual system will be significantly reduced. In addition, such measurements are taken periodically, since the IDZ model can estimate, with a reasonable approximation, the evolution of the water height around the initial point. Indeed its parameters

are derived through a linearisation process. For long-term simulations, in which the system state varies significantly, it is necessary to recalculate the parameters of the IDZ model using an updated system state, that is measured periodically. This chapter deals with the problem of sensor placement within a open channels network in order to measure flow and height. In particular, the aim is to identify the minimum set of channel to be equipped with sensor in order to estimate the flows of all the unobserved channel. This problem is also call network sensor location problem (NSLP).

4.1 State of the art

The NSLP has relevance in many field, such as traffic planning and management. Gentili and Mirchandani (2012) [26] provide a review of the NSLP. In particular they classify it into two main types: sensor location flow-observability problem and sensor location flow-estimation problem. The first one proposes a design for the optimal placement of sensors with the purpose to obtain the unique determination of the unobserved flows. The flow-estimation problem identifies the optimal placement of sensors to improve the estimation quality. Yang et al.(2006) [27] formulates the NSLP as integer linear-programming models and propose a solution to find an optimal locations without considering the uncertainty of measurements. Other works overcome this assumption as Fei and Mahmassani (2011) [28] by employing the Kalman filtering method to identify the sensor locations minimizing the uncertainties of the estimates. However, this study and, in general, the majority of the literature of flow-estimation problem deals with origin-destination (OD) flows. This type of flow is defined as the flow that travels from a origin to a destination. This type of flow is suitable for the study of transportation networks and it is not the type of flow uses this thesis, since water, unlike cars, has a dynamic determined by deterministic physics law, while the cars flow is composed of discrete units that are free to choose the path according to the needs of the driver.

The sensor location flow-observability problem consists of finding the minimum number of sensors that guarantees the optimal locations ensuring the full observability of the network flows. This strategy has been addressed by Hu et al.(2009) [29] followed by Castillo et al. (2010) [30] that provides some matrix tools to solve the observability problems. Ng (2012) [31] propose a node-based approach based on the node–link incidence matrix to solve this problem. Xu et al. (2016) [32] proposes a different approach which identifies the minimum set of links to be equipped

with sensors in order to obtain the full observability of flows and to minimise in the inferred link flows errors. This is the paper to which this chapter mainly refers. In particular, this chapter focuses on the sensor location flow-observability problem to obtain the complete link flow observability in a network minimizing the uncertainty of the estimated flow.

4.2 Problem description

In this chapter, the network of open-channels is represented by a directed graph (digraph) $\mathcal{G} = (\mathcal{V}, \mathcal{E})$ identified by a set of vertices (nodes) V and a set of edges (links) $\mathcal{E}$. The cardinality of the sets are denoted as $|\mathcal{V}| = N$ and $|\mathcal{E}| = M$. Also it is used the set $E(j)$ which contains the label of the links incident to node j. The cardinality of the this set is called $n_j = |E(j)|$ and it is the number of links incident to node j . The set $E(j)$ is composed of two subsets $O(j)$ and $I(j)$, which are respectively the sets that contain the labels of the incoming and outgoing links of the node j.

The links of the graphs represent the channels of the network: to each of them is assigned a variable which is the value of the flow Q_i that passes through the related channel. This variable is scalar and it is positive, if the direction of the actual flow is in agreement with the direction of the link, otherwise it is negative. In practice, the flow of a channel cannot be modelled with a scalar value. Even if in this thesis the flow it is approximated as a 1D-dimensional quantity called $Q(x, t)$, it can vary along the length of the channel x and over time. However, there is a particular case in which this assumption is valid, namely when the flow is uniform. Therefore, in this chapter, the flow is assumed to be uniform so that its velocity and height are constant over the channel length. The other fundamental element of the graph are the nodes, classified into two types: the first one are called non-centroid nodes, they represent a junction between channels that connect two or more links together. The second type of nodes represent the entry and exit points of the network flow, they connect links with the external environment and they are called centroid nodes. The set of non-centroid nodes is called $\mathcal{V}_{NC}$ and it has cardinality $|\mathcal{V}_{NC}| = N_{NC}$. To each non-centroid nodes it is associated a flow conservation equation:

$$\sum_{i \in E(j)} Q_i = 0, \quad \forall j \in \mathcal{V}_{NC}; \tag{4.1}$$

where the value Q_i is the flow of the i-th branch of the junction j. The value Q_i is chosen positive, if the flow enters in the junction (regardless of the direction of

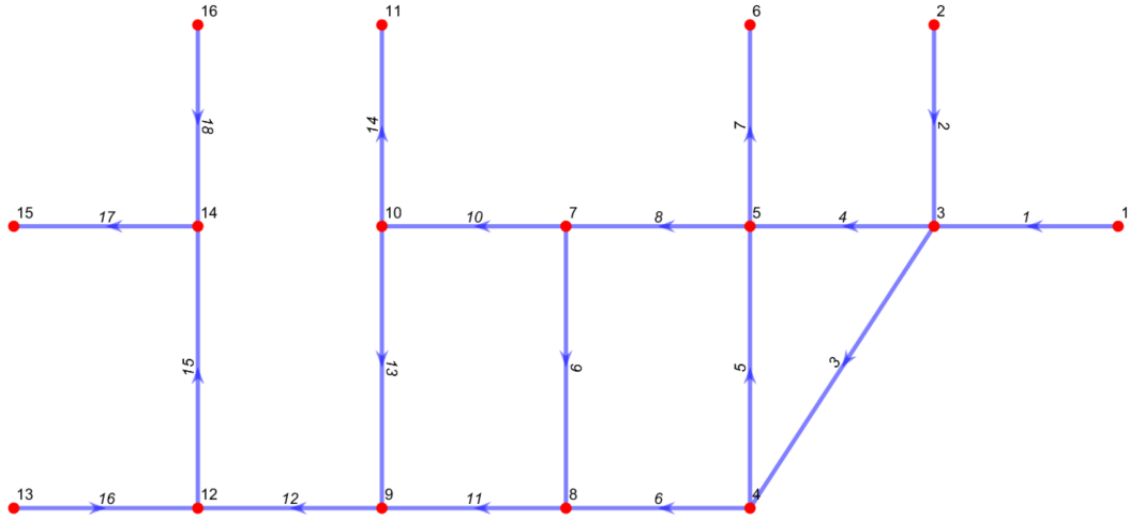

Figure 4.1: Subgraph of the Cavallino network.

the edge), otherwise it is chosen negative, if the flow exits from the junction. Note that the flow variables are not time dependent. This is due to the fact that (4.1) is derived from the principle of mass conservation under the assumption that the flows are steady, i.e. they are constant in time. Therefore, it is necessary to assume that the flow in the network is steady to use the equation (4.1) (as well as uniform as explained above). The equation (4.1) is the starting point of the proposed procedures to solve the NLSP. However, given these considerations, it is necessary to keep in mind that this procedure is only valid for the estimation of uniform and steady flows.

Figure 4.1 shows the graph $\mathcal{G}$ used in this chapter: it represents the main connected part of the Cavallino network. In particular, that is the main network of the peninsula facing the Adriatic Sea, in which blind canals are neglected since they are not relevant for the study of flow. The graph is derived associating to each junction of this network a non-centroid node, while to each inlet or outlet it is assigned a centroid node and, finally, an edge is associated to each canals.

The graph $\mathcal{G}$ is composed of $M = 18$ edges and 16 nodes of which $N_{NC} = 9$ represent channel junctions (i.e. non-centroid nodes), while the remaining 7 represent entry and exit points of the flow, i.e. centroid nodes. Note that a flow conservation equation (4.1) is associated to each junction, hence to each non-centroid node. Every equation provides a constraint that can be used to estimate the flow of a channel, so it is possible to estimate the flows of N_{NC} channels. Since the network $\mathcal{G}$ has M channels, where $M > N_{NC}$, it is necessary to measure the others $M - N_{NC}$ flows. It is possible to represent all the junction constraints using the incidence matrix E of

the non-centroid nodes of the graph G. The element of this matrix are:

$$E_{ij} = \begin{cases} +1, & \text{if } j \in I(i) \\ -1, & \text{if } j \in O(i) \\ 0, & \text{otherwise} \end{cases} \tag{4.2}$$

where $i \in \mathcal{V}$, $j \in \mathcal{E}$. The sets $I(i)$ and $O(i)$ are the sets of incoming and outgoing links at node i. From the incidence matrix of the overall graph is retrieved the incidence matrix of the non-centroid node $\mathcal{V}_{NC}$. This matrix is called E_{NC} and it is calculated by taking the rows of the matrix E related to only the $i \in \mathcal{V}_{NC}$.

The number of rows and columns of E_{NC} matrix are, respectively, the number of non-centroid nodes N_{NC} and the number of links M, so the matrix has dimension $N_{NC} \times M$. Also, it is introduced the column vector Q: it is the vector whose i-th element is the flow value of the i-th link. Using E_{NC} and Q, it is possible to represent the flow conservation equations imposed by the network junctions with a simple equation $E_{NC}\, Q = 0$. Furthermore, with a permutation of the columns of the matrix E_{NC} it is possible to write the nodal flow conservation equation as follows:

$$(E_U, E_O) \begin{pmatrix} Q_U \\ Q_0 \end{pmatrix} = 0, \quad \text{or} \quad E_U Q_U + E_O Q_O = 0; \tag{4.3}$$

where the vector Q_U collects the unobserved flows and Q_O collect the observed flows. Note that, since the junction provide N_{NC} independent equations, the maximum number of unobserved flows Q_U are N_{NC}, as consequence the minimum number of the observed flows Q_O are $M - N_{NC}$. Note that, it is not possible to estimate more than N_{NC} flows because there is N_{NC} equation each of which can estimate at most one flow. However, it is possible to estimate less than N_{NC} always with $M - N_{NC}$ sensors exploiting the redundancy to reduce the estimation error. This procedure is proposed in [32], but as anticipated, the objective of this thesis is to find the minimum number of the observed flows Q_O. So, in this case, the number of unobserved flows Q_U is fixed to N_{NC}, and the number of the observed flows Q_O is fixed to $M - N_{NC}$.

Consequently, the matrix E_U has dimension $N_{NC} \times N_{NC}$ while E_O has dimension $N_{NC} \times (M - N_{NC})$. From (4.3) is possible to derive a formula to calculate Q_U that is:

$$Q_U = -E_U^{-1} E_O Q_O. \tag{4.4}$$

This equation is valid only if the matrix E_U is invertible, i.e if it is square and full rank. Note that the observed flows Q_O are subject to a measurement error. In particular the measurements Q_O can be seen as sample of a random vector $\overline{Q}_O$ whose expected value is the true value of the flows (that is unknown), while the covariance matrix is Σ_O represent the measurement error. In particular, for simplicity, it is assumed that the measurement are independent with equal variance σ^2, so that the matrix Σ_O can be written as $\sigma^2\ I_{(M-N_{NC})}$, where $I_{(M-N_{NC})}$ is the identical matrix of dimension $(M - N_{NC}) \times (M - N_{NC})$. Also Q_U can be seen as sample of a random vector $\overline{Q}_U$ whose expected value is the true value of the flows, while the covariance matrix is Σ_U represent the estimation error. In particular, Q_U and Q_O are linked by a linear equation, then under the assumption that the variables of Q are independent, it is possible to calculate its covariance matrix of Q_U (and so the variance of the estimated flows) using the following formula:

$$\Sigma_U = (E_U^{-1}E_O)\ \Sigma_O\ (E_U^{-1}E_O)^T. \tag{4.5}$$

Note that the matrix E_U and E_O are not unique because there are various combinations of the observed and unobserved links that can be choosen. In particular, the sensor location problem requires to find N_{NC} links to be equipped with sensors in order to obtain the full observability of flows. The set X is defined as the set of the possible combinations of unobserved-observed links; in other words, it is the set of possible solutions to the sensor location problem. Set X is composed by vectors x that describe which link is equipped with a sensor and which are not. These vectors can be of three forms: the first one x is a Boolean vector with dimension M and each element x_i is :

$$x_i = \begin{cases} 1, & \text{if link i is unobserved} \\ 0, & \text{if link i is observed.} \end{cases} \tag{4.6}$$

To describe which links are equipped with a sensor it is also possible to use the vector x that contains only the $M - N_{NC}$ labels of the observed links, or the N_{NC} labels of the unobserved links. Note that it is sufficient to know only one of these two vectors because the other is found by exclusion because, if a link in the graph if not classified as observed, it is classified as unobserved. Following, x is considered a Boolean vector that lives in a space X, which in turn is a subspace of $\{0, 1\}^M$. In particular, the sensor location problem requires to find N_{NC} links to be equipped with sensors in order to obtain the full observability of flows. Since the number of unobserved flows are N_{NC}, the problem requires to choose $M - N_{NC}$ distinct links

to be observed without repetitions on a set of dimension M. In other words, this problem is equivalent to finding all possible subset of cardinality $M - N_{NC}$ of a set with cardinality M. The number of all possible combinations of N_{NC} unobserved links can be thus calculated using the binomial coefficient [1]:

$$|X| = \binom{M}{M - N_{NC}} = \binom{M}{N_{NC}}, \tag{4.7}$$

where $|X|$ is the cardinality of X that is the set of all possible solution for the sensor location problem. Note that the problem requires to chose $M - N_{NC}$ distinct links to be observed on a set of dimension M is equivalent to chose N_{NC} distinct unobserved links. Indeed, each set of observed links is associated with a unique set of unobserved link. For example, considering the network $\mathcal{G}$ in figure 4.1, the total combination are $|X| = \binom{18}{9} = 48620$. However in general, these combinations do not guarantee that the matrix E_U is invertible, therefore it is necessary to develop a method able to generate all possible combination of observed/unobserved links (then possible couple of matrices E_O and E_U) such that E_U is square and full rank, this method is presented in the next section.

4.3 Unobserved link selection

In this section, it is proposed a procedure to build the set of the possible combinations of unobserved links. Each element of this set is composed by N_{NC} links that cannot be chosen randomly because it has to guarantee that the matrix E_U is invertible, otherwise is not possible to estimate Q_U. In particular, the proposed method is an iterative algorithm in which a non-centroid node is scanned at each cycle. For simplicity in this case, they are scanned in the ascending order given by their labels. However, any order is acceptable, the key point is to visit all the nodes only once. For each non-centroid node, i.e for each cycle i, the set A_i is retrieved, which is the set of links connected to the current non-centroid node and not connected to the nodes analysed in previous cycles. With this simple procedure, the sets $A_1, ..., A_N$ are obtained. From these sets it is possible to extract the possible solutions x: they are all combinations of the elements in the obtained sets A_1,A_2,...,A_N by taking only one element from each set. This particular set of solution is called C: it is defined as the subset of X which contains the solution x find with the algorithm just described.

[1] These are the combinations of N_{NC} unobserved links, all possible combinations with any number of observed links are 2^M.

In particular, the solution $x \in C$ is represented with a Boolean vector. However, the proposed algorithm find the sets of unobserved links, to write the x as a Boolean vector can be used the definition (4.6). In this way the candidate solutions $x \in C$ obtained ensure that the matrix E_U is invertible, this can be proved with the two following observation:

- To generate a candidate solution x from sets A_i, only a single link is selected for each set. Since these sets are N_{NC} by construction, the number of selected link (i.e unobserved link) is equal to the number of non-centroid nodes. The matrix E_U has N_{NC} rows by definition and a number of columns equal to the number of unobserved flows, so in this case, it is a square matrix $N_{NC} \times N_{NC}$;
- Each selected link belongs to a different A_i, so it is not connected to the nodes visited in the previous cycles from 1 to $i-1$. In this way, the column associated with the link belonging to any set A_i has null elements in correspondence to the rows of the nodes analysed in the previous cycles w.r.t. i. This implies that the column vector associated with link i is linearly independent of the previous columns. Hence, all columns in E_U are linearly independent.

In conclusion, these two remarks show that this procedure generates candidate solutions x such that E_U is square and full rank, so it is invertible. To conclude this section, the method just described is applied to the graph in figure 4.1. The first node taken into analysis is node 3, the links connected to it are $[1, 2, 3, 4]$. Since it is the first iteration, all the links are good candidates so $A_1 = [1, 2, 3, 4]$. In the second iteration, the next non-centroid node to be analysed in ascending order is 4, the links connected to it are $[3, 5, 9]$. Note that link 3 is already connected to node 3, so it is discarded; in this way the set of candidates is $A_2 = [5, 9]$. This procedure is repeated for all non-centroid nodes, all set A_i obtained in this example are reported in table 4.1, for a total of 256 combinations.

Note that the combinations found are only a part of those that guarantee, the invertibility of E_U, indeed there are different ways to construct the sets A_i which can give solutions different from those shown in the table 4.1. In particular, changing the order with which the algorithm explores the nodes also changes the sets A_i. For example, in the solutions found, the links 1 and 3 are never classified as unobserved at the same time because they belong to the same set A_1, from which only one link is extracted to determine the candidate solutions. However, if in the first iteration the algorithm visits node 4 and in the second it visits node 3, set A_1 becomes $[3, 5, 6]$ while A_2 becomes $[1, 2, 4]$. In this way, links 1 and 3 are in two separate sets, meaning that there are now different combinations.

Iteration	Node i	Connected links	Candidates links A_i
1	3	1,2,3,4	1,2,3,4
2	4	3,4,5	5,6
3	5	4,5,7,8	7,8
4	7	8,9,10	9,10
5	8	6,9,10	11
6	9	11,12,13	12,13
7	10	10,13,14	14
8	12	12,15,16	15,16
9	14	15,17,18	17,18

Table 4.1: Set of candidates links A_i that guarantees the invertibility of E_U.

4.4 Adopted optimization approaches

The aim of this section is to set up an optimisation problem to solve the objective of this chapter. In particular, it is necessary to position the sensors in the network in order to observe the flow of whole network minimizing the estimation error of the inferred flow. To solve the problem, it is necessary to find an equation that expresses the variance Σ_U representing the estimation error as a function of x that describes which link is observed and which is estimated. In this way it is possible to find the optimal value of x which minimises the sum of variance of the estimated flow with a classical optimisation problem approach:

$$\underset{\mathbf{x}\in X}{\operatorname{argmin}} \sum_{i\in\mathcal{E}} \Sigma_{U,ii}(x). \tag{4.8}$$

Unfortunately, in this case, is not possible to obtain a relation between Σ_U and x. Indeed, even if Σ_U is related with E_O and E_U by equation (4.5), there is no explicit and general formulation that allows to express these matrix as a function of x. Hence, Σ_U does not have an explicit expression as a function of x. In conclusion, it is necessary to find an approach that provides a solution that minimises the sum of variance of the estimated flow even if it does not use it explicitly. In the next paragraph a different optimisation problem with this feature is proposed.

Instead of directly minimizing the accumulated variance of the inferred link flows, it is possible to minimise the number of unobserved links connected to the non-centroid nodes. To explain why this may be a suitable alternative, an example

is provided. Considers the graph $\mathcal{G}$ focusing on the nodes 3 and 5 and the links connected to them. To estimate the flow in link 7 with the flow conservation equation of node 5, the flow of links $4, 5, 6$ are needed. If these links are measured directly, their variance is σ^2; consequently, with the assumption that the measurements are independent, the variance of the estimated flow of link 7 is the sum of the variance measurement, then it is $3\sigma^2$. However, for example, if the flow of link 4 is not measured directly, but estimated using the equation of node 3, its variance is $3\sigma^2$, therefore the variance of the estimated flow of link 7 is $5\sigma^2$. In the second case, it is observed that the estimation of the flows of unobserved link 7 involves an estimated flow leading to an accumulation of measurement error. In conclusion, it can be stated that the smaller the number of unobserved links involved in the link flow inference equations, the lower is the possibility of error accumulation and, therefore, the lower the uncertainty in the inferred link flows.

Therefore two alternative methods are presented. Their aim is to minimise the number of unobserved links connected to each non-centroid node. The first minimisation problem presented is called *min-max problem*: it minimises the largest number of unobserved links connected to each non-centroid node as follows:

$$\underset{\mathbf{x}\in X}{\operatorname{argmin}} \max_{\mathbf{i}\in\mathcal{V}_{NC}} \sum_{j\in\mathcal{E}} x_j \gamma_j^i; \tag{4.9}$$

where i is a non-centroid node and x_j is the j-th element of vector x that is equal to 1 if the link j is an unobserved link and 0 otherwise. The variable γ_j^i is called node–link indicator: it is equal to 1 if link j is connected to the node i and 0 otherwise. Note that the variable x changes according to the link combination, while γ_j^i depends on the structure of the graph, indeed this coincides with the absolute value of the element of the incidence matrix $\gamma_j^i = |E_{ij}|$. Therefore, the function $Z_i(x) = \sum_{j\in\mathcal{E}} x_j \gamma_j^i$ counts how much unobserved links are connected to the non-centroid node i for the combination x. In this case, the cost function is defined as $f_{MAX} = \max_i Z_i(\mathbf{x})$ that is the largest number of unobserved links connected between all the non-centroid node i for a given combination x.

The second one is called *min-sum problem*: this method minimises the sum of all unobserved links connected to non-centroid nodes.

$$\underset{x\in X}{\operatorname{argmin}} \sum_{i\in\mathcal{V}_{NC}} \sum_{j\in\mathcal{E}} x_j \gamma_j^i. \tag{4.10}$$

In this case, the cost function is defined as $f_{SUM}(x) = \sum_{i\in\mathcal{V}_{NC}} Z_i(\mathbf{x})$, that is the sum

of the unobserved links connected to all the non-centroid node i for a given combination x.

4.5 Numerical results

In this section, the proposed methods for solving the sensor placement problem are tested using the graph in figure 4.1, which represents the main connected part of the Cavallino network. It is also assumed that the measured flows Q_i, $\forall i \in [0, M]$ are independent random variables with variance $\sigma^2 = 0,2\ m^6/s^2$. Note that this value is arbitrary set, indeed recall that the variance values are not available to solve the problem. In this case, they are used to test performance of optimisation problems.

To solve the two optimisation problems (4.9)-(4.10), Matlab solver functions can be used. Indeed, as shown in [32], it is possible to reformulate (4.9)-(4.10) as Mixed-integer linear programming problem (MILP) that can be solved by the Matlab function `intlinprog()`. However, since the combinations to be tested are only 256, the brute force approach is used to get a complete overview of the performance for all combinations. In particular, the cost functions $f_{MAX}(x)$ and $f_{SUM}(x)$ are computed for all candidate solutions $x \in C$ and, for each solution, the variance of the estimated flows is calculated using (4.5). Since for each x there are N_{NC} flows estimated with N_{NC} distinct variances, to compare the results, it is used their mean values calculated as:

$$\overline{\sigma}_U = \frac{1}{N_{NC}} \sum_{i \in \mathcal{E}} \Sigma_{U,ii}(x), \tag{4.11}$$

where $\Sigma_{U,ii}(x)$ are the elements in the diagonal of matrix $\Sigma_U(x)$ obtained with the combination x.

In figure 4.2 the relation between the mean variance $\overline{\sigma}_U$ and the cost functions are plotted for each candidate combinations $x \in C$. These comparisons are performed to check whether the optimisation problem (4.9)-(4.10) are able to find a solution that minimises the mean variance (4.11). In particular, this test aims to prove that minimising the two proposed cost functions is equivalent to minimising the variance of the inferred link flows. Then ideally, the relation plotted in 4.2 increases monotonically.

In figure 4.2.a the variance $\overline{\sigma}_U$ and the cost functions of min-max approach $f_{MAX}(x)$ is plotted for each candidate combinations $x \in C$. The figure 4.2.a shows that the cost function takes two values and, for each of these, there is a set of candidate combinations x that generate different values of variance $\overline{\sigma}_U$. In particular, there is more than one solution that minimises the cost function, but such solutions do

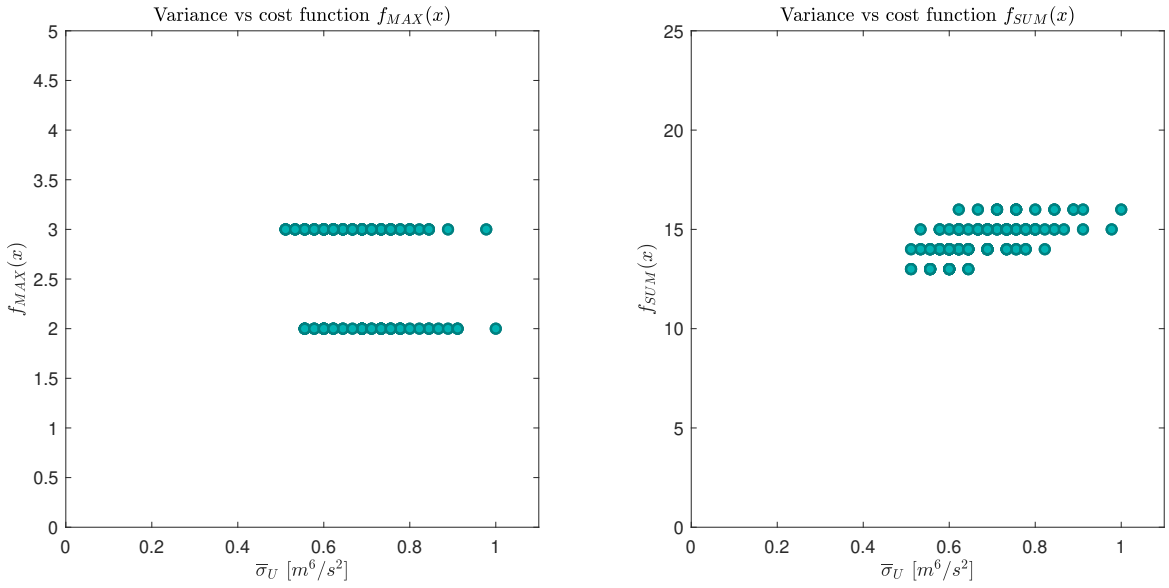

(a) (b)

Figure 4.2: Relations between the mean variance $\overline{\sigma}_U$ and the cost function $f_{MAX}(x)$ in (a) and $f_{SUM}(x)$ in (b).

not also minimise the variance $\overline{\sigma}_U$. This can also be seen in the table 4.2, in which it is reported the number of solutions x generating each value of the cost function and the maximum and minimum value of $\overline{\sigma}_U$ for each value of the cost functions. In particular, the minimum variance obtained with the solutions that minimise the cost function is $\overline{\sigma}_U = 0.54\ m^6/s^2$. Whereas, there are solutions that generates a smaller variance $\overline{\sigma}_U = 0.51\ m^6/s^2$ even if the cost function $f_{MAX}(x) = 3$. Therefore, it can be concluded that the solutions that minimise the cost function do not guarantee to minimise $\overline{\sigma}_U$. In figure 4.2.b, the mean variance $\overline{\sigma}_U$ and the cost functions $f_{SUM}(x)$ is plotted for each candidate combinations $x \in C$. The min–sum model seems to have a better distinguishing capability compared to the min–max model. Indeed, given a set of candidates solution with $f_{MAX}(x) = 2$, the corresponding values of $f_{SUM}(x)$ could ranging from 13 to 16. Figure 4.2.b also shows that, as the cost function increases, the variance $\overline{\sigma}_U$ also increases. In particular, as soon as the cost function value is equal to 13 and 14, there are optimal solutions with minimum variance 0.51. For higher values of the cost function, as for $f_{SUM}(x) = 15$, one has $\overline{\sigma}_U \in [0.53, 0.97]\ m^6/s^2$ and for $f_{SUM}(x) = 16$, one has $\overline{\sigma}_U \in [0.62, 1]\ m^6/s^2$.
In conclusion it can be stated that, as $f_{SUM}(x)$ increases, candidate solution x generates with more likely higher inferred flow variance. However, the min-sum approach provides solutions which tend to minimise the total value of unobserved

$f_{MAX}(x)$	# x	min $\overline{\sigma}_U$	max $\overline{\sigma}_U$
2	104	0.55	1
3	152	0.51	0.98

(a)

$f_{SUM}(x)$	# x	min $\overline{\sigma}_U$	max $\overline{\sigma}_U$
13	32	0.51	0.64
14	96	0.51	0.82
15	96	0.53	0.97
16	32	0.62	1

(b)

Table 4.2: Overview of the relevant parameters obtained in figures 4.2: (a) shows the results for $f_{MAX}(x)$, (b) shows the results for $f_{SUM}(x)$.

links considering all the junctions, but it is possible that such solutions have a high value of $f_{MAX}(x)$. Therefore, even if total value of unobserved links is minimised, this approach allows some junctions to have a high number of unobserved links and therefore there might be some estimated flows with a high variance. In conclusion, it can be said that choosing a solution that minimises a $f_{MAX}(x)$ or $f_{SUM}(x)$ does not guarantee that it is optimal (i.e. it minimises the variance $\overline{\sigma}_U$). However, a more accurate solution is obtained combining the two methods together. It consist to select the candidate solutions $x \in C$ that minimise both cost functions $f_{MAX}(x)$ and $f_{SUM}(x)$. Then, in this case, it is selected the solutions x that has $f_{MAX}(x) = 2$ and $f_{SUM}(x) = 13$. In table 4.3 all solutions that minimise the cost $f_{MAX}(x)$ and $f_{SUM}(x)$ are reported. Note that the selected combination generates the variance that is not equal to the minimum value $\overline{\sigma}_U = 0.51\ m^6/s^2$, but it varies in a narrow range $\overline{\sigma}_U \in [0.55, 0.6]\ m^6/s^2$. Although the mean variance $\overline{\sigma}_U$ is not minimised, the chosen solution minimises the largest and the cumulative number of unobserved links connected to each non-centroid node minimising the risk of uncertainty accumulation and propagation. Moreover, the variance that is used in this simulation is an arbitrary value, so choosing a solution that minimises at most $\overline{\sigma}_U$ with $\sigma^2 = 0,2\ m^6/s^2$ for each measured flow can be deleterious. Indeed, such a solution applied in a practical context, where each channel has different variance, may lose its performance. In conclusion, it can be stated that solutions that minimise both cost functions can be considered good solutions because, even if they do not minimise variance, the values obtained are close to the minimum. In table 4.3 all solutions that minimise the cost function $f_{MAX}(x)$ and $f_{SUM}(x)$ are presented, in particular it is shown the observed and unobserved links and the mean variance $\overline{\sigma}_U$. In total there are 14 solutions, figure 4.3 illustrates the combination shown in row 3 of table 4.3. In particular, the red links are the links whose flow is estimated, while the blue

links are equipped with a sensor. This solution is chosen as an example, indeed the others solution in Tab.4.3 have similar performance. The fact that there is more than one solution is an advantage because it is possible to exploit this degree of freedom to satisfy a secondary task. For example, it is possible to choose the combination that measures directly channels that are more critical for the task, e.g. the channels with an higher risk of overflow can be choosen.

Unobserved link	Observed link	$\overline{\sigma}_U$ $[m^6/s^2]$	$\max_i \Sigma_{U,ii}(x)$ $[m^6/s^2]$
$[1,5,7,9,11,12,14,16,17]$	$[2,3,4,6,10,12,15,18]$	0.6	1
$[1,5,7,9,11,12,14,16,18]$	$[2,3,4,6,8,10,12,15,17]$	0.6	1
$[1,5,7,9,11,13,14,16,17]$	$[2,3,4,6,8,9,13,15,18]$	0.55	0.8
$[1,5,7,9,11,13,14,16,18]$	$[2,3,4,6,8,9,13,15,17]$	0.55	0.8
$[1,5,7,10,11,12,14,16,17]$	$[2,3,4,5,8,9,13,15,18]$	0.55	0.8
$[1,5,7,10,11,12,14,16,18]$	$[2,3,4,5,8,9,13,15,17]$	0.55	0.8
$[1,6,7,10,11,12,14,16,17]$	$[1,3,4,6,8,10,13,15,18]$	0.60	1
$[1,6,7,10,11,12,14,16,18]$	$[1,3,4,6,8,10,13,15,17]$	0.60	1
$[2,5,7,9,11,12,14,16,17]$	$[1,3,4,6,8,10,12,15,18]$	0.60	1
$[2,5,7,9,11,12,14,16,18]$	$[1,3,4,6,8,10,12,15,18]$	0.60	1
$[2,5,7,9,11,13,14,16,17]$	$[1,3,4,6,8,10,12,15,18]$	0.55	0.8
$[2,5,7,9,11,13,14,16,18]$	$[1,3,4,6,8,10,12,15,17]$	0.55	0.8
$[2,5,7,10,11,12,14,16,17]$	$[1,3,4,6,8,9,13,15,18]$	0.55	0.8
$[2,5,7,10,11,12,14,16,18]$	$[1,3,4,6,8,9,13,15,17]$	0.55	0.8
$[2,6,7,10,11,12,14,16,17]$	$[1,3,4,5,8,9,13,15,18]$	0.60	1
$[2,6,7,10,11,12,14,16,18]$	$[1,3,4,5,8,9,13,15,17]$	0.60	1

Table 4.3: All solutions that minimise both the cost function $f_{MAX}(x)$ and $f_{SUM}(x)$ with corresponding mean variance and maximum variance.

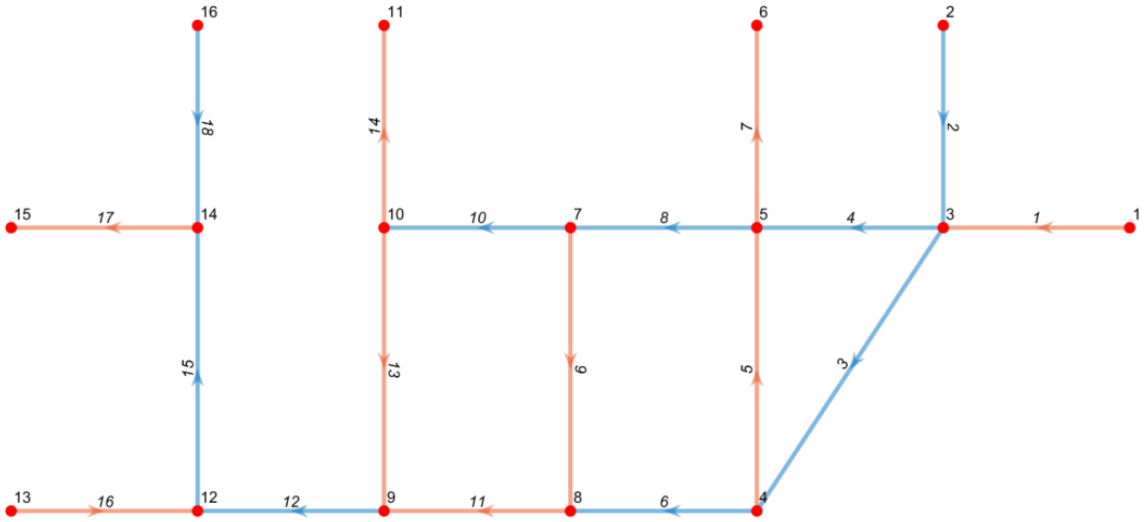

Figure 4.3: Example of solution that minimises both the cost function $f_{MAX}(x)$ and $f_{SUM}(x)$. The links highlighted in blue are those equipped with sensors, while the flow of those highlighted in red are estimated.

CHAPTER 5

Network Model for open-channel systems

In the previous chapters, models for open-channel and junctions have been presented. In this chapter they are used to create a model for open-channel networks. The purpose of this model is to analyse the functionality of the network under stress, i.e. when the drainage capacity is low and there is a large amount of rainwater to drain. In particular, the proposed model describes the flow and water heights of the channels taking into account the backwater effect. In a channel, this phenomenon is generated by the fact that if the outflow of the channel is smaller than the inflow, the water is slowed down and it accumulates generating a rise the water level. The IDZ model accurately describes this phenomenon for a channel but, in a network, the backwater effect also propagates through the junctions; hence, it is necessary to develop a model. To model a open-channel network, it is divided into components that can be classified into the following groups: channels, control structures and junctions. Each element is described using an appropriate model and then these are coupled to build up the model of the network. To represent the network, it is used a digraph $\mathcal{G} = (\mathcal{V}, \mathcal{E})$ identified by a set of vertices (nodes) $\mathcal{V}$ and a set of edges (links) $\mathcal{E}$. The cardinality of the sets are denoted as $|\mathcal{V}| = N$ and $|\mathcal{E}| = M$. In this chapter, the index i is used for referring to a link, therefore $i \in [0, M]$. While for referring to a node it is used index $j \in [0, N]$. Also it is used the set $E(j)$ which contains the label of the links incident to node j. The cardinality of the this set is called $n_j = |E(j)|$ and it is the number of both incoming and outgoing links incident to node j . The set $E(j)$ is composed of two subsets $O(j)$ and $I(j)$, which are respectively the sets that contain the labels of the incoming and outgoing links of the node j. Each link and node of the digraph $\mathcal{G}$ represents an element of the network (i.e channel, control structures or junctions). In the following paragraphs, it is provided a more detailed description of this network.

Network link

Edge links represent the channel branches, they are defined as any section of watercourse at which extremities there are control structures or junctions. In this way, in each channel branch, the flow enters only from upstream end and exits from downstream. The direction of the link is chosen in agreement with the usual direction of the flow, which is given by the slope of the channel. Hence, the tail of the links indicates the inlet of flow into the channel, while the head indicates the outlet. Note that, in this thesis, the flow directions are fixed according to the initial conditions and during the simulation of the model, the directions do not change.

The objective of this definition is to divide the watercourses into sections that meet the conditions necessary to apply the IDZ model. In particular, this definition guarantees that flow enters only from upstream end and exits from downstream end. Moreover, it is guaranteed that there is not any control structures within the branch. The other hypotheses necessary to apply the IDZ model are described in detail in the chapter 2. The most important assumptions are listed below:

- The lateral inflow of branches is negligible, so the flow enters only from upstream end and exits only from downstream end;
- The branch needs to be straight with a cross-section with a know shape (in this case it is used a trapezoidal cross-section). Also the variations of the cross-section sizes as bottom width and lateral slope along the channel need to be small;
- The slope $S_b(x)$ is considered constant over the channel length;
- The effect of friction is modeled using Manning's equation, this formula is reported in appendix A.1;
- The pressure to which water is subject is hydrostatic, namely the pressure increases in proportion to depth measured from the surface downward.

The first two assumptions require that the channels have constant cross-section sizes. In addition, the effect of the bends on the flow state is neglected for simplicity. Therefore, a link can represent a segment of a real channel with many bends. The last assumption requires that the pressure to which water is subject is hydrostatic and it is guaranteed in the case where the channel has a cross-section on top and the bed slope S_b is small enough to ensure that $\arctan(S_b) \simeq 0$. (see section 2.1 for more details). However, the Cavallino network has channels with a cross-section closed

on top also called pipelines. These channels can be modelled as an open-channel as long as the pipes are partially full and, therefore, when the pressure on the water is hydrostatic. However, when the pipe is full, the pressure increases and the flow becomes pressurised. The advantage of this situation is that it is no longer necessary to model the height of the water because it is constant and imposed by the size of the pipe. The flow through the pipe is influenced by the pressure, it can be derived using the Bernoulli equations A.4. In this chapter, the pressurised flow is not considered, it is indeed assumed that the pipelines have a constant flow over time.

Network nodes

The nodes of the graph represent the junctions, the control structures, the inlet and the outlet of the network. They can be grouped into the following categories:

- Junction nodes represent the the junctions between channel;
- Control nodes represent the control structure;
- Inlet nodes represent the entry points of the network flow;
- Outlet nodes represent the outlet points of the network flow.

To each junction node is assigned a model that describes the flow of a junction between two or more branches. In particular, the proposed model does not describe in detail the dynamics within the junction, but it only provides a relationship between the boundary conditions of the junction. The control nodes represent the control structures. For example, given a water course in which there is a gate along its path, this channel cannot be modelled as a single branch link because the IDZ model is not able to describe the control structures. Therefore, it is necessary to split the channel into two branches (i.e links) connected by a control node. In this way one has two channel sections in which there are no control structures along their path, so it is possible to describe both of them through the IDZ model. Often control structures are allocated in proximity to junctions or to an outlet of the network. In this case, the structures are not represented by a control node but they are integrated in the junction node or in the outlet node. Inlet and outlet nodes represent the entry and the exit points of the network. The flow at these points it is usually regulated by a control structure such as a gate or a water pump. To the inlet nodes it is assigned the value of the inflow known a priori without considering any control structure model. To outlet node, if it represents a water pump, it is assigned the value of the flow that exits such a node, while if it represents a gate, it is assigned the of control structure.

In conclusion, these paragraphs present the various components of the network, the models assigned to each type of node and link are introduced in the following.

5.1 Notation

Before introducing the models that describe the elements of the network, it is necessary to present the variables used to denote the flow state of the network. The variables used to describe the flow state of each link i (i.e the i-th channel branch) are the water flow $Q_i(x,t)$ and water height $Y_i(x,t)$. These quantities have already been introduced in section 2.1 for an individual channel and they are inherited by the network model. In particular, recall that flow and height are considered one-dimensional quantities: they are assumed to vary only along the channel length, while they are constant over the cross-section. The direction of the flow is given by the slope of the channels or, in case they are flat, by the direction of the flow at the initial instant the simulation, this direction coincides with the direction of the digraph links $\mathcal{E}$. The variables $Q_i(x,t)$ are considered positive if the flow is oriented along this direction, otherwise they take a negative value.

The variables just introduced describe the flow of a single channel. To describe the flow state for the whole network vectors $Q(x,t)$ and $Y(x,t)$ are used. Vector $Q(x,t)$ collects the flows of all channels $Q_i(x,t)$, $\forall\, i \in [1,M]$. Vector $Y(x,t)$ collects the heights of all channels $Y_i(x,t)$ $\forall\ i \in [1,M]$. In this case, since the IDZ model is used, it is necessary to know only $[Q_i(0,t), Q_i(L_i,t)]$ and $[Y_i(0,t), Y_i(L_i,t)]$, which are respectively the inflow and outflow of the i-th channel, also called boundary condiction of the channel. Indeed, this model describes the height of water the channel using only $[Q_i(0,t), Q_i(L_i,t)]$ and, therefore, it is not necessary to know the flows for each value of t and x. In particular, the IDZ model describes the dynamics of the height $[Y_i(0,t), Y_i(L_i,t)]$. The most interesting height is $Y_i(L_i,t)$ because, according to the IDZ model, the water tends to accumulate towards the downstream side. Then, since we want to study the capacity to resist overflow, the most sensitive point is considered to be $x = L_i$. In conclusion, the state of the network is represented by the vectors $Q(x,t)$ and $Y(x,t)$, whose i-th element is defined as:

$$Q_i(x,t) = [Q_i(0,t),\ Q_i(L_i,t)] \ \text{ and } \ Y_i(x,t) = [Y_i(0,t),\ Y_i(L_i,t)],\ \ \forall i \in \mathcal{E} \qquad (5.1)$$

The dimension of both vectors is $2 \times M$. To describe the flow state of the nodes, it is not necessary to introduce any other variables. The junction model that is used does

not provide the evolution of a flow within the junction but only provides relationships between the boundary conditions of the junction. The latter coincides with the boundary conditions of the channels connected to that junction. In particular, given the node $j \in [0, N]$ the flow state is described by the following element of the vectors $Q(x,t)$ and $Y(x,t)$:

$$[Q_i(0,t), Y_i(0,t)], \ \ \forall i \in O(j) \ \text{ and } \ [Q_i(L_i,t), Y_i(L_i,t)], \ \ \forall i \in I(j); \tag{5.2}$$

where $I(j)$ is the set of the incoming links to node j, and $O(j)$ is the set of the outgoing links from node j.

5.2 Open channel modeling

In the previous paragraphs, links are defined as the elements of the network $\mathcal{G}$ that represent the channel branches. To model these elements, the discrete-time version of IDZ model is used. The latter is presented in detail in section 2.5.2, in the following its equations are reported.

$$\begin{cases} y_i(L, t+T_s) = y_i(L,t) + \frac{T_s}{A_{d,i}}(q_i\,(0, t-\tau_{d,i}) - q_i(L,t)); \\ \\ y_i(0, t+T_s) = y_i(0,t) + \frac{T_s}{A_{u,i}}(q_i\,(0,t) - q_i(L, t-\tau_{u,i})); \end{cases} \tag{5.3}$$

where, for each channel $i \in \mathcal{E}$:

- $q_i(0,t)$ and $q_i(L_i,t)$ stand for the deviations of upstream and downstream discharges respectively from the initial conditions $Q_i(0,0)$ and $Q_i(L_i,0)$;
- $y_i(0,t)$ and $y_i(L_i,t)$ stand for the deviations of upstream and downstream water depths respectively from the initial conditions $Y_i(0,0)$ and $Y_i(L_i,0)$;
- $A_{d,i}$ and $A_{u,i}$ are respectively the upstream and downstream equivalent backwater area.
- $\tau_{d,i}$ is defined as the time required for a perturbation of input flow $q_i(0,t)$ to travel from the upstream to the downstream end of channel and to have effect on the downstream height $Y_i(L,t)$.
- $\tau_{u,i}$ is defined as the time required for a perturbation of output flow $q_i(L_i,t)$ to travel from the downstream to the upstream end and to have effect on the downstream height $Y_i(0,t)$.

- T_s is the sampling time;

Recall that the IDZ model also has parameters $P = [p_{11}, p_{12}, p_{21}, p_{22}]$; in this chapter they are neglected by setting them to zero. This simplification does not lead to a radical change of the IDZ model dynamics, indeed parameters P give a small contribution compared to the integrator effect, which is the core of the model. The discrete-time version of IDZ model is used because open channel network models include nonlinearities such as the backwater effect propagation on the junction and control structure structures. For this reason it is chosen to implement the network model in discrete time. Consequently, since the IDZ model is used to model the channels, it has to be discrete. Note that the IDZ model calculates the heights $y_i(0,t)$ and $y_i(L_i,t)$ given the boundary conditions of flow $q_i(0,t),\ q_i(L_i,t),\ \forall t$. These four quantities are respectively the deviations of heights and the flows with respect to the initial conditions and then they are calculated as:

$$\begin{aligned} y_i(0,t) &= Y_i(0,t) - Y_i(0,0), \quad y_i(L_i,t) = Y_i(L_i,t) - Y_i(L_i,0) \\ q_i(0,t) &= Q_i(0,t) - Q_i(0,0), \quad q_i(L_i,t) = Q_i(L_i,t) - Q_i(L_i,0) \end{aligned} \tag{5.4}$$

where $Y_i(0,0),\ Y_i(L_i,0)\ Q_i(0,0)$ and $Q_i(L_i,0)$ are the initial conditions of the flow in the channel i. Thus note that, given the initial conditions, it is possible to switch from the notation of the model 5.3 to the notation used to define the state of the network 5.1 (and vice versa) without difficulty. In general, the initial condiction of the system is represented by $[Q_i(x,0), Y_i(x,0)]\ , \forall x \in [0, L_i]$ for each channel $i \in \mathcal{E}$ of the network. In particular, the IDZ model assumes that, at the initial time, the flow in the channel i is steady and it is constant along it. This implies that:

$$Q_i(x,0) = Q_{0,i}, \forall x \in [0, L_i] \tag{5.5}$$

Then the flow of each channel at the initial time can be represented by a scalar value called $Q_{0,i}$ which has to be known a priori. Moreover, it is defined the vector Q_0 that collects these values, i.e. its i-th element is $Q_{0,i}$. Furthermore, it is assumed that the height along each channel $i \in \mathcal{E}$ is uniform:

$$Y_i(x,0) = Y_{0,i},\ \forall x \in [0, L_i]. \tag{5.6}$$

Then, at the initial time, the water height can be represented by a scalar value called $Y_{0,i}$. Also, it is defined the vector Y_0 that collects these values $\forall i \in \mathcal{E}$, i.e. its i-th

element is defined as $Y_{0,i}$. Note that, given the values of flows Q_0, the water height Y_0 can be calculated in closed form using the inverse Manning's formula A.1. In conclusion, according to the assumptions of IDZ model, the initial conditions of all channels in the network are characterised only by the vector Q_0, that has to be known a priori.

5.3 Junction modeling

The aim of the proposed junction model is to provide relationships between the boundary conditions of the junction. Indeed, the IDZ model 5.3 calculates the height $Y_i(0,t)$ and $Y_i(L_i,t)$ given the boundary conditions of flow $[Q_i(0,t), Q_i(L_i,t)]$, $\forall t$. The latter are provided by models associated with the nodes connected to link. This model is based on flow conservation equation that, for the j-th junction, it is written as:

$$\sum_{i \in I(j)} Q_i(L_i,t) = \sum_{i \in O(j)} Q_i(0,t), \tag{5.7}$$

where summation on the l.h.s. is the sum of flows entering in the junction j, while the summation on the r.h.s. is the sum of its outflows. Therefore, Eq.(5.7) states that, in a junction, the sum of inflows is equal to the sum of outflows.

However, note that (5.7) is derived under the assumption that the flows are steady, i.e they do not change over time. This assumption is not valid in general, indeed the IDZ model describes the behaviour of the water assuming that the flow is steady only at the initial condition $t = 0$; while for $t \neq 0$ the flow is unsteady. Then (5.7) is valid only for the initial time. Therefore, it is necessary to find a model that is able to describe the flow through a junction for the unsteady flow. Also, this model needs to be suitable for junctions with an arbitrary number of branches.

Another aspect that the model has to consider is the propagation of backwater effect over the junction. In the channels, the backwater effect occurs if the outflow $Q(L,t)$ is smaller compared to the inflow $Q(0,t)$. In this case, the water is slowed down and it accumulates generating a rise of the level. This accumulation develops from the downstream side of the channel and it propagates towards the upstream side. When this phenomenon affects the flow over the entire length of the channel, it causes a reduction of the flow passing trough the channel. In this situation, the channel is said to be in *full backwater* state. In particular, if the outflow $Q(L,t)$ is equal to the inflow $Q(0,t)$, there is no water accumulation in the channel so, its height does not rise. In this case, the channel is not affected by backwater. On the

other hand, suppose that its outflow $Q(L,t)$ is less than $Q(0,t)$ because it is regulated by a water pump with constant drainage capacity. In this case, the water level at the downstream end of channel rises due to accumulation of water and this growth propagates towards the upstream side. When this phenomenon affects also the upstream end, i.e height of channel at the upstream side increases due to accumulation of water, it causes a reduction of the flow passing trough the channel. In particular, the input flow is enforced by the output flow and therefore, since $Q(L,t)$ is less than $Q(0,t)$, the input flow is reduced.

At this point, i.e when a channel is in *full backwater* state, it is expected that this effect propagates also through the junction toward the entrance of the channel.

Therefore, to model the propagation of this phenomenon over the junction, two elements are required:

- The condition to detect whether a channel connected to the junction is in full backwater state;
- A procedure to redistribute flows among the channel junctions.

Backwater detection

The condition presented to detect whether the channel connected to the junction is in a full backwater state is based on the height of the channels. Let us consider a generic junction j, the water heights at its boundaries are represented by the following variables

$$Y_i(0,t) \ \ \forall i \in O(j) \ \text{ and } \ Y_i(L_i,t) \ \ \forall i \in I(j); \tag{5.8}$$

which are respectively the heights of the flows leaving the junction j from the links $O(j)$ and heights of the flows entering the junction from the links $I(j)$.

The proposed condition is based on the observation that water flows out from the junction through the channel $i \in O(j)$ only if the water height in the junction is higher than the one of the channel. Thus, it is necessary to define the water level inside the junction. Indeed, so far, it is introduced only the water levels at the boundaries of the junction (5.8) which coincide with the heights at the boundary of the connected channels. The water level inside the junction is thus defined as the average value of these heights and calculated as follows:

$$Y_{mean,j} = \frac{1}{|E(j)|} \left(\sum_{i \in O(j)} Y_i(0,t) + \sum_{i \in I(j)} Y_i(L_i,t) \right). \tag{5.9}$$

Therefore, the junction is affected by the backwater effect there exists at least one channel $i \in O(j)$ in full backwater state. This happens if:

$$Y_i(0,t) > Y_{mean,j}. \tag{5.10}$$

All the channels $i \in O(j)$ of junction j that satisfy (5.10), (i.e the channel in full backwater state) are collected in the *backwater set*, denoted with $B(j)$.

Flow distribution

The other fundamental aspect to define is how the water flow is redistributed once the backwater effect influences the junction. In particular, the junction can be in three situations:

- No channel is in full backwater state;
- Only part of the outgoing channels are in full backwater state;
- All outgoing channels are in full backwater state.

In the first case, when the junction is affected by backwater effect, the output flows of the junction j are established by the inflows. In particular, it is used a vector called split ratio SR_j in which each of the elements $SR_j(i)$ indicates the portion of the total inflow that flows out from the junction branch $i \in O(j)$. This vector is derived using the flows at the initial time, i.e each element $SR_j(i)$ is calculated as:

$$SR_j(i) = \frac{Q_i(0,0)}{\sum_{k \in I(j)} Q_k(L_k,0)}, \ \ \forall i \in O(j), \tag{5.11}$$

where $Q_i(0,0)$ is the flow that goes out from the junction branch $i \in O(j)$, while the denominator is the total inflow of the junction j.

This vector is used to model the flow during simulation. In particular, it calculates the output flow of each junction branch $i \in O(j)$ given the total input flow in the following way:

$$Q_i(0,t) = SR_j(i) \sum_{k \in I(j)} Q_k(L_k,t), \ \ \forall i \in O(j), \tag{5.12}$$

where $Q_i(0,t)$ is the inflow of the branches $i \in O(j)$ at time t and $\sum_{k \in I(j)} Q_k(L_k,t)$ is the total inflow of junction at time t. Note that $Q_i(0,t)$ is the inflow of the branches, but it is also the outflow of the junction through the branch $i \in O(j)$.

In the case when only a part of the outgoing channels are in full backwater state, it is necessary to calculate the reduction of outflow caused by the backwater effect. This can be obtained by using the following formula:

$$Q_{BW,j} = \sum_{i \in B(j)} Q_i(0,t) - Q_i(L_i,t), \tag{5.13}$$

where $Q_i(0,t)$ is the outflow from each channels $i \in B(j)$ calculated without considering backwater effect, so with (5.12). While $Q_i(L_i,t)$ is the outflow of the junction branches $i \in B(j)$ calculated considering backwater effect. In conclusion, $Q_{BW,j}$ is the difference between the junction outflow that would have occurred, if no channel had been in backwater and the junction outflow affected by backwater effect. The flow $Q_{BW,j}$ is supposed to be redirected into the other outgoing channels not yet in the backwater; in particular, it is split between them uniformly.

In the last scenario, all the output channel of the junction are affected by the backwater. In this case, there is no output channels in which the flow can be redirected. Therefore the backwater affects the input flow. In particular, the inflow is reduced and it is given by the following formula:

$$Q_{IN,j} = \sum_{i \in O(j)} Q_i(0,t) = \sum_{i \in O(j)} Q_i(L_i,t), \tag{5.14}$$

where $Q_{IN,j}$ is the total inflow of the junction. The first equality represents the flow conservation equation which states that, in a junction, the total inflow is equal to the outgoing flow. The second equality derives from the fact that, since all output channels are in backwater state, $Q_i(0,t) = Q_i(L_i,t)$, $\forall i \in O(j)$. In this case, the backwater effect reduces the input flow of the junction. Eq.(5.14) gives the total incoming flow of the junction when all the output channels of the junction are affected by the backwater. However, it is necessary to understand how the flow of each individual input branch is affected.

To do that, it is used a vector called input split ratio ISR_j in which each elements $ISR_j(i)$ indicates the portion of flow entering from the branch $i \in I(j)$. This is derived by using the flow of the initial conditions; in particular, each element $ISR_j(i)$ is calculated dividing the inflow of each junction branch by the total inflow as follows:

$$ISR_j(i) = \frac{Q_i(L_i,0)}{\sum_{k \in I(j)} Q_k(L_k,t)}, \quad \forall i \in I(j). \tag{5.15}$$

This vector is used to split $Q_{IN,j}$ calculated by (5.14). In particular, given $Q_{IN,j}$, the inflow of each junction branch $i \in I(j)$ is determined in the following way:

$$Q_i(L_i, t) = ISR_j(i)Q_{IN,j}, \quad \forall i \in I(j), \tag{5.16}$$

where $Q_i(L_i, t)$ is the inflow of the branch $i \in I(j)$ and the $Q_{IN,j}$ is the total inflow of junction. Note that the model presented is designed for junctions with more than two channels. However, this model can also be used to describe a junction with only one input and one output branch. In particular, this junction can be characterized by two conditions. In the first, the outgoing channel is not in backwater, so one has $SR_j = 1$. Therefore, the outflow is imposed by the inflow, i.e $Q_k(L_k, t) = Q_i(0, t)$ where $i \in I(j)$ and $k \in O(j)$. Instead, if the unique outgoing channels are in backwater, the input flow is imposed by the output flow, hence one has $Q_i(0, t) = Q_k(L_k, t)$, where $i \in I(j)$ and $k \in O(j)$.

5.4 Control node modeling

Control nodes have only two incident links, representing two channels, one with a flow entering the node and one with an outgoing flow. The links are respectively labelled with $i \in O(j)$ and $k \in I(j)$, where j is the label of the node. The control nodes represent the control structures. For simplicity, in this thesis only the submerged gate structures are considered. They consists in a movable bulkhead that allow water to pass through a hole between the channel bed and their submerged crest of bulkhead. (for more detail see appendix A.5). The flow passing through the gate is determined by the water heights at both sides of the structures. Therefore, these structures impose a flow that is determined by the following formula:

$$Q_k(L_k, t) = C_d W_j H_j \sqrt{2g(Y_k(L_k, t) - Y_i(0, t))}; \tag{5.17}$$

where H_j is the height of the gate hole, W_j is the width of gate hole and $Y_k(L_k, t)$ is the water level of the gate side in which flow enters and $Y_i(0, t))$ is the water level of the gate side in which the flow exits. Parameter C_d is called discharge coefficient and, for the gate, it is set to 0.6. Note that this formula is valid only if the gate is in submerged flow condition, i.e. when the flow is subcritical on both sides of the junction. This condition is guaranteed in the simulations proposed in 5.6 , indeed the channels analysed are almost flat. Consequently, the flow is characterised by a slow speed and thus also the Froude number is low; typically it is about $F_d \simeq 0.1$. Recall that

the flow is considered subcritical if its Froude number is less than 1. Furthermore, (5.18) is valid under the assumption that the flows upstream and downstream of the control structure are steady. This assumption is not verified in general, indeed it is assumed that the flows are steady only at the initial instant of the simulation. During the simulations, in general, the flows are unsteady so (5.18) is invalid. However, this formula is still used because, if the flows vary slowly overtime, they can be approximated as steady since their variation over time is small and then it can be neglected. However, (5.18) can be used although it has to be taken into account that it gives an approximate result.

5.5 Inlet and outlet node modeling

The inlet nodes have one incident link that represents a channel with an outgoing flow from the node. This link is labeled with $i \in O(j)$, where j is the label of inlet node. These nodes are not assigned to a model, but they are associated with the value of the flow entering the network which is $Q_i(0,t)$. In particular, the inflow can be decomposed as $Q_i(0,t) = Q_i(0,0) + q_i(0,t)$, where $Q_i(0,0)$ is the value of flow at $t = 0$, (i.e it is the initial value of flow), while $q_i(0,t)$ is the variation of the inflow at time t w.r.t the initial value. Both quantities have to be known a priori, since these are respectively the initial conditions and the boundary conditions of the inflow.

The outlet nodes represent the points at which the flow leaves the network. They have only one incident link that represents a channel with an incoming flow into the node. This link is labeled with $k \in I(j)$, where j is the label of outlet node. To this type of node two models can be assigned. In the first one the outlet flow $Q_k(L_k,t)$ is considered constant and known a priory. This model represents the case where the outlet flow is regulated by a water pump that forces a fixed outflow. The second possibility is that the outlet node is assigned to a model of a control structure, as for the control node. Also in this case it is considered only the submerged gate structure, thus the outflow of the node is

$$Q_k(L_k,t) = C_d W_j H_j \sqrt{2g(Y_k(L_k,t) - Y_E)}, \tag{5.18}$$

where H_j is the height of the gate hole, W_j is the width of gate hole and C_d is the discharge coefficient usually set to 0.6. Note that, in this case, it is know only the height $Y_k(L_k,t)$ which is the water height at the downstream side of the channel k.

Lastly, the Y_E stands for the height of the water of the external environment. In this thesis, for simplicity, this quantity is considered constant over time.

5.6 Numerical results

In this section, the model for open channel networks just presented is tested. In the first simulation, the model is tested with a simple network $\mathcal{G}_1$ in order to verify its proper functioning. The network $\mathcal{G}_1$, shown in Figure 5.1, is composed of $M = 4$ links and $N = 5$ nodes. Table 5.1 shows the type of each node in the network and the associated parameters.

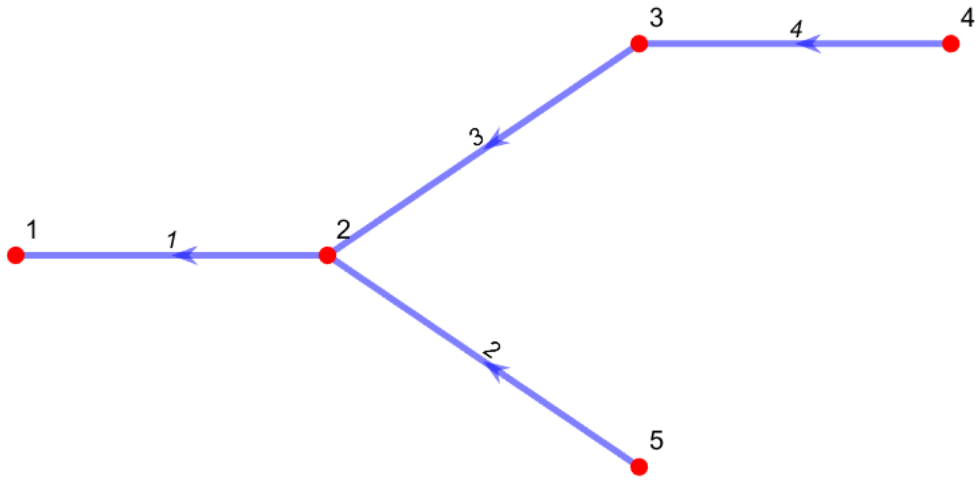

Figure 5.1: Network $\mathcal{G}_1$.

Node index	Type of node	Parameters
1	Outlet node with constant outflow	$q_2(L_2, t) = 0\ m^3/s$
2	Three-branches junction node	$n_2 = 3$
3	Two-branches junction node	$n_3 = 2$
4	Inlet node	$q_2(0, t) = 0.5\ m^3/s$
5	Inlet node	$q_4(0, t) = 0.5\ m^3/s$

Table 5.1: Summary of network $\mathcal{G}_1$ nodes parameters.

In the simulation it is assumed that the state of the network at the beginning (i.e $t = 0$) is in a steady equilibrium, so the flows are assumed to be steady, i.e they do not vary over time. Furthermore, the flow of each channel is assumed to be uniform, so it has a constant height over the length of each channel. Subsequently, this equilibrium is interrupted by a rainfall event that introduces a flow perturbation

into the network. Recall that IDZ assumes that the lateral inflow of branches is negligible, so the flow enters in the branches only from upstream end and exits only from downstream end. To satisfy this assumption it is supposed that the rainfall event introduces the flow into the network only through the input nodes. For the network $\mathcal{G}_1$, this nodes are $j = 4, 5$. Since the initial instant the flow is uniform and steady, flow conservation equation (3.2) and Equality model (3.3) can be used to describe the flow in the junction. The first one states that in a junction with two or more branches the incoming flows are equal to the outgoing ones. The initial conditions of the flow Q_0 are chosen according to this principle. In particular, network $\mathcal{G}_1$ has two junction nodes; therefore, flow conservation equation (3.2) provides two constraints which are required to be satisfied by the vector Q_0. These constraints are:

$$Q_{0,3} = Q_{0,4} \text{ and } Q_{0,1} = Q_{0,2} + Q_{0,3}. \tag{5.19}$$

Hence, for the choice of vector Q_0 two flows are fixed, in this case: $Q_{0,2}$ and $Q_{0,4}$; while the remaining two are found using (5.19). Flows $Q_{0,2}$ and $Q_{0,4}$ are chosen equal to 0.5 m^3/s; consequently, one has $Q_0 = [1, 0.5, 0.5, 0.5]$ m^3/s. These values are selected because, under the assumption that the flow is uniform, they are characterised by a velocity of nearly 0.15 m/s, which is a realistic value.

Furthermore, it is assumed that the water height is constant through the whole network. This statement results from the study of the Equality model 3.2. Indeed, if the Froude number that characterises the flow of each branch is sufficiently low (less than about 0.35), it is plausible to assume that the water height trough the junctions is constant. For the network $\mathcal{G}_1$, the flows Q_0 are characterised by a Froude number $F_d \simeq 0.01$, so the water height trough the junctions can be assumed equal. However, according the IDZ model, the flow is assumed to be uniform and then it is possible to calculate the water height with formula (A.3). According to the latter formula, if all the channels of $\mathcal{G}_1$ has the same geometrical sizes, the channel with a flow $Q_{0,i} = 0.5$ m^3/s have different water level respect channel 1 which has a flow $Q_{0,1} = 1$ m^3/s (i.e channel 1).

This is in opposition to the Equality model, since junction 2 of $\mathcal{G}_1$ has the inlet channel with an height of $Y_2(L_2, 0) = Y_3(L_3, 0) = 1.1$ m while the outlet channel has $Y_1(0, 0) = 1.40$ m. In order to match the IDZ model that uses (A.3) and the Equality model, it is adapted the geometrical dimensions of the channels. Table 5.2 shows the geometric parameters associated to each link (i.e. channel branches) of network $\mathcal{G}_1$. They are equally set for simplicity, with the only exception of the bottom width B_i which: for branch $i = 1$, $B_1 = 4$ m is chosen to ensure the height to be the same

along the whole network at the initial instant of simulation. For completeness, Table 5.2 also shows the values of the IDZ model parameters.

Link	$L[m]$	$m[\,]$	$B[m]$	$S_b[\,]$	$n[m^{1/3}/s]$	$A_{u,i}\ [m^2]$	$A_{d,i}[m^2]$	$\tau_{u,i}\ [s]$	$\tau_{d,i}\ [s]$
$i = 1$	500	1.5	4	0.0001	0.05	$3.93\ 10^3$	$3.31\ 10^3$	186	165
$i \in [2, 4]$	500	1.5	2	0.0001	0.05	$2.62\ 10^3$	$2.17\ 10^3$	200	179

Table 5.2: List of the channels parameters of network $\mathcal{G}_1$.

The other quantities required to simulate the model are the boundary conditions of the network. The latter are the outflow of the network $Q_1(L_1, t)$ and the inflows $Q_2(0, t)$, $Q_4(0, t)$. These quantities are equal to each other at the initial time. For $t \neq 0$ $Q_2(0, t)$ and $Q_4(0, t)$ increase due to the rain perturbation. Their variations are set to $q_2(0, t) = 0.5\ m^3/s$ and $q_4(0, t) = 0.5\ m^3/s$. The outflow $Q_1(L_1, t)$ is kept constant $\forall t$ and it is equal to its initial value $Q_1(L_1, t) = Q_{0,1} = 1\ m^3/s$, $\forall t$. In this way, at the initial time, the network is in equilibrium state with the network inflow equal to the network outflow. However, the outflow does not adapt to the perturbation $q_2(0, t)$ and $q_4(0, t)$; therefore, it is expected an accumulation of water over time and a consequent increase of the water depth in the network. In the sequel, it is reported the result of the simulation performed on the network $\mathcal{G}_1$ with the initial and boundary conditions just described. In particular, the simulation duration is one hour (i.e from $t = 0$ to $t = T_{sim} = 1\ h$) and it is executed with a sampling time $T_s = 60\ s$.

Numerical results for $\mathcal{G}_1$

Figures 5.2 shows the variables $Q_i(0, t), Q_i(L_i, t), Y_i(0, t), Y_i(L_i, t)$ for each branch $i \in \mathcal{E}$ of the network $\mathcal{G}_1$. To analyse the evolution of these variables over time, one may observe the branches $i = 2, 4$. The latter are the links from which the perturbations $q_2(0, t), q_4(0, t)$ enter in the network. In particular, in channel 2 it is observed that $Y_2(0, t)$ increases in time already from the initial instant, while $Y_i(L_i, t)$ does not vary. This is due to the IDZ model which assumes that the inflow $q_2(0, t)$ takes a time $\tau_{d,2}$ to reach the downstream end of the channel and thus to influence $Y_i(L_i, t)$. Therefore, at $t = \tau_{d,2}$, the perturbation $q_2(0, t)$ reaches the downstream end of branch 2. Indeed from Figure 5.2.b it is shown that, at this instant, the inflow becomes equal to the outflow (the instant $t = \tau_{d,2}$ is shown in figure 5.2.a with a red dashed line). This leads to the following events:

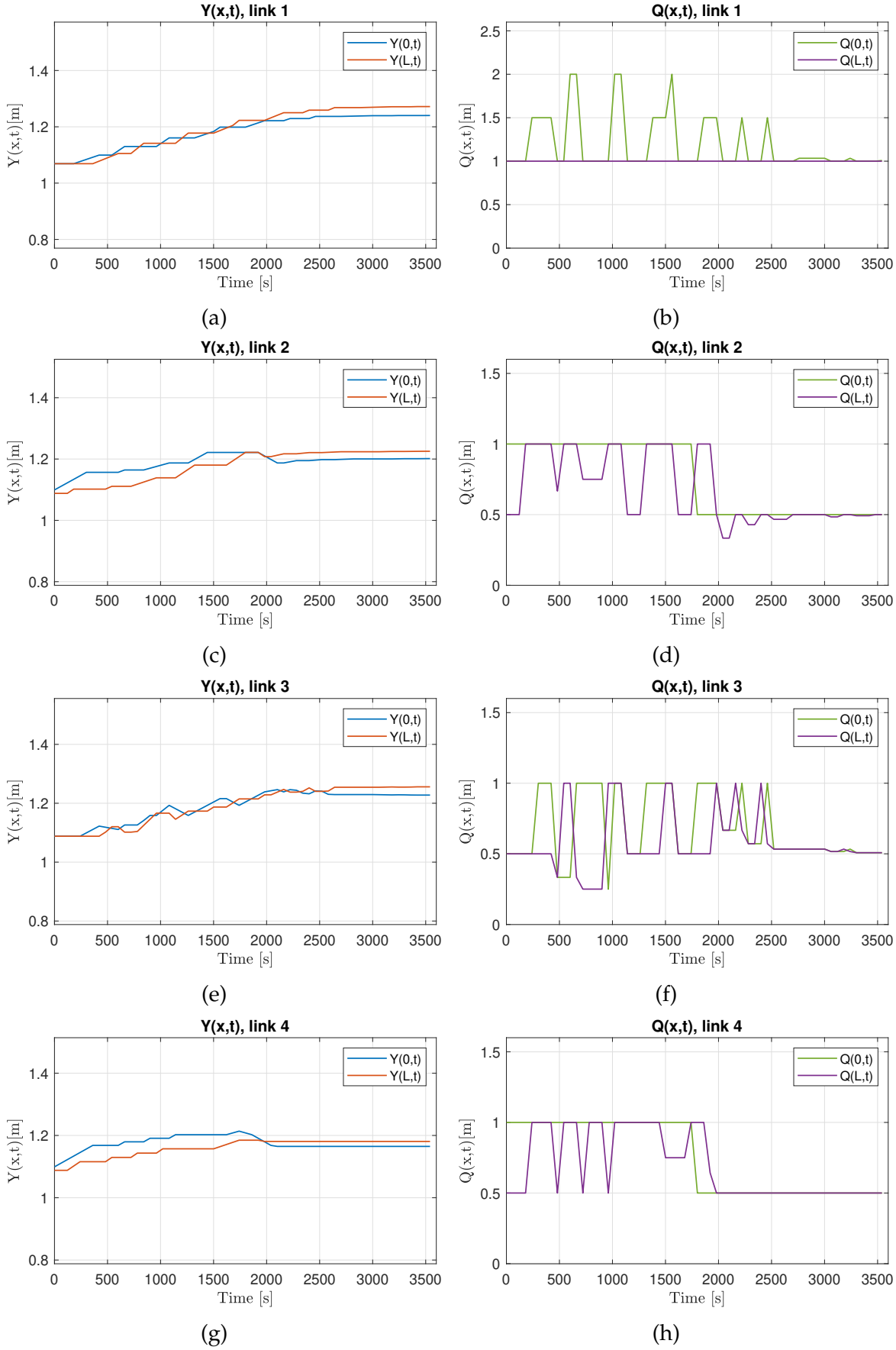

Figure 5.2: Flow states of all channel of network $\mathcal{G}_1$. The plots on the left column shows variables $Y_i(0,t)$ and $Y_i(L_i,t)$. The plots on the right column show variables $Q_i(0,t)$ and $Q_i(L_i,t)$.

- The flows $Q_2(0, \tau_{d,2})$ and $Q_2(L_2, \tau_{d,2})$ are equal since the latter is not influenced by backwater;
- The heights of channel 2 no longer increase since $Q_2(0, \tau_{d,2}) = Q_2(L_2, \tau_{d,2})$.
- The flow perturbation $q_2(0, t)$ has reached the junction, so it is instantly propagated to the output branch 1 whose inflow grows by $q_1(0, \tau_{d,2}) = 0.5\ m^3/s$.

Note that at $t = \tau_{d,2}$, the perturbation coming from node 5 has not yet reached the junction since it has to pass through two branches with the same size of branch 2. Then it takes a time $\tau_{d,3} + \tau_{d,4}$ to reach the junction that it is longer than $\tau_{d,2}$. Subsequently, $q_1(0, \tau_{d,2})$ propagates along channel 1 until it reaches the downstream end of it and thus to influence $Y_1(L_1, t)$. Recall that $Q_1(L_1, t)$ is considered constant at its initial value, so when the perturbation arrives at the downstream end, the channel cannot drain it. This generates a growth of the height $Y_1(L_1, t)$ and consequently of $Y_1(0, t)$, because the channel is flat, so the heights at the two ends grow almost simultaneously. The heights of channel $i = 1$ continue to grow until the backwater condition (5.10) is satisfied. Indeed, according to the junction model 5.3, if the $Y_1(0, t)$ exceeds $Y_{mean,2}$, the junction is subject to the backwater effect. In this case $Y_{mean,2}$ is the mean value of $Y_2(L_2, t)$ and $Y_3(L_3, t)$, since the inlet channels of the junction $j = 2$ are channels 2 and 3. At this point the following events occur:

Event 1 The input flow of channel 1 is reduced, in particular $Q_1(0, t)$ is imposed by $Q_1(L_1, t)$, i.e $Q_1(0, t) = Q_1(L_1, t)$. This implies that the water height in this channel stops rising;

Event 2 The backwater effect is propagated thought the junction, therefore downstream flow of branches 2 and 3 are reduced according to (5.14).

It follows that the heights in the branches 2 and 3 start to increase, because the backwater effect has reduced their outflow. In particular, $Y_2(L_2, t)$ and $Y_3(L_3, t)$ grow until they overtake $Y_1(0, t)$, so until the backwater condition 5.10 does not hold again. This leads to the following facts:

Event 3 Since the backwater condition is not satisfied the propagation of backwater effect is interrupted;

Event 4 $Y_2(L_2, t)$ and $Y_3(L_3, t)$ stop growing;

Event 5 $Y_1(0, t)$ increases until backwater condition (5.10) is satisfied again;

At this point, events 1 and 2 repeat, then $Y_2(L_2, t)$ and $Y_3(L_3, t)$ grow until they overtake $Y_1(0, t)$ again and hence also the events 3, 4 and 5 repeat. This process (i.e from events 1 to 5) repeats as long as the perturbation $q_2(0, t), q_4(0, t)$ end at time $t = 30\ min$. In practice, the backwater condition is satisfied repeatedly. Therefore:

- When this condition is not met, the water level in channel 1 increases until the condition (5.10) is met;
- When backwater condition is satisfied, the water height in the downstream channels of the junction (i.e. $Y_2(L_2, t)$ and $Y_3(L_3, t)$) increases until the condition (5.10) is not satisfied again.

This process leads to an increase in height over all the branches of the junctions during the period in which $q_4(0, t), q_5(0, t) \neq 0$. Figure 5.2 shows that the flows of the channels, during the period $[0, 30]\ min$, vary repeatedly. For example, Figure 5.2.b shows that $Q_1(L_1, t)$ is constant in time as imposed by the boundary condiction. Furthermore, it is observed that $Q_1(0, t)$ oscillates. This is due to the fact that the junction 2 is repeatedly affected by the backwater effect:

- When $Q_1(0, t) > Q_1(L_1, t)$, channel 1 is not in a full backwater state, then the water height along it grows;
- When $Q_1(0, t) = Q_1(L_1, t)$, backwater condition (5.10) is satisfied.

When $Q_1(0, t) = Q_1(L_1, t)$, the growth of the height in channel 1 is interrupted and the water height of the downstream channels of the junction (i.e. $Y_2(L_2, t)$ and $Y_3(L_3, t)$) grow. Therefore, to summarise, the plots in Figure 5.2 show that:

- The water heights of the channel increases while the network $\mathcal{G}_1$ is subject to the perturbations $q_2(0, t), q_4(0, t)$;
- When the latter end, i.e the network inflow returns to its initial value, the heights stabilise around a steady value reported in Table 5.3.

This is due to the fact that the output flow $Q_1(L_1, t)$ of the network is assumed to be constant during the whole simulation. As long as $q_2(0, t), q_4(0, t) \neq 0$, the input flow of the network is higher than $Q_1(L_1, t)$, so there is an accumulation of water inside the network. Whereas, when the inflow of network returns to its initial value, the inflow of the network equals the outflow. In this condition, the water quantity that flows out from the network coincides with the quantity that enters, so the accumulation caused by the disturbance is not drained and the water level remains

Link	$Y_i(x,0)$	$Y_i(L_i,T_{sim})$	$Y_i(0,T_{sim})$	$Q_i(x,0)$	$Q_i(L_i,T_{sim})$	$Q_i(0,T_{sim})$
1	1.1	1.27	1.23	1	1	1
2	1.1	1.23	1.21	0.5	0.5	0.5
3	1.1	1.24	1.22	0.5	0.5	0.5
4	1.1	1.23	1.20	0.5	0.5	0.5

Table 5.3: Comparison between the flow state at the initial and final instants of simulation with network $\mathcal{G}_1$. Note that Y(x,0) and Q(x,0) are constant $\forall x \in [0, L_i]$.

constant. In order to restore water heights to their initial values, it is necessary to have an outflow greater than inflow and this would generate a reduction of water levels in the network.

The latter case is tested in the following. In particular, the simulation for $\mathcal{G}_1$ is repeated with a different value of $Q_1(L_1,t)$ that is set to 1 m^3/s, which is slightly larger value than the one used so far. Figures 5.3 shows the variables $Q_1(0,t)$ $Q_1(L_1,t), Y_1(0,t), Y_1(L_1,t)$. Note that in the period of time ranging about from $[0, 360]$ s, $Y_1(L_1,t)$ decreases. This is due to the fact that $Q_1(L_1,t)$ is greater than $Q_1(0,t)$, so, according to the IDZ model, the water levels in the channels are reduced. At time $t = 360$ s perturbations $q_2(0,t), q_4(0,t)$ affect the flow in channel 1, then its water height starts to rise. This is due to the fact that, even if $Q_1(0,t)$ is higher than in the previous simulation, channel 1 is not able to drain completely the perturbations $q_2(0,t)$ and $q_4(0,t)$. Thus, the water levels still rise, yet more slowly than in the simulation 5.2.a. Finally, once the effect of the perturbations $q_2(0,t), q_4(0,t)$ is over at time $t = 30$ min, the network water height in the channel 1 does not start to decrease immediately (i.e immediately after $t = 30$ min), before channels 2 and 3 are drained. Indeed, figure 5.3.c shows the heights $Y_2(0,t)$ and $Y_2(L_2,t)$. Note that the latter decrease, since $t = 30$ min, while $Y_1(0,t)$ and $Y_1(L_1,t)$ remain constant at least in a first moment. This implies that, as $Y_2(L_2,t)$ decreases, the backwater condition (5.10) remains satisfied; then the difference between $Y_1(L_1,t)$ and $Y_{mean,2}$ increases, so that channel 1 stays in a full backwater state. This means that, according to the model in Sec.5.3, channels 2 and 3 are discharged, while channel 1 keeps at a constant water height. However it is expected that after the channels 2 and 3 are discharged, also channel 1 starts to discharge, but the model does not seem to be able to describe this aspect. To extend the model to describe this behaviour as well, backwater condiction (5.10) is modified. In particular, it is added another condition whereby if $Y_1(0,t) - Y_{mean,2} > 0.1$ m, then also the 1 channel starts to discharge.

Figure 5.3.a, shows the effects of this adjustment. In particular, when channels

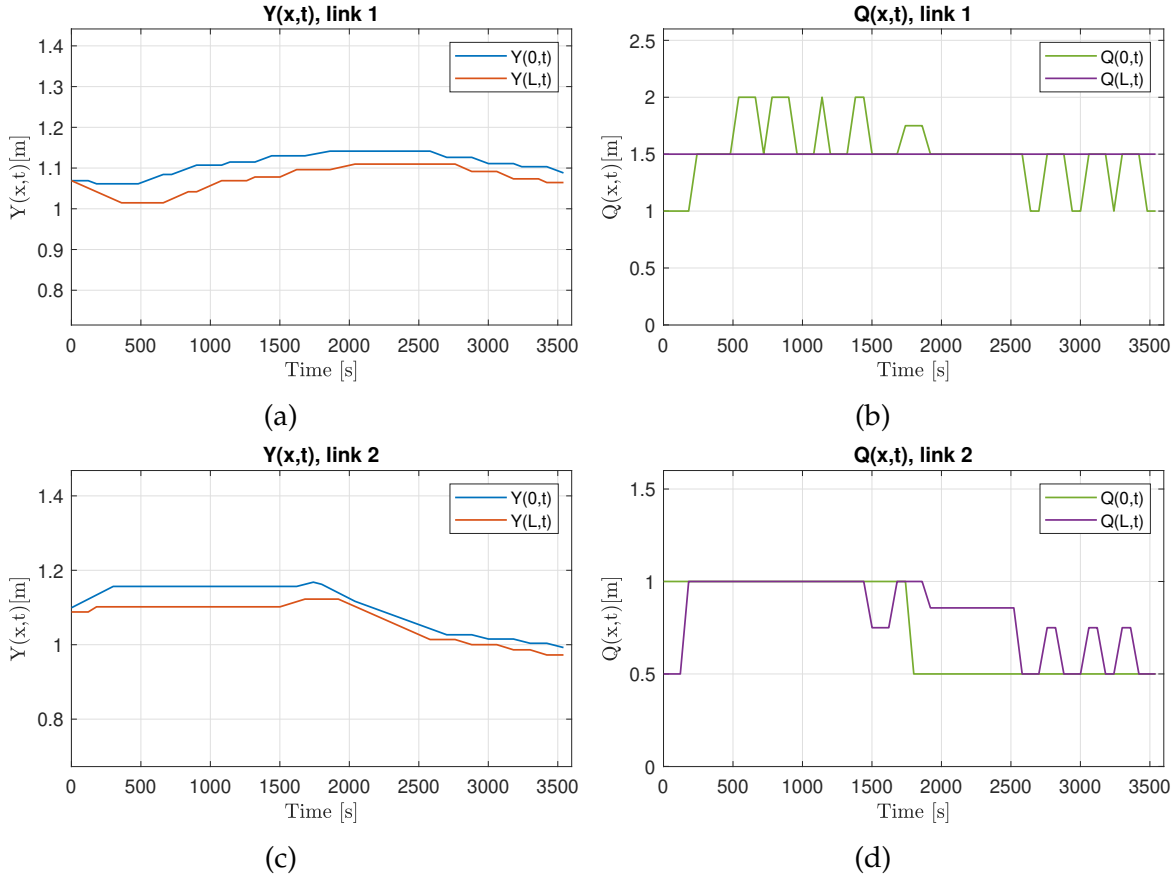

Figure 5.3: Flow states of channel $i = 1, 2$ of network $\mathcal{G}_1$. Simulation version with $Q_1(L_1, t) = 1\ m^3/s$.

2 and 3 have discharged sufficiently such that the average between $Y_2(L_2, t)$ and $Y_3(L_3, t)$ is 0.1 m less than $Y_1(0, t)$, then the channel downstream of junction 1 is reduced to $Q_1(0, t) = Q_2(L_2, t) + Q_3(L_3, t)$. By doing so, one has $Q_1(0, t) < Q_1(L_1, t)$, then the channel 1 is drained. In conclusion, from the simulations presented so far, it can be seen that the proposed model works correctly during the phase in which there is a disturbance that increases the height of the water. This phase is the most important for our purposes, since it allows to understand where the water accumulates in the network and, consequently, it can be used to understand which channels are most probable to overflow. However, it has been observed that the model has criticalities at describing situations in which the network is drained down. The proposed solution to overcome this issues works correctly, but is valid only for this specific simulation. Therefore, the next research direction is represented by the extension of the junction model presented in section 5.3 in order to describe also the case in which the network is drained down.

Link index	$L[m]$	$m[\,]$	$B[m]$	$S_b[\,]$	$n\ [m^{1/3}/s]$
Branches $i \in [1,9]$	500	1.5	2	0.001	0.05

Table 5.4: List of the channels parameters used in the simulation.

Numerical results of $\mathcal{G}_2$

In the third simulation the model is tested with the network $\mathcal{G}_2$ shown in Figure 5.4. This network is more complex than $\mathcal{G}_1$, indeed the links within it create a loop. It is composed of $M = 9$ links and $N = 9$ nodes. Table 5.4 shows the geometric

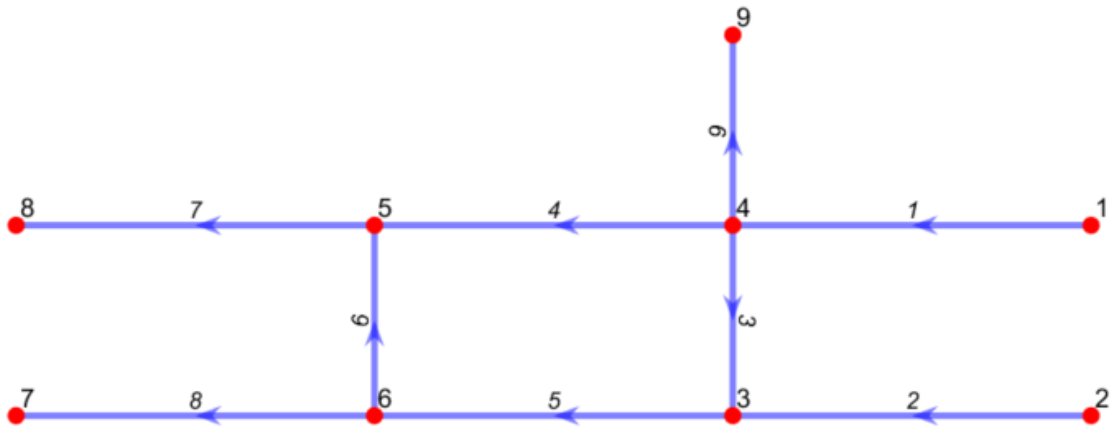

Figure 5.4: Network $\mathcal{G}_2$.

parameters associated to each link (i.e. channel branches). For simplicity, they are choosen with the same dimension.

As for $\mathcal{G}_1$, the initial conditions of the flow Q_0 are choose according to flow conservation principle (3.2). Then a part of the flows (i.e $i \in [1,2,3,4,7]$) are arbitrarily chosen such that they have plausible values [1] and the others are calculated with the equations provided by (3.2). Consequently, one has $Q_0 = [1, 0.25, 0.25, 0.5, 0.5, 0.25, 0.75, 0.25, 0.25]\ m^3/s$. In accordance with IDZ model, it is assumed that each channel has a uniform flow, i.e. it is characterised by a constant height over its entire length that can be calculated by means of the Manning's formula (A.3). In addition, unlike the simulations presented so far with $\mathcal{G}_1$, the Equality model is not used, therefore the water heights at the boundaries of the junctions are not set equal. The boundary conditions of network $\mathcal{G}_2$ are inflows $Q_1(0,t)$ and $Q_2(0,t)$ and outflow $Q_7(L_7,t)$. $Q_8(L_8,t)$, $Q_9(L_9,t)$. In particular, the inflows for $t \neq 0$ increase due

[1] The flow are choosen such that the water velocity is realistic therefore about $[0.1, 0.5]\ m/s$.

Link	$Y_i(x,0)$	$Y_i(L_i,T_{sim})$	$Y_i(0,T_{sim})$	$Q_i(x,0)$	$Q_i(L_i,T_{sim})$	$Q_i(0,T_{sim})$
1	1.39	1.42	1.5	1	2	2
2	0.69	1.4	1.40	0.25	1.25	1.25
3	0.69	0.91	0.91	0.25	0.86	0.86
4	0.99	1.55	1.55	0.5	0.27	0.5
5	0.99	1.05	1.05	0.5	0.77	2.11
6	0.69	1.04	1.04	0.25	0.48	0.48
7	1.21	1.29	1.28	0.75	0.75	0.75
8	0.68	1.17	1.17	0.25	0.25	0.25
9	0.68	1.20	1.16	0.25	0.25	0.86

Table 5.5: Comparison between the flow state at the initial and final instants of simulation of $\mathcal{G}_2$. Note that Y(x,0) and Q(x,0) are constant $\forall x \in [0, L_i]$.

to the rain perturbation; their variations are set to $q_1(0,t) = q_2(0,t) = 1\ m^3/s$. The outflows are kept constant $\forall t$ and equal to their initial values.

In the sequel, it is reported the result of the simulation performed on network $\mathcal{G}_2$ with the initial and boundary conditions just described. In particular, the simulation duration is one hour (i.e from $t = 0$ to $t = T_{sim} = 1\ h$) and it is executed with a sampling time $T_s = 60\ s$. Given the high number of channels in the network, the plots of the flow state of all channels are given at the end of this section. Table 5.5 summarises the flow state of each channel at the instant $t = 0$ (i.e. the initial condition) and at the final instant $t = T_{sim}$. From Table 5.5 it is possible to infer in which channels the water level has increased the most and which channels are subject to an high flow. In particular, the table shows some heights highlighted in red: these are the largest heights of network $\mathcal{G}_2$ at the final moment of the simulation. These values are analysed below.

Channel 1 has a height $Y_1(0,T_{sim}) = 1.5\ m$. The latter is high w.rt the height of other channel of the network $\mathcal{G}_2$ because the inflow is equal to $Q_1(0,t) = 2\ m^3/s$. Therefore, this channel has a high height because also the inflow is high and a not because the channel has difficulty at draining out the inflows. Indeed, Figure 5.5.a shows that the height is constant over time and that the channel is never in a backwater state since $Q_1(0,t) = Q_1(L_1,t),\ t \in [0,T_{sim}]$.

Channel 2 has a high water level that is $Y_2(L_2,T_{sim}) = 1.47\ m$. The latter is much higher than its initial value of $Y_2(x,0) = 0.71\ m$. This growth is due to the large flow entering on junction 3, indeed this junction is not able to drain completely the inflow, generating a backwater effect that affects the channels 2 e 3. However, unlike channel 2, channel 3 propagates the backwater effect towards downstream

links. Therefore, it keeps a height equal to $Y_3(L_3, T_{sim}) = 0.91\ m$ to the detriment of upstream channels (i.e channel 4 and 9) that are affected by an increase of inflow. On the other hand, channel 2 does not have any link on which it can propagate the backwater effect, so its water level increases more than channel 3.

Channel 4 has a high water heights at the end of simulation. From Figure 5.5.h it can be observed that this is due to two factors. The first is that the inflow is high since the initial moments of the simulation. This is due to the equation (5.15) which regulates the distribution of flow in the junctions. For junction 3, half of the input flow $Q_1(L_1, t)$ is directed to the branch 4, so, considering the flow perturbation, the inflow of branch 4 is equal to $Q_4(0, t) = 0.9\ m^3/s$. The other important aspect is that the outflow of channel 4 is limited by the backwater effect; indeed, its value is about $Q_4(L_4, t) = 0.5\ m^3/s$. The combination of these two effects generates a significant increase in the heights of channel 4, which has the greatest height variation of all the channels in the network $\mathcal{G}_2$.

An important aspect to study is the water heights in channels 7, 8 and 9. These are the channels connected to the outlet nodes of the network, so they are the channels in which water accumulates when the drainage capacity of the outlet node is not sufficient to drain off the flow perturbation.
Channel 7 is the one that undergoes the smallest height variation; indeed, one has $Y_7(L_7, T_{sim}) - Y_7(L_7, 0) = 0.08\ m$. This is followed by channel 8, which has a variation of $Y_8(L_8, T_{sim}) - Y_8(L_8, 0) = 0.49\ m$ and by channel 9 which has a variation of $Y_9(L_9, T_{sim}) - Y_9(L_9, 0) = 0.52\ m$. From figure 5.6.h, it can observed that the growth of water height in channel 8 is due to the flow of channel 5, which is $Y_8(0, T_{sim}) = 1.75\ m^3/s$. In junction 6, this flow is equally split between links 6 and 8. Although the flow is split, the part that passes through link 8 is $Q_8(0, t) = 0.875\ m^3/s$. The latter is higher compared to the drainage capacity of the channel which is only $Q_8(L_8, t) = 0.25\ m^3/s$. This generates a significant increase in height along 8 channel.
The height variation in channel 9 is due to the backwater effect acting on junction 4. Indeed, the incident links of this junction are: $i = 1, 3, 4, 9$. As seen above, the perturbation $q_1(L_1, t)$ has difficulty to pass through links 3 and 4 since both channels are in full backwater state. Then the inflow of the junction falls back in link 9 causing a significant increase of water height along it.

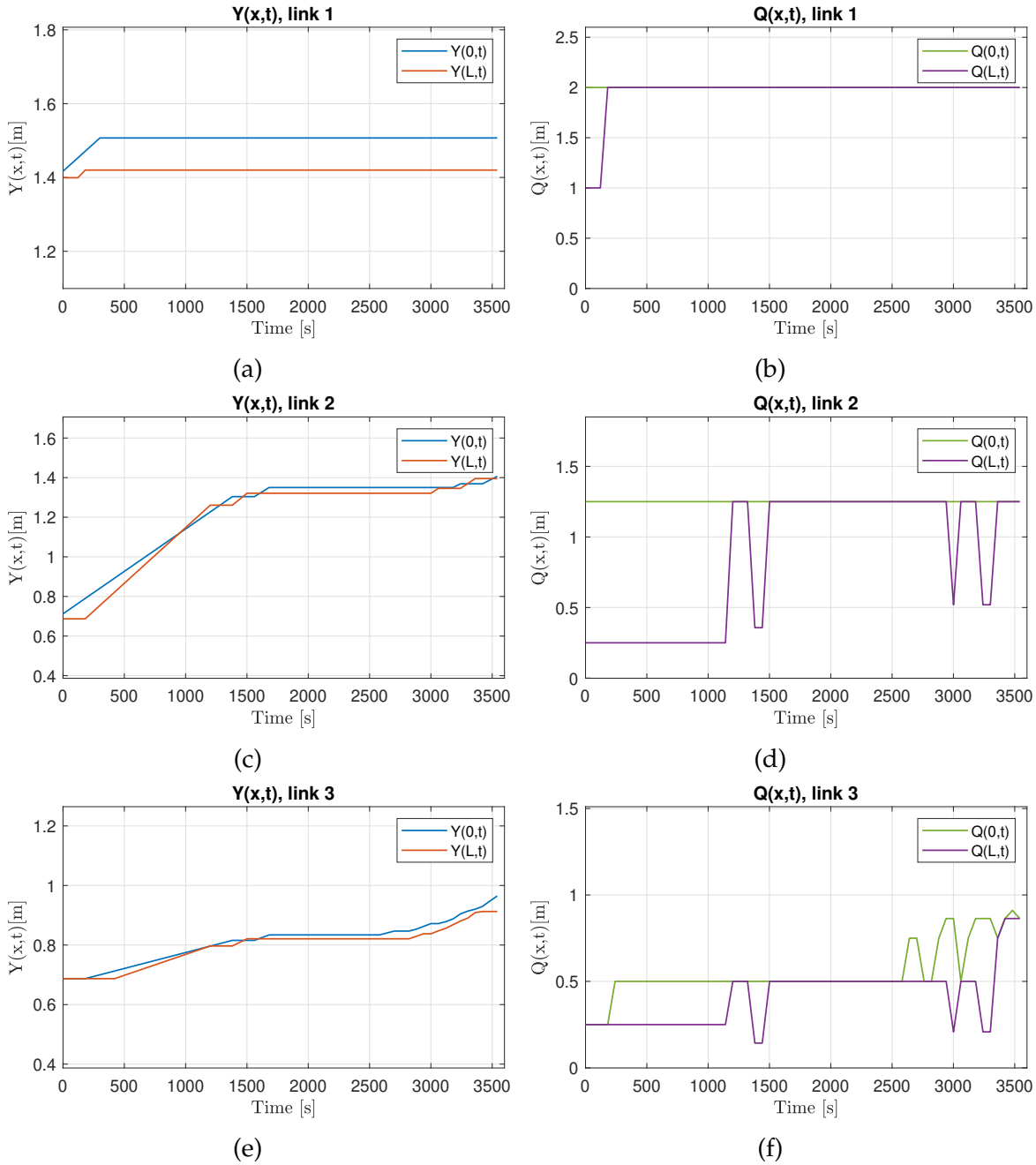

Figure 5.5: Flow states of all of channels $i \in [1,2,3]$ of network $\mathcal{G}_2$. The plots on the left column shows variables $Y_i(0,t)$ and $Y_i(L_i,t)$. The plots on the right column show variables $Q_i(0,t)$ and $Q_i(L_i,t)$.

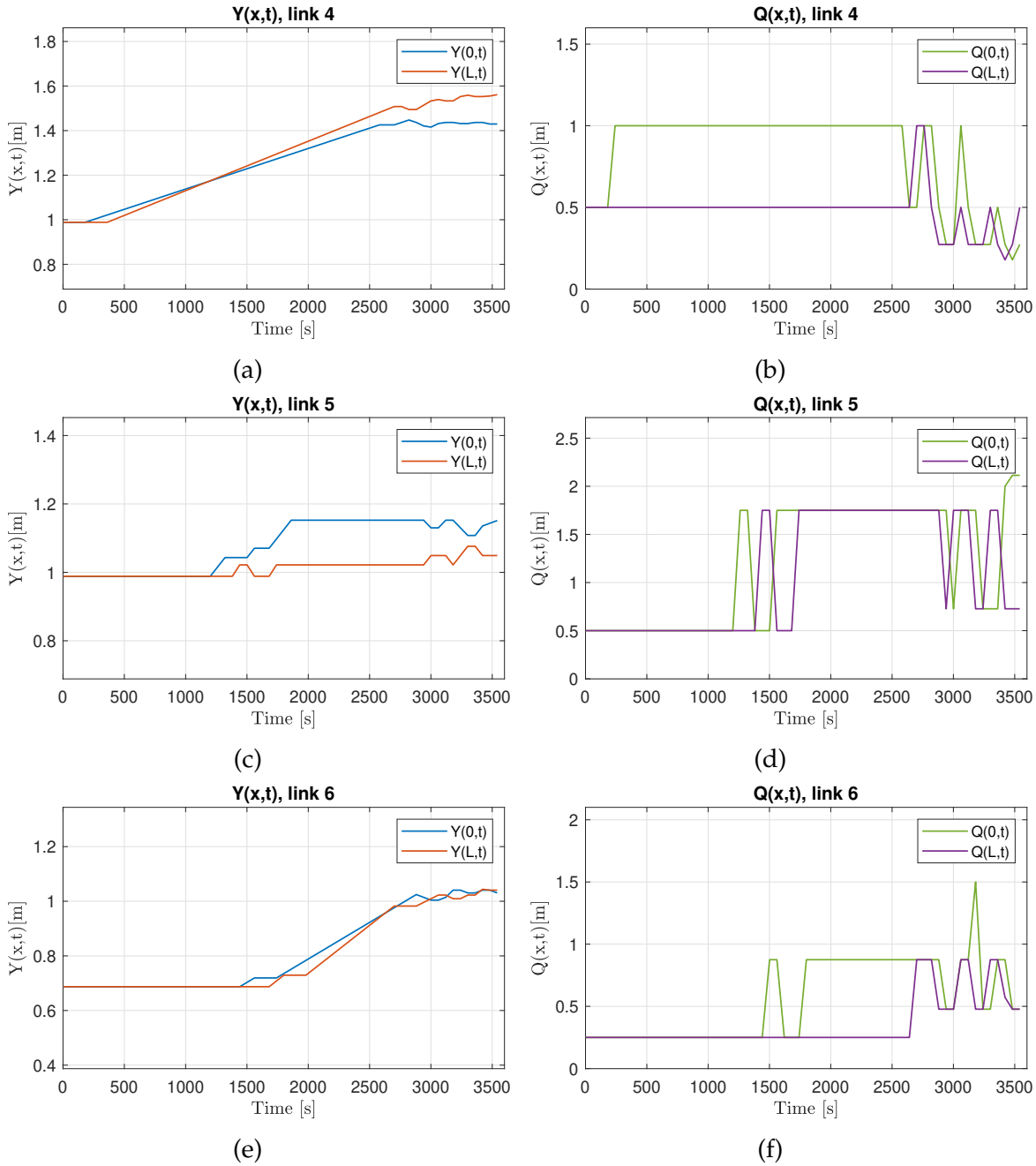

Figure 5.6: Flow states of channels $i \in [4,5,6]$ of network $\mathcal{G}_2$. The plots on the left column shows variables $Y_i(0,t)$ and $Y_i(L_i,t)$. The plots on the right column show variables $Q_i(0,t)$ and $Q_i(L_i,t)$.

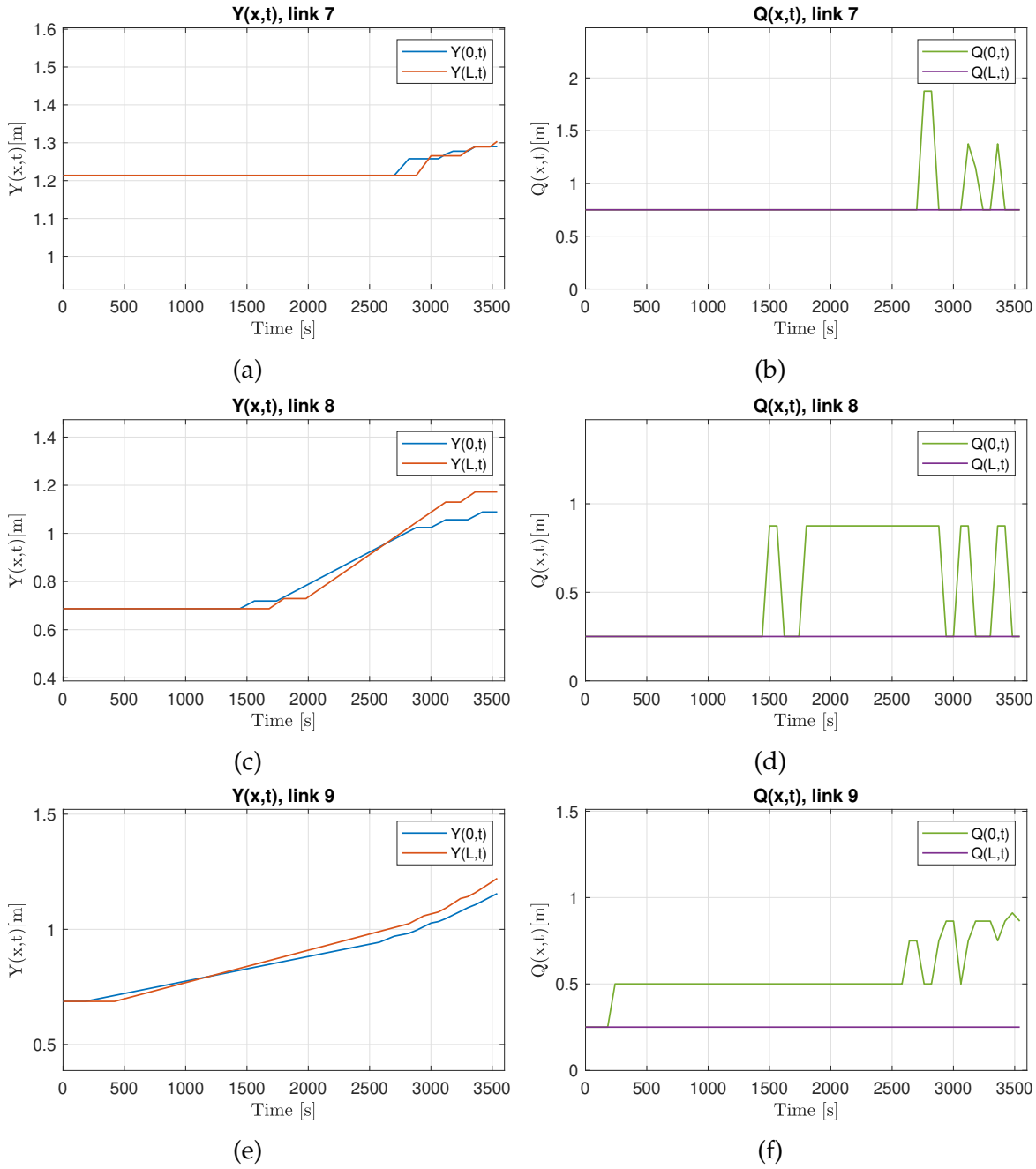

Figure 5.7: Flow states of all of channel $i \in [7,8,9]$ of network $\mathcal{G}_2$. The plots on the left column shows variables $Y_i(0,t)$ and $Y_i(L_i,t)$. The plots on the right column show variables $Q_i(0,t)$ and $Q_i(L_i,t)$.

Conclusions

In this thesis, it is proposed a model to describe the water flow dynamics in an open-channel network. To do that, models for open-channels and junctions are described and analysed in detail. In the first chapter, the IDZ model is discussed. This represents the core of the network model, indeed it is able to capture the main physical behaviour of open channel dynamics through linear equations. In particular, the IDZ model is tested in different scenarios. For example, its step response is analysed when the channel outflow is regulated by an undershoot gate. In this case, the channel heights $y(L,t)$ and $y(0,t)$ stabilise at a steady state value instead of growing linearly, as in the case in which the outflow is kept constant over time. Furthermore, it is proposed a discrete-time version of the IDZ with a regard to the choice sampling time. From this study, rules are derived for the design of sampling time which are used for the choice of sampling type of network model. The second chapter deals with junction models. In particular, different models are presented and validated through real data. From this analysis, it can be said the *Shabayek model* attains the best agreement with the experimental data while the *Equality model* has generated the greatest errors among all. Moreover, the latter model has been subject to further study. Indeed, it is shown that the *Equality model* has good performance if the downstream flow has a low Froude number, i.e. if it is a flow characterised by low speed and high depth. Note that *Shabayek model* and *Gurram model* use non-linear equations calculated for the junction with two inflow branches and one outflow. One possible development is to extend these models also for other types of junctions; for example, for a junction with one inlet branch and two outlet branches. This thesis also deals with the problem of sensor placement in the open-channel network in order to observe the flow of the whole network by minimizing the estimation error. This aspect is crucial for the IDZ model, which accounts for the values of water heights using the known-a-priori inflow and outflow. To solve this task, it is to set up an optimisation problem. In particular, two cost functions are proposed. The latter are used to find the optimal position of the sensors within an example network. From this example, it observed that solutions that minimise only one of the two cost

functions, do not minimise the estimation error. However, it is observed that the solutions minimising both the cost functions also minimise the estimation error.

In the last chapter, it is presented the model for open-channel networks. This uses the models presented in the previous chapters to describe the flow state in the network. In particular, this model leverages the discrete time IDZ model to capture the open-channel dynamics. To model the junctions, conservation equations are employed and it is also considered the propagation of backwater effect through the junction.

Finally, the network model is tested on two networks. The first one has a simple structure and it is used to verify that the model works correctly. The second one is a slightly more complex network. In this case, it can be observed that the model is able to provide the evolution of the heights when the network is subjected to an undesired increase in the input flow. However, it has been observed that the model has criticalities at describing situations in which the network is drained down. In particular it is proposed a solution to overcome this issues. The next research direction is represented by the extension of the junction model in order to describe also the case in which the network is drained down. Furthermore, note that the presented model is able to describe the flow for open-channels. However, drainage networks such as the one of the *Cavallino* peninsula has also pipelines. Then the network model can be extended by introducing an improvement to describe the flow within the pipe, also called pressurised flow.

APPENDIX A

Elements of hydraulics

A.1 Classification of Flows

A flow is called *steady flow*, if both flow velocity $V(x,t)$ and height $Y(x,t)$ does not change with respect to time, instead if the velocity or height changes, a flow is called *unsteady flow*. If the flow velocity and height does not vary along the channel (with respect to the position), then the flow is called *uniform flow*. Conversely, if the flow velocity or the height at a time varies with respect to x, then the flow is called *nonuniform flow*. Note that this classification is based on the variation of velocity $V(x,t)$ and height $Y(x,t)$ respect to time t or space x, thus it is possible to classify the flow into these types using the derivatives, as reported in table A.1.

Uniform flow

In the uniform flow, if the channel bottom slope is positive, the weight of water causes acceleration of flow, whereas the friction stress at the channel bottom and sides generate resistive force. As figure A.1 shows, in a open water channel the input flow accelerates for a distance until the accelerating and resistive forces are

Type of flow	Steady flow	Unsteady flow	Uniform flow	Non uniform flow
	$\frac{\partial V(x,t)}{\partial t} = 0$	$\frac{\partial V(x,t)}{\partial t} \neq 0$	$\frac{\partial V(x,t)}{\partial x} = 0$	$\frac{\partial V(x,t)}{\partial x} \neq 0$
Condition	AND	OR	AND	OR
	$\frac{\partial Y(x,t)}{\partial t} = 0$	$\frac{\partial Y(x,t)}{\partial t} \neq 0$	$\frac{\partial Y(x,t)}{\partial x} = 0$	$\frac{\partial Y(x,t)}{\partial x} \neq 0$

Table A.1: Summary of flow types with their conditions.

equal. After this point the flow velocity and flow depth remain constant along the channel. Such a flow is called uniform flow and the corresponding flow depth is called the normal depth Y_n. In the next paragraph, it is presented a formula that describes the effect of the friction on the water flow.

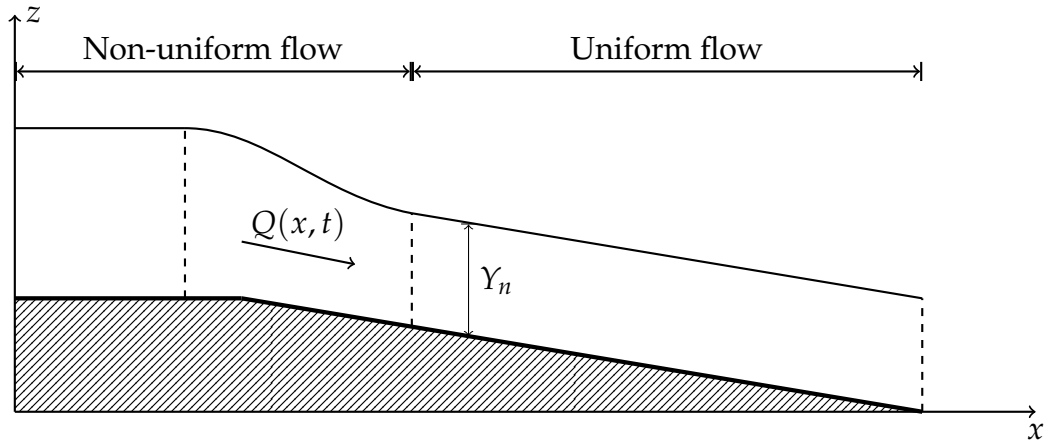

Figure A.1: Example of transition from a non uniform to a uniform flow.

Manning formula

In steady open channel flows, a fundamental problem is determining the relation between the water depth and the flow velocity. An empirical formulation, called the Gauckler–Manning formula, was developed to find a solution to this problem; its expression is given by

$$Q = \frac{1}{n} R^{2/3} A \sqrt{S_f}, \tag{A.1}$$

where Q is the flow rate, A is the cross-sectional area of flow normal to the flow direction and R is the hydraulic radius defined as the ratio between cross section area A and the wetted perimeter P. Parameters n is a constant called Manning roughness coefficient whose unit of measurement is $[m^{1/3}/s]$. This parameter represents the friction effect generated between the bed of channel and the water mass. Its value depends on the material of which the channel bed is composed, its roughness and irregularity, as accumulation of debris, the amount of vegetation or abrupt changes of the channel sizes. Note that all these factors are difficult to measure accurately and they are often unpredictable. It follows that n is difficult to estimate, however it is possible to provide an indicative values, some of these are shown in the table A.2.

Material	$n[m^{1/3}/s]$
Corrugated metal	0.025
Smooth Concrete	0.013
Rough Concrete	0.017
Clay	0.013
Natural watercourse in earth	0.030 - 0.040
Natural watercourse in earth with vegetation	0.050 - 0.070

Table A.2: Collection of Manning's numbers .

The last parameters of (A.1) is called friction slope S_f. To describe this parameter it is necessary to introduce the concept of energy reported in paragraph A.4, for now it is sufficient to know that this parameter is used by SVEs to model the friction forces and it can be calculated reversing the Manning formula in the following way:

$$S_f = \frac{Q^2 n^2}{A^2 R^{4/3}}. \tag{A.2}$$

In case of uniform flow, the Manning's formula can be used to calculate the normal depth. Given a channel having uniform flow, constant bed slope, cross-section sizes and roughness along its entire length, it is possible to demonstrate that the friction slope S_f is equal to the bed slope S_b, so the equation (A.2) becomes

$$Q = \frac{1}{n} R^{2/3} A \sqrt{S_b}. \tag{A.3}$$

Note that the quantities R and A depend on the height Y_n, so by reversing this formula, it is possible to calculate the normal depth given the flow Q. Taking the trapezoid profile as an example, the radius R and the area A are non-linear equations so, in general, the equation (A.3) cannot be inverted analytically. However using the Matlab function `fsolve()` it is possible to obtain a estimate of Y_n with high precision. Note that the Manning's coefficient is one of many parameters used to describe the friction effect, in this thesis it is also used an analogous coefficient called the Chezy coefficient C. In this case, the formula (A.1) and all the previous discussions still valid since exist a formula that relates which allows to find n from C or vice versa, this formula is:

$$C = \frac{1}{n} R^{1/6}, \tag{A.4}$$

where C is the Chezy coefficient, n the Manning's number and R the hydraulic radius.

A.2 Froude Number

An important parameter uses to describe the flow is the Froude number. It is a dimensionless number defined as follows:

$$\mathrm{F_d} = \frac{\mathrm{V}}{\sqrt{\mathrm{gh}}}. \tag{A.5}$$

This index is the rate between the velocity of water V and the celerity. This quantity is defined as the speed of propagation of a small amplitude wave on the surface. It can be calculated as $\mathrm{C} = \sqrt{\mathrm{gh}}$, where g is the gravity constant and h is the hydraulic depth. The latter parameter is the rate between cross section area and the top water surface width. Note that the Froude number is dimensionless index since numerator and denominator have the same unit of measure $[m/s]$.

If a flow have a Froude number $F_d \geq 1$, the velocity of water flow is bigger than the wave velocity. This means that waves cannot propagate upstream, they can propagate only towards downstream direction. In this case the flow is called *supercritical*. Instead if $F_d \leq 1$, the flow velocity of water flow is smaller than the wave velocity, so the waves can propagate both upstream and downstream direction. In this case the flow is called *subcritical* except for $F_d = 1$ which is called *critical*. The figure A.2 shows three examples of how waves move across the surface of the water with subcritical, supercritical, and critical flows. In particular the direction x is the direction of propagation of the flow, while the circles represent the waves generated by the disturbance at the origin O.

This index is used to classify the water flow, in particular, a water flow with a low Froude number is a flow that tend to be deep and slow, whereas a flow with a high Froude number tends to be shallow and fast.

A.3 Pressure

Pressure p is defined as the normal force F per unit area A over which the force is applied, so its unit of measurement is $[N/m^2]$. In a open-channel the fluid is subject to several forces: the component of the gravity force normal to the water surface, the component of the gravity force parallel to the direction of flow given by the slope of the channel S_b and the friction forces. In this thesis it is often used a special case where the water is not subject to any force parallel to the direction of flow. This situation can occur when the slope of the channel $S_b = 0$ and therefore the gravity

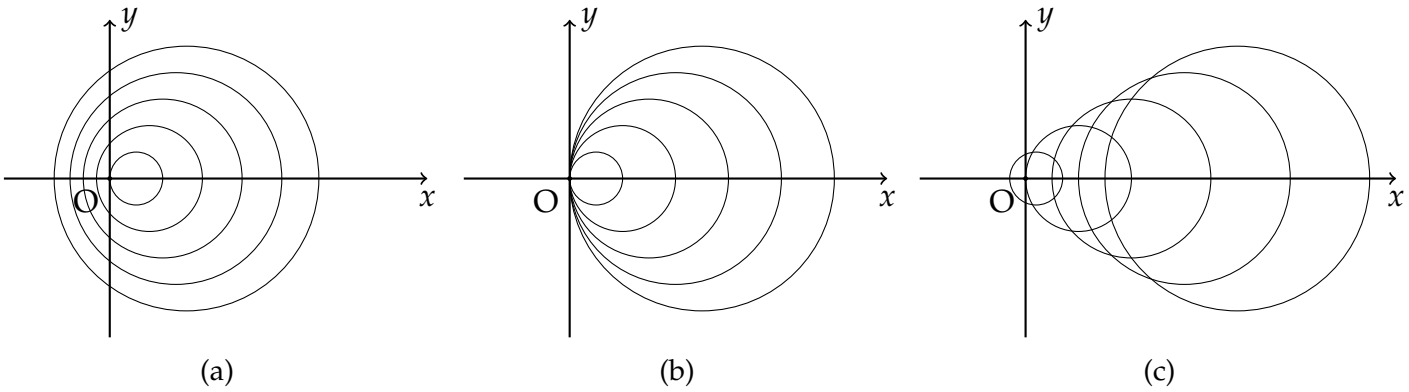

Figure A.2: Propagation of waves generated by a perturbation in O: (a) Sub-critical flow (b) Critical flow (c) Super-critical flow.

force does not accelerate the flow. In this case, the pressure is called *hydrostatic* and is given by the following equation:

$$p = \rho g h = \gamma h; \tag{A.6}$$

where γ is specific weight of the liquid given by the product of the fluid density ($\rho = 1\ kg/m^3$ for water) and the gravity acceleration $g = 9.81\ m/s^2$. The variable h is the distance between the water surface and the point at which the pressure is calculated. Also for the uniform flow the pressure can be approximated to hydrostatic. In the latter case the flow is in equilibrium state where the gravity component parallel to the flow direction is compensated by the friction forces keeping constant the flow velocity and height along the channel. Then the pressure acting on the water mass is only the component of the gravity force normal to the surface and is given by the following equation:

$$p = \gamma h cos^2(\theta), \tag{A.7}$$

where θ is the angle that represents the slope of channel bed: it is defined as:

$$\theta = \arctan(S_b). \tag{A.8}$$

Note that in this case the pressure distribution is not hydrostatic since (A.9) is different to (A.6). However, if the bed slope is sufficiently small, the pressure distribution can be considered hydrostatic because $\theta \simeq 0$ implies $cos(\theta) \simeq 1$. Hence,

$$p = \gamma h cos^2(\theta) \ \simeq \gamma h. \tag{A.9}$$

Figure A.3 shows the distribution of hydrostatic pressure along the cross section of

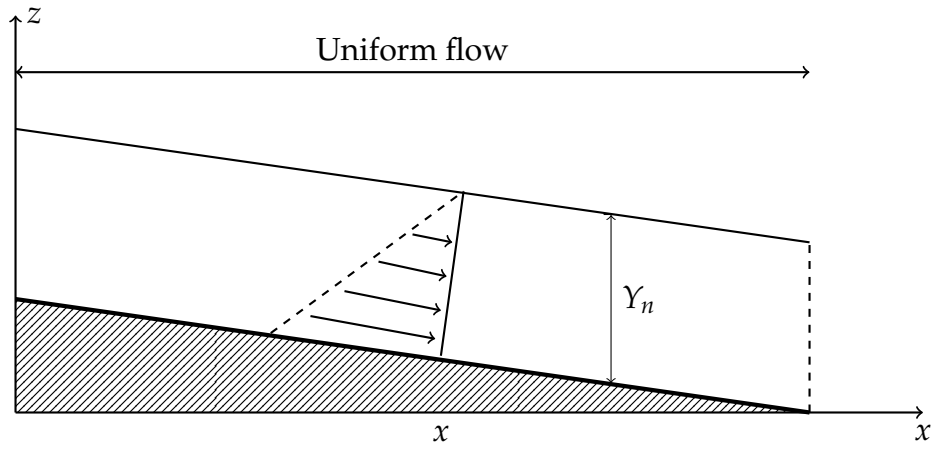

Figure A.3: Example of hydrostatic pressure distribution in a channel with uniform flow.

the channel in position x. The arrows represent the intensity of pressure generated by the water mass. Note that the pressure increases linearly as depth h increases. This linear growth is highlighted by the dashed line positioned adjacent to the tails of the arrows in the figure.

A.4 Energy of open-channel flow

The energy of liquid at a given pose x on the channel can be expressed as the sum of three element, as reported in the flowing formula:

$$E = \rho V^2/2 + p + \rho g z. \tag{A.10}$$

They are in order the kinetic energy, pressure energy and potential energy, where:

- p is the pressure imposed by the water mass upstream of the considered point and it is measured in $[N/m^2]$. Note that it is assumed that the pressure is hydrostatic, namely the pressure increases in proportion to depth measured from the surface;
- V is the mean velocity of the fluid over the cross-section measured in $[m/s]$;
- z is the bed elevation above the given reference that is x axis;
- g is the acceleration due to gravity;
- ρ is the water density measured in $[Kg/m^3]$.

Usually the expression of energy E is divided by γ, that is the specific weight defined as the product of water density ρ and the acceleration due to gravity g(its unit of measurement is $[N/m^3]$). The normalized energy is called also 'head' H and it is defined as :

$$\frac{E}{\gamma} = H = \frac{V^2}{2g} + \frac{P}{\gamma} + z. \tag{A.11}$$

Note that the head relative to pressure energy is equal to the height of the water flow y. This result is not straightforward to obtain, it is derived from the assumption that pressure is hydrostatic. Note that the unit of measurement for the energy head H is meter $[m]$. According to the energy conservation principles, the energy across any two points in space x_1 and x_2 of the channel must balance. In particular, if the energy is reduced by friction or other disturbances the loss should be considered. This loss in energy is called head loss H_L and it is considered in the energy conservation equation as follows:

$$\frac{p_1}{\gamma} + z_1 + \frac{V_1^2}{2g} = \frac{p_2}{\gamma} + z_2 + \frac{V_2^2}{2g} + H_L. \tag{A.12}$$

This is the general form of the energy conservation equation. In the special case in which there is no energy loss (i.e. $H_L = 0$), it is known as Bernoulli equation. The determination of head loss H_L is challenging, indeed it is depends on phenomena that are difficult to quantify precisely. One of these is the internal friction between fluid particles traveling at different velocities. Other causes of energy loss are turbulence of flow, friction with the channel bed and channel shape variations, such as a reduction in cross-section sizes or channel curve.

An equivalent parameter to head loss is the friction slope S_f: this is the rate at which energy is lost along a given length of channel, so it is:

$$S_f = \frac{H_L}{\Delta x}, \tag{A.13}$$

where H_L is the head loss along the channel with length Δx. This quantity is usually expressed as dimensionless value or with length by length unit $[m/m]$.

If the flow is uniform, the friction slope S_f is equal to the bed slope S_b, in fact under conditions of uniform flow a channel has constant flow velocity and height. Therefore, given a section of channel ranging from x_1 to x_2 and applying the formula (A.12), the terms kinetic energy and pressure energy can be simplified, and thus the following relation is obtained:

$$z_1 = z_2 + H_L. \tag{A.14}$$

Dividing this equation on both sides by the length of the channel $x_2 - x_1$, the equation become:

$$\frac{H_L}{x_2 - x_1} = \frac{z_1 - z_2}{x_2 - x_1} \quad \Rightarrow \quad S_f = S_b. \tag{A.15}$$

A.5 Hydraulic structure

A hydraulic structure is a submerged or partially submerged structure, which changes the natural flow of water. The main types of these structures are weirs and gates: the weirs are barriers anchored to the channel bed that allow the passage of water only over their crest. The undershot gates are movable structures that allow water to pass through a hole between the channel bed and their submerged crest. Figures A.4 and A.5 show these two types of hydraulic structures. In this section the weirs and undershot gates are modeled using a static nonlinear equations derived from the Bernoulli's equation. In particular, these equations provide a relationship between the water heights at both sides of the structure and the flow passing through it. These equations also depend on the state of the flow, two cases can occur. If the downstream flow is critical or supercritical, the hydraulic structure is said to be in *free flow condition* and, in this case, the downstream level has no influence on the discharge that depends on the upstream water level only. Whereas, a hydraulic structure is said to be in *submerged flow condition* if the downstream flow remains subcritical, in that case, the outflow of hydraulic structure can be influenced by the downstream water depth. Figure A.4.a shows a weir in *free flow condition*, it can be observed that the flow passing through the weir is not affected by Y_2 since $Y_2 < W$. Figure A.4.b shows a weir in *submerged flow condition*, note that the downstream flow has a depth that covers the whole weir, so upstream and downstream parts are not decoupled as in *free flow* case. Figure A.5.a shows an undershoot gate in *free flow condition*, while figure A.5.b shows an undershoot gate in *submerged flow condition*. Below it is reported the model for the weir and for the undershot gate.

Weir

In the free flow condition, the flow passing over the gate is given by:

$$Q = C_d W \left(Y_1 - H\right)^{3/2}, \tag{A.16}$$

where H the weir crest height from channel bed, W is the width of the weir throat and Y_1 is the upstream water level. Coefficient C_d is called discharge coefficient

and is equal to $C_d \simeq (2/3)\sqrt{(2g/3)} = 1.705$. If the structure is in submerged flow condition, the flow is given by:

$$Q = C_d W \left(Y_1 - Y_2\right)^{3/2}, \tag{A.17}$$

where Y_1 is water height at the upstream side of the structure and Y_2 is water height at the downstream side.

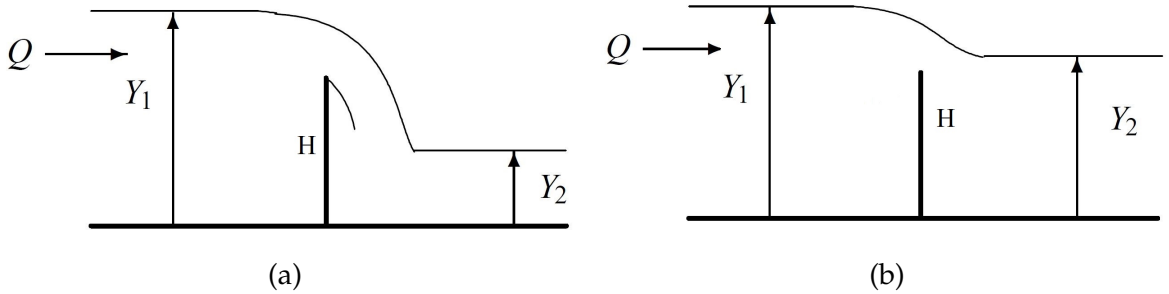

Figure A.4: Example of Weir structure in *free flow condition* for (a) and *submerged flow condition* for (b).

Submerged gate

Under free flow condition the flow passing through the gate is described by the following equation:

$$Q = C_d W H \sqrt{2gY_1}, \tag{A.18}$$

where H the height of the gate hole, W is the width of gate hole and Y_1 the upstream water level. The discharge coefficient C_d for the gate is usually set to 0.6. In the submerged flow condition the flow is given by:

$$Q = C_d H W \sqrt{2g\left(Y_1 - Y_2\right)}, \tag{A.19}$$

where Y_1 is water height at the upstream side of the structure and Y_2 is water height at the downstream side.

Linearized models

In order to include the hydraulic structure models in the IDZ model, it is necessary to linearise their equations. As linear approximation of these functions, it is used the first order Taylor expansion computed around a working point called (Y_1, Y_2, H).

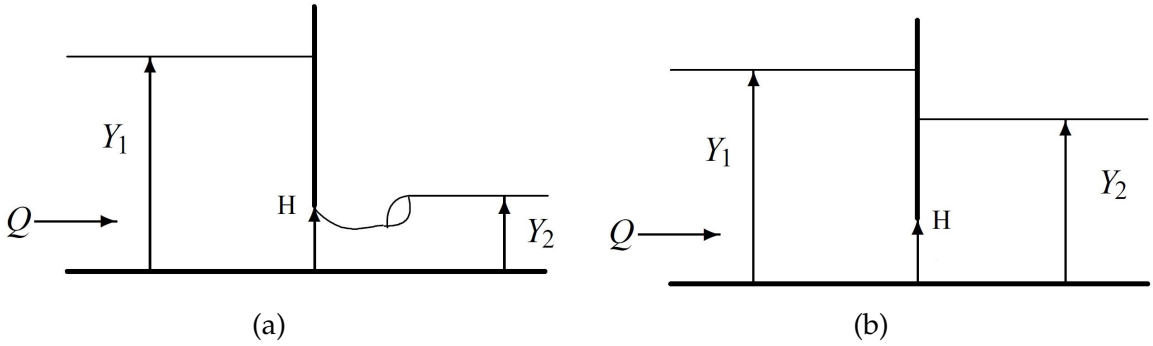

Figure A.5: Example of Gate structure in *free flow condition* for (a) and *submerged flow condition* for (b) .

The linearized model is represented by the equation:

$$Q(t) = f(Y_1, Y_2, H) + k_u y_1(t) + k_d y_2(t) + k_h h(t), \tag{A.20}$$

where $Q(t)$ is the total flow the pass thought the gate, $f(Y_1, Y_2, H)$ is the function that models the behavior of hydraulic structure evaluated at the working point. The variables $y_1(t), y_2(t)$ are, respectively, the deviation of water levels from Y_1 and Y_2, also $h(t)$ is the deviation of the gate hole height from H. The coefficients k_u, k_d, and k_w are defined as the derivatives of the function $f()$ evaluated at Y_1, Y_2, and W, so they are:

$$\begin{aligned} k_u &= \frac{\partial f}{\partial Y_1}(Y_1, Y_2, H), \\ k_d &= \frac{\partial f}{\partial Y_2}(Y_1, Y_2, H), \\ k_h &= \frac{\partial f}{\partial H}(Y_1, Y_2, H). \end{aligned} \tag{A.21}$$

In this thesis it is used on only the undershoot gate in free flow condiction. Note that its flow (A.18) doesn't depends on Y_2, also it is assumed that W is constant in time, so the linearized equation is

$$Q(t) = f(Y_1, Y_2, H) + f'(Y_1, Y_2, H)(y_1(t)), \tag{A.22}$$

where $f(Y_1, Y_2, H)$ is the non-linear equation (A.18) and $f'(Y_1)$ is its derivative respect to Y_1

$$f'(Y_1, Y_2, H) = \frac{\partial f}{\partial Y_1}(Y_1, Y_2, H) = \frac{g C_d W H}{\sqrt{2 g Y_1}}. \tag{A.23}$$

For the gate in submerged-flow condiction, the equation (A.22) and (A.24) are not valid since $Q(t)$ depends on Y_2. However if Y_2 is assumed constant in time , $y_2(t)$ is

null, therefore even if $k_d \neq 0$, only K_u is used an it is

$$f'(Y_1, Y_2, H) = \frac{\partial f}{\partial Y_1}(Y_1, Y_2, H) = \frac{g C_d W H}{\sqrt{2g(Y_1 - Y_2)}}. \tag{A.24}$$

APPENDIX B

IDZ parameters

B.1 Linearized Saint-Venant model

The SVEs are the starting point from which the parameters of the IDZ model. They are linearised around a given steady state flow regime defined by $[Q_0(x), Y_0(x)]$. The first step is to simplify the SVEs assuming that flow and height do not vary in time (i.e. steady state), in particular this condition is satisfied if:

$$\frac{dY(x,t)}{dt} = 0 \quad \text{and} \quad \frac{dQ(x,t)}{dt} = 0. \tag{B.1}$$

Substituting these conditions into the SVEs become:

$$\begin{aligned} &\frac{\mathrm{d}Q_0(x)}{\mathrm{d}x} = 0, \\ &\frac{\mathrm{d}Y_0(x)}{\mathrm{d}x} = \frac{S_b - S_{f0}(x)}{1 - F_0(x)^2}, \end{aligned} \tag{B.2}$$

where $Q_0(x)$, $Y_0(x)$ denoting the variables corresponding to the equilibrium regime.

B.2 Backwater curve approximation

The backwater curve defines the water level along the entire length of the channel at the initial state for a given flow Q_0 and a downstream boundary water depth $Y(L, 0)$. It is described by the SVEs in the steady-state condiction reported below:

$$\frac{dY_0(x)}{dx} = \frac{S_b - S_{f0}(x)}{1 - F_0(x)^2}, \tag{B.3}$$

where F_0 is the Froude number calculated at the initial state using (A.5), S_b is the channel bottom slope and S_{f0} is the friction slope modeled by the Manning-Strickler formula (A.2).

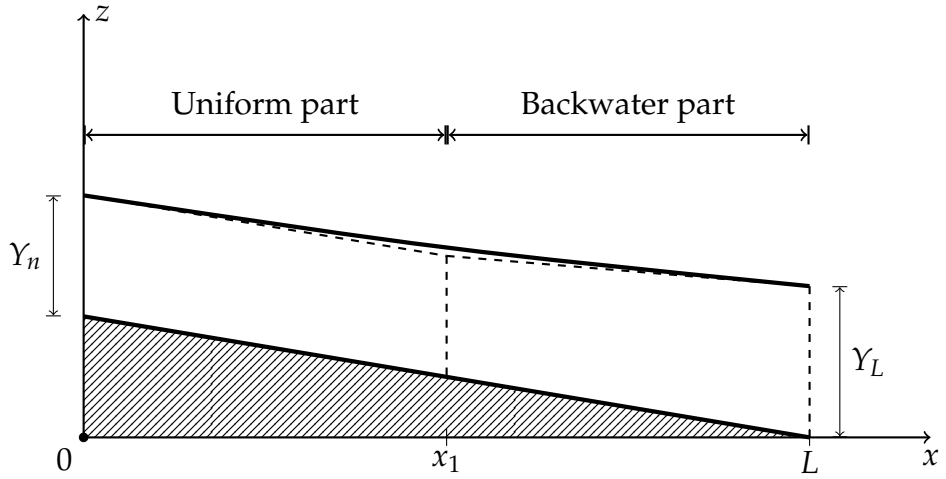

Figure B.1: Lateral section of a open channel with it backwater profile $(-)$ and its approximation $(--)$.

In figure B.1, a continuous line shows backwater curve described by equation (B.3), while the dashed line represents the approximation of the backwater curve used by the IDZ model. In particular, along the first part of channel $x \in [x_1, L]$ this approximation assumes that the height is equal to the normal depth Y_n. The second part the height is modeled with a line defined as the tangent to the original backwater curve at the point $x = L$. The slope of this line can be calculated evaluating equation (B.3) at $x = L$:

$$S_L = \frac{S_b - S_{f0}(L)}{1 - F_0^2(L)}. \tag{B.4}$$

Using B.4 it is possible to calculate the point x_1, which is the position that separates the "uniform part" to "backwater part". This position can be calculated with the following formula:

$$x_1 = \begin{cases} \max\left\{L - \frac{Y_L - Y_n}{S_L}, 0\right\} & \text{if } S_L \neq 0 \\ L & \text{if } S_L = 0. \end{cases} \tag{B.5}$$

In conclusion the height of the channel at a generic point x can be calculate with the following formula:

$$Y(x) = \begin{cases} Y_1 & \text{for } x \in [0, x_1] \\ Y_1 + (x - x_1)\, S_L & \text{for } x \in [x_1, X]\,, \end{cases} \tag{B.6}$$

with

$$Y_1 = \begin{cases} Y_n & \text{if } x_1 \neq 0 \\ Y_L - LS_L & \text{if } x_1 = 0. \end{cases} \tag{B.7}$$

To sum up, these results presented above say that, knowing the inlet flow Q and the height Y_L, it is possible to estimate the height of the water for any position $x \in [0, L]$, so it is sufficient to know these two quantities in order to know entire state of the channe.

B.3 IDZ parameters calculation

To calculate the parameters of IDZ model, it is necessary to linearize Saint-Venant equations around a given steady flow regime $[Q_0, Y_0(x)]$. For a channel with trapezoidal cross-section, the Saint-Venant equations linearized around a given steady flow regime are:

$$\begin{aligned} &T_0(x)\frac{\partial y}{\partial t} + \frac{\partial q}{\partial x} = 0, \\ &\frac{\partial q}{\partial t} + 2V_0(x)\frac{\partial q}{\partial x} - \beta_0(x)q + \left[C_0(x)^2 - V_0(x)^2\right] T_0(x)\frac{\partial y}{\partial x} - \gamma_0(x)y = 0. \end{aligned} \tag{B.8}$$

where $y = Y - Y_0$ is the variation of water depth respect to the steady-state regime and $q = Q - Q_0$ m^3/s is the variation of water flow respect to the steady-state regime. The variable $T_0(x)$ is the width for water surface at the equilibrium regime m; $A_0(x)$ is the wetted area. $V_0(x)$ is the average water velocity in section $A_0(x)$ calculated as $V_0(x) = Q_0/A_0(x)$. C_0 is the wave celerity m/s and it is calculated as $C_0 = \sqrt{gA_0/T_o}$. F_0 is the Froude number that is assumed to be less than one, i.e the flow is assumed subcritical. The parameters S_{f0} is the friction slope modeled with the Manning-Strickler formula (A.3):

$$S_{f0}(x) = \frac{Q_0^2 n^2}{A_0(x)^2 R_0(x)^{4/3}}. \tag{B.9}$$

Where n is the Manning's number $m^{1/3}s$ and $R_0(x)$ is the hydraulic radius. The equation (B.8) use also two parameters γ_0 and β_0:

$$\begin{aligned}\gamma_0 &= V_0^2\frac{\partial T_0}{\partial x} + gT_0\left\{(1+\kappa_0)\,S_b - \left[1+\kappa_0-(\kappa_0-2)\,\mathrm{F}_0^2\right]\frac{\partial Y_0}{\partial x}\right\},\\ \beta_0 &= -\frac{2g}{V_0}\left(S_b - \frac{\partial Y_0}{\partial x}\right),\end{aligned} \tag{B.10}$$

where $\kappa_0 = 7/3 - 4A_0/\left(3T_0P_0\right)\partial P_0/\partial Y$ and $P_0(x)$ is the wetted perimeter of area $A_0(x)$. Below are reported the formulas for deriving the parameters of the IDZ model. The calculation process is composed by four step:

1. The SVEs are linearised on this work point; starting from the initial conditions of the system $[Q_0, Y_0(L)]$, it is assumed that the system is in steady state conditions, so that the flow and heights are constant over time and equal to initial conditions $[Q_0, Y_0(L)]$.

2. The Normal depth and other quantities describing the backwater profile are calculated at the initial conditions. This part is described in the previous section B.2;

3. The channel is considered as union of two channel: one with uniform flow and the another one with backwater flow (i.e non-uniform flow), the model parameters are calculated separately for both channels;

4. The global IDZ model is obtained merging the parameters of both channels with a interconnection rules.

Therefore each parameter of the model is calculated for the uniform part and the backwater part and finally are merge together with interconnection formula. In particular, the parameters calculated for the uniform part are marked with a "hat", while the parameters for the backwater part are marked with a "bar". In the following, the formulae are only given for the calculation of the parameters of the uniform part because the parameters of the backwater part are calculated with the same formulae, the only difference are the variables x and l. x indicates the point on which the variables (as C_0, V_0,S_{f0}) are calculated. For the uniform part parameters it is $x = 0$ while for the backwater part it is $x = (x_1 + L)/2$. The variable l indicates the length of the channel part, for the uniform part parameters it is $l = x_1$ while for the backwater

part it is $l = L - x_1$. The areas parameters for the upstream uniform flow part are:

$$\begin{aligned}\hat{A}_d &= \frac{T_0^2\left(C_0^2 - V_0^2\right)}{\gamma_0}\left[1 - e^{-\gamma_0/T_0\left(C_0^2 - V_0^2\right)l}\right],\\ \hat{A}_u &= \frac{T_0^2\left(C_0^2 - V_0^2\right)}{\gamma_0}\left[1 - e^{\gamma_0/T_0\left(C_0^2 - V_0^2\right)l}\right].\end{aligned} \tag{B.11}$$

The interconnection rules are:

$$\begin{aligned}A_u &= \hat{A}_u\left(1 + \frac{\bar{A}_u}{\hat{A}_d}\right),\\ A_d &= \bar{A}_d\left(1 + \frac{\hat{A}_d}{\bar{A}_u}\right).\end{aligned} \tag{B.12}$$

The delay times are:

$$\begin{aligned}\hat{\tau}_d &= \frac{x_1}{C_0(x) + V_0(x)},\\ \hat{\tau}_u &= \frac{x_1}{C_0(x) - V_0(x)}.\end{aligned} \tag{B.13}$$

The interconnection rules are:

$$\begin{aligned}\tau_u &= \hat{\tau}_u + \overline{\tau}_u,\\ \tau_d &= \hat{\tau}_d + \overline{\tau}_d.\end{aligned} \tag{B.14}$$

The gains in high frequencies for uniform part are:

$$\begin{aligned}\hat{p}_{11} &= \frac{1}{T_0C_0\left(1 - \mathrm{F}_0\right)}\sqrt{\frac{1 + \left(\frac{1-\mathrm{F}_0}{1+\mathrm{F}_0}\right)^2 e^{\alpha l}}{1 + e^{\alpha l}}},\\ \hat{p}_{12} &= \frac{2}{T_0C_0\left(1 - \mathrm{F}_0^2\right)}\frac{e^{-\frac{\gamma_0}{2T_0\left(C_0^2 - V_0^2\right)}l}}{\sqrt{1 + e^{\alpha l}}},\\ \hat{p}_{21} &= \frac{2}{T_0C_0\left(1 - \mathrm{F}_0^2\right)}\frac{e^{\gamma_0/2T_0\left(C_0^2 - V_0^2\right)l}}{\sqrt{1 + e^{\alpha l}}},\\ \hat{p}_{22} &= \frac{1}{T_0C_0\left(1 + \mathrm{F}_0\right)}\sqrt{\frac{1 + \left(\frac{1+\mathrm{F}_0}{1-\mathrm{F}_0}\right)^2 e^{\alpha l}}{1 + e^{\alpha l}}},\end{aligned} \tag{B.15}$$

where for uniform part $x = x_1$ and

$$\alpha = \frac{T_0\left[2 + \left(\kappa_0 - 1\right)\mathrm{F}_0^2\right]S_b}{A_0\mathrm{F}_0\left(1 - \mathrm{F}_0^2\right)}.$$

For backwater part, to find $\overline{p}$, the same expressions are valid, it is necessary to substitute x with $x = L - x_1$, the variable are evaluated at $x_2 = (x_1 + L)/2$ and α is substituted with

$$\bar{\alpha} = \frac{T_0}{A_0 \mathrm{F}_0 \left(1 - \mathrm{F}_0^2\right)} \left\{ \left[2 + (\kappa_0 - 1)\, \mathrm{F}_0^2 \right] S_b - \left[2 + (\kappa_0 - 1)\, \mathrm{F}_0^2 \; - \left(\frac{A_0}{T_0^2} \frac{dT_0}{dY} + \kappa_0 - 2 \right) \mathrm{F}_0^4 \right] S_L \right\}.$$

The interconnection rules are:

$$\begin{aligned} p_{11} &= \hat{p}_{11} + \frac{\hat{p}_{12}\hat{p}_{21}}{\overline{p}_{11} + \hat{p}_{22}}, \\ p_{12} &= \frac{\hat{p}_{12}\overline{p}_{12}}{\overline{p}_{11} + \hat{p}_{22}}, \\ p_{21} &= \frac{\hat{p}_{21}\overline{p}_{21}}{\overline{p}_{11} + \hat{p}_{22}}, \\ p_{22} &= \overline{p}_{22} + \frac{\overline{p}_{12}\overline{p}_{21}}{\overline{p}_{11} + \hat{p}_{22}}. \end{aligned} \tag{B.16}$$

B.4 Cross-section variables

In this section it is presented the variables that describe the trapezoidal and rectangular cross-section shape used in this thesis.

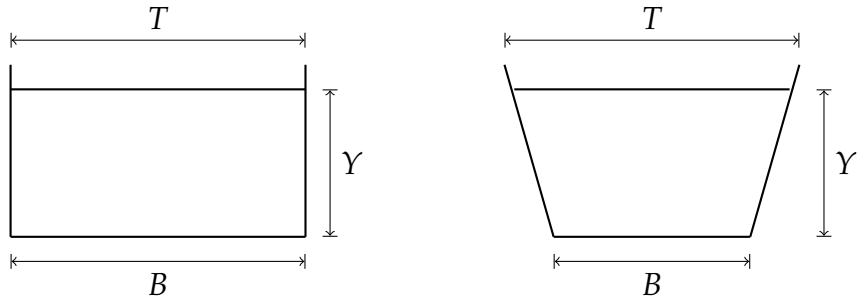

(a) (b)

Figure B.2: Cross-section shape. (a) Rectangular cross-section (b) Trapezoidal cross-section.

The rectangular cross-section is shown in figure B.2.a, only two parameters are required to describe it: the bottom width B and water height Y, both measured in meters. The trapezoidal cross-section is shown in figure B.2.b, in this case the cross section is described by four parameters:

- The smaller base of the trapezoid B, which is also the width of the channel bed;
- The bigger base of the trapezoid T, which the width of the water surface also called top width;
- The water height Y;
- The coefficient m represent the slope of the oblique side of the trapezoid,

In particular the latter coefficient is defined as :

$$m = \frac{T - B}{2Y}. \tag{B.17}$$

This parameter can be found with any value of the Y and the associated value of T. For example, it is possible to use the maximum value of the water height Y_{max} and the maximum top width T_{max}, the advantage is that they are constant values which do not depend on the state of the water. In addition, other variables are used in this thesis, they are listed below:

- A is the cross-section area of water flow;
- P is the perimeter of the cross-section area A;
- R is called hydraulic radius and it is defined as the ratio between cross-section area and its perimeters: $R = A/P$;
- D_h is called hydraulic depth and it is defined as the ratio between cross-section area and its top width: $R = A/T$;

Table B.1 it is shown the formulas to calculate the variables just describe for the rectangular and trapezoidal cross-sections.

Variable	Symbol	Rectangular cross-section	Trapezoidal cross-section
Cross-section area	$A\ [m^2]$	$B\ Y$	$(B + mY)Y$
Wetted perimeter	$P\ [m]$	$B + 2Y$	$B + 2Y\sqrt{1 + m^2}$
Hydraulic radius	$R\ [m]$	$\frac{B\ Y}{B+2Y}$	$\frac{(B+mY)Y}{B+2Y\sqrt{1+m^2}}$
Top width	$T\ [m]$	B	$B + 2mY$
Hydraulic depth	$D_h\ [m]$	Y	$\frac{(B+mY)Y}{B+2mY}$

Table B.1: Formulas to calculate the cross-section variables.

References

[1] Michael J Hammond et al. "Urban flood impact assessment: A state-of-the-art review". In: *Urban Water Journal* 12.1 (2015), pp. 14–29.

[2] CNR ISMAR. *Acqua alta a Venezia*. 2022. URL: http://www.ismar.cnr.it/infrastrutture/previsioni/acqua-alta-venezia.

[3] Luís García et al. "Modeling and real-time control of urban drainage systems: A review". In: *Advances in Water Resources* 85 (2015), pp. 120–132.

[4] Gregory Conde, Nicanor Quijano, and Carlos Ocampo-Martinez. "Modeling and control in open-channel irrigation systems: A review". In: *Annual Reviews in Control* (2021).

[5] Tim D Fletcher, Herve Andrieu, and Perrine Hamel. "Understanding, management and modelling of urban hydrology and its consequences for receiving waters: A state of the art". In: *Advances in water resources* 51 (2013), pp. 261–279.

[6] Romuald Szymkiewicz. *Numerical modeling in open channel hydraulics*. Vol. 83. Springer Science & Business Media, 2010.

[7] FR Garcia and R Kahawita. "Numerical solution of the shallow water equations with a MacCormack type finite difference scheme". In: *Mathematical Modelling in Science and Technology*. Elsevier, 1984, pp. 669–673.

[8] Pierre-Olivier Malaterre and J Rodellar. "Multivariable predictive control of irrigation canals. Design and evaluation on a 2-pool model". In: *Proceedings of the International Workshop on Regulation of Irrigation Canals: State of the Art of Research and Applications*. Citeseer. 1997, pp. 239–248.

[9] R Szymkiewicz. "Finite-element method for the solution of the Saint Venant equations in an open channel network". In: *Journal of hydrology* 122.1-4 (1991), pp. 275–287.

[10] A Tavakoli and F Zarmehi. "Adaptive finite element methods for solving Saint-Venant equations". In: *Scientia Iranica* 18.6 (2011), pp. 1321–1326.

[11] Shoitiro Hayami. "On the propagation of flood waves". In: *Bulletins-Disaster Prevention Research Institute, Kyoto University* 1 (1951), pp. 1–16.

[12] G Corriga, S Sanna, and G Usai. "Frequency response and dynamic behaviour of canal networks with self-levelling gates". In: *Applied Mathematical Modelling* 4.2 (1980), pp. 125–129.

[13] Xavier Litrico and Vincent Fromion. "Analytical approximation of open-channel flow for controller design". In: *Applied Mathematical Modelling* 28.7 (2004), pp. 677–695.

[14] Jan Schuurmans. "Control of water levels in open-channels". In: (1997).

[15] Gerald T McCarthy. "The unit hydrograph and flood routing". In: *proceedings of Conference of North Atlantic Division, US Army Corps of Engineers, 1938*. 1938, pp. 608–609.

[16] Erik Weyer. "System identification of an open water channel". In: *Control engineering practice* 9.12 (2001), pp. 1289–1299.

[17] Ali Osman Akan and Ben Chie Yen. "Diffusion-wave flood routing in channel networks". In: *Journal of the Hydraulics Division* 107.6 (1981), pp. 719–732.

[18] Georges Kesserwani et al. "Simulation of subcritical flow at open-channel junction". In: *Advances in Water Resources* 31.2 (2008), pp. 287–297.

[19] Sampath Kumar Gurram, Karam S Karki, and Willi H Hager. "Subcritical junction flow". In: *Journal of Hydraulic Engineering* 123.5 (1997), pp. 447–455.

[20] Chung-Chieh Hsu, Wen-Jung Lee, and Cheng-Hsi Chang. "Subcritical open-channel junction flow". In: *Journal of Hydraulic Engineering* 124.8 (1998), pp. 847–855.

[21] Shazy Shabayek, Peter Steffler, and FE Hicks. "Dynamic model for subcritical combining flows in channel junctions". In: *Journal of Hydraulic Engineering* 128.9 (2002), pp. 821–828.

[22] Mouhamadou Samsidy Goudiaby and Gunilla Kreiss. "A Riemann problem at a junction of open canals". In: *Journal of Hyperbolic Differential Equations* 10.03 (2013), pp. 431–460.

[23] Mohamed Elshobaki, Alessandro Valiani, and Valerio Caleffi. "Numerical modelling of open channel junctions using the Riemann problem approach". In: *Journal of Hydraulic Research* (2018).

[24] Xavier Litrico and Vincent Fromion. *Modeling and control of hydrosystems*. Springer Science & Business Media, 2009.

[25] Chung-Chieh Hsu, Feng-Shuai Wu, and Wen-Jung Lee. "Flow at 90 equal-width open-channel junction". In: *Journal of Hydraulic Engineering* 124.2 (1998), pp. 186–191.

[26] Monica Gentili and Pitu B Mirchandani. "Locating sensors on traffic networks: Models, challenges and research opportunities". In: *Transportation research part C: emerging technologies* 24 (2012), pp. 227–255.

[27] Hai Yang, Chao Yang, and Liping Gan. "Models and algorithms for the screen line-based traffic-counting location problems". In: *Computers & operations research* 33.3 (2006), pp. 836–858.

[28] Xiang Fei and Hani S Mahmassani. "Structural analysis of near-optimal sensor locations for a stochastic large-scale network". In: *Transportation Research Part C: Emerging Technologies* 19.3 (2011), pp. 440–453.

[29] Shou-Ren Hu, Srinivas Peeta, and Chun-Hsiao Chu. "Identification of vehicle sensor locations for link-based network traffic applications". In: *Transportation Research Part B: Methodological* 43.8-9 (2009), pp. 873–894.

[30] Enrique Castillo et al. "Matrix tools for general observability analysis in traffic networks". In: *IEEE Transactions on Intelligent Transportation Systems* 11.4 (2010), pp. 799–813.

[31] ManWo Ng. "Synergistic sensor location for link flow inference without path enumeration: A node-based approach". In: *Transportation Research Part B: Methodological* 46.6 (2012), pp. 781–788.

[32] Xiangdong Xu et al. "Robust network sensor location for complete link flow observability under uncertainty". In: *Transportation Research Part B: Methodological* 88 (2016), pp. 1–20.